Integrated Sensing and Communications: Toward Dual-Functional Wireless Networks for 6G and Beyond

Fan Liu, *Member, IEEE*, Yuanhao Cui, *Member, IEEE*, Christos Masouros, *Senior Member, IEEE*, Jie Xu, *Member, IEEE*, Tony Xiao Han, *Senior Member, IEEE*, Yonina C. Eldar, *Fellow, IEEE*, and Stefano Buzzi, *Senior Member, IEEE*

***Abstract*— As the standardization of 5G solidifies, researchers are speculating what 6G will be. The integration of sensing functionality is emerging as a key feature of the 6G Radio Access Network (RAN), allowing for the exploitation of dense cell infrastructures to construct a perceptive network. In this IEEE Journal on Selected Areas in Communications (JSAC) Special Issue overview, we provide a comprehensive review on the background, range of key applications and state-of-the-art approaches of Integrated Sensing and Communications (ISAC). We commence by discussing the interplay between sensing and communications (S&C) from a historical point of view, and then consider the multiple facets of ISAC and the resulting performance gains. By introducing both ongoing and potential use cases, we shed light on the industrial progress and standardization activities related to ISAC. We analyze a number of performance tradeoffs between S&C, spanning from information theoretical limits to physical layer performance tradeoffs, and the cross-layer design tradeoffs. Next, we discuss the signal processing aspects of ISAC, namely ISAC waveform design and receive signal processing. As a step further, we provide our vision on the deeper integration between S&C within the framework of perceptive networks, where the two functionalities are expected to mutually assist each other, i.e., via communication-assisted sensing and sensing-assisted communications. Finally, we identify the potential integration of ISAC with other emerging communication technologies, and their positive impacts on the future of wireless networks.**

***Index Terms*— Integrated sensing and communications, 6G, performance tradeoff, waveform design, perceptive network.**

Manuscript received August 24, 2021; revised January 29, 2022; accepted February 18, 2022. Date of publication March 17, 2022; date of current version May 18, 2022. This work was supported in part by the National Natural Science Foundation of China under Grant 62101234 and in part by the Engineering and Physical Sciences Research Council under Project EP/S028455/1. The work of Jie Xu was supported in part by the National Natural Science Foundation of China under Grant U2001208 and in part by the Science and Technology Program of Guangdong Province under Grant 2021A0505030002. The work of Stefano Buzzi was supported by the Ministero dell'Istruzione, dell'Università e della Ricerca (MIUR) Program "Dipartimenti di Eccellenza 2018–2022." *(Corresponding author: Yuanhao Cui.)*

Fan Liu is with the Department of Electronic and Electrical Engineering, Southern University of Science and Technology, Shenzhen 518055, China (e-mail: liuf6@sustech.edu.cn).

Yuanhao Cui is with the Department of Communication Engineering, Beijing University of Posts and Telecommunications, Beijing 100876, China (e-mail: cuiyuanhao@bupt.edu.cn).

Christos Masouros is with the Department of Electronic and Electrical Engineering, University College London, London WC1E 7JE, U.K. (e-mail: chris.masouros@ieee.org).

Jie Xu is with the School of Science and Engineering and the Future Network of Intelligence Institute (FNii), The Chinese University of Hong Kong, Shenzhen 518172, China (e-mail: xujie@cuhk.edu.cn).

Tony Xiao Han is with Huawei Technologies Company Ltd., Shenzhen 518129, China (e-mail: tony.hanxiao@huawei.com).

Yonina C. Eldar is with the Faculty of Mathematics and Computer Science, Weizmann Institute of Science, Rehovot 7610001, Israel (e-mail: yonina.eldar@weizmann.ac.il).

Stefano Buzzi is with the Department of Electrical and Information Engineering, University of Cassino and Southern Lazio, 03043 Cassino, Italy, also with the Consorzio Nazionale Interuniversitario per le Telecomunicazioni (CNIT), 43124 Parma, Italy, and also with GBB Wireless Research, 80143 Naples, Italy (e-mail: buzzi@unicas.it).

Color versions of one or more figures in this article are available at https://doi.org/10.1109/JSAC.2022.3156632.

Digital Object Identifier 10.1109/JSAC.2022.3156632

I. Introduction

A. Background and Motivation

NEXT-GENERATION wireless networks (such as beyond 5G (B5G) and 6G) have been envisioned as key enablers for many emerging applications. These applications demand high-quality wireless connectivity as well as highly accurate and robust sensing capability. Among many visionary assumptions about B5G/6G networks, a common theme is that *sensing* will play a more significant role than ever before [1].

While the speculative study for future wireless systems has just begun, the technological trends clearly show that we are ready to embrace the new sensing functionality in the forthcoming B5G and 6G eras. Indeed, radio sensing and communication (S&C) systems are both evolving towards higher frequency bands, larger antenna arrays, and miniaturization, thereby becoming increasingly similar in terms of hardware architectures, channel characteristics, and signal processing. This offers an exciting opportunity of implementing sensing by utilizing wireless infrastructures, such that future networks will go beyond classical communication and provide ubiquitous sensing services to measure or even to image surrounding environments. This sensing functionality and the corresponding ability of the network to collect sensory data from the environment are seen as enablers for learning and building intelligence in the future smart world, and may find extensive usage in numerous location/environment-aware scenarios. To name but a few, vehicle-to-everything, smart home, smart manufacturing, remote sensing, environmental monitoring, and human-computer interaction, as shown in Fig. 1, which will be detailed in Sec. II-A. Towards that end, there is a strong need to jointly design the S&C operations in B5G/6G networks,

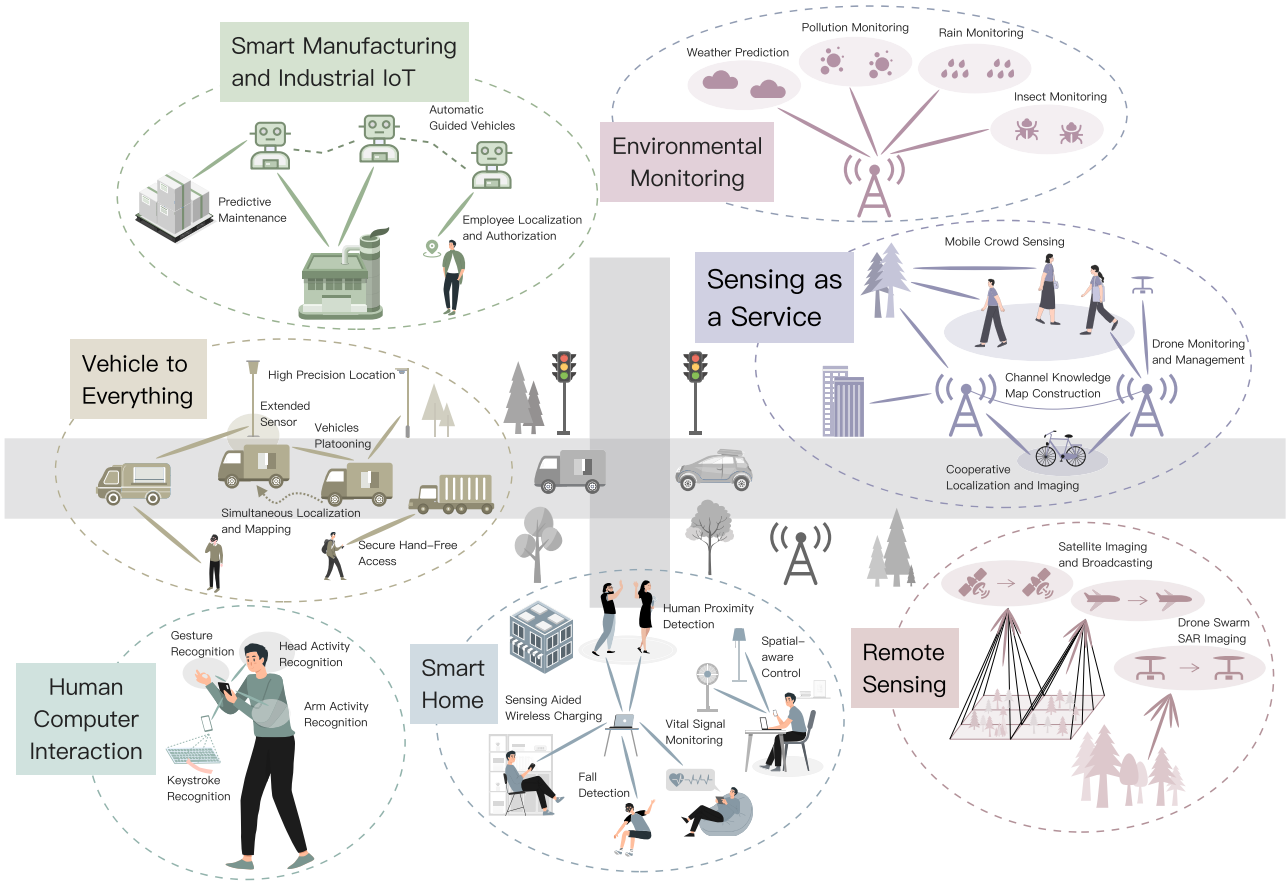

Fig. 1. ISAC technology for future wireless networks.

which motivates the recent research theme of *Integrated Sensing and Communications (ISAC)* [2].

The information processing for S&C shows a striking distinction. Sensing collects and extracts information from noisy observations, while communication focuses on transferring information via specifically tailored signals and then recovering it from a noisy environment. The ultimate goal of ISAC is to unify these two operations and to pursue direct tradeoffs between them as well as mutual performance gains. On the one hand, ISAC is expected to considerably improve spectral and energy efficiencies, while reducing both hardware and signaling costs, since it attempts to merge sensing and communication into a single system, which previously competed over various types of resources. On the other hand, ISAC also pursues a deeper integration paradigm where the two functionalities are no longer viewed as separate end-goals but are co-designed for mutual benefits, i.e., via communication-assisted sensing and sensing-assisted communication.

Although it has only recently gained growing attention from both the academia and wireless industry, ISAC has been investigated by various research communities under different names for decades, e.g., Radar-Communications (RadCom) [3], Joint Communication and Radar (JCR) [4], Joint Radar and Communication (JRC) [5], and Dual-functional Radar-Communications (DFRC) [5]. While these terminologies may have varying connotations, the sensing functionality therein mainly refers to *radar sensing*, which has long been a mainstream in ISAC. In this overview, we use ISAC as a unified term to refer to all the joint designs of radar sensing and communications.

B. Historical View of ISAC

In the earliest ISAC implementation (1960s) [6], communication information was embedded into a group of radar pulses via pulse interval modulation (PIM), where the radar was used as missile range instrumentation. Although the scheme seems fairly simple, the researchers at that time, long before the birth of modern digital communications, had already realized that certain communication functions could be implemented into military radars. In fact, as a major representative of sensing technologies, radar's development has been profoundly affected by wireless communications, and vice versa. In this subsection, we overview the development of ISAC technologies from a historical view.

1) Early Development of Radars: Early radars were driven by mechanical motors, searching for targets in the space via periodically rotating its antenna(s). Such radars, however, face several critical challenges, e.g., the lack of multi-functionality and flexibility, as well as being relatively easy to jam and interfer with. In view of this, the phased-array, a.k.a. the electronically-scanned array technique, was developed to circumvent many of these drawbacks [7]. Instead of mechanically rotating its antennas, phased-array systems generate spatial beams of signals that can be electronically steered in different directions. The first long-range early warning phased-array radar, named "FuMG 41/42 Mammut" (or "Mammut" for short), was developed by the German company GEMA during

World War II, capable of detecting targets flying at an altitude of 8 km at a range of 300 km [8].

2) How Radar and Communication Inspire Each Other: "Mammut" might be not only the first phased-array radar system, but also the first multi-antenna system, which inspired the invention of multi-input multi-output (MIMO) communication systems. In 1994, the first patent on MIMO communications was granted to Paulraj and Kailath [9], which led to the new eras of 3G, 4G, and 5G wireless networks [10], [11]. Triggered by MIMO communication techniques, colocated MIMO radar was proposed ten years later at the 2004 IEEE Radar Conference by the MIT Lincoln Lab [12]. In MIMO radar, each antenna transmits individual waveforms instead of phase-shifted counterparts of a benchmark waveform [13]. This leads to an enlarged virtual aperture, which improves the flexibility and sensing performance compared to phased-array radars. Concepts such as *degrees-of-freedom (DoFs)* and *diversity*, which were "borrowed" from MIMO communication theory, became cornerstones of the theoretical foundation of MIMO radar [14], [15].

Research on radar and communication began to merge in the early 1990s-2000s. In the 1990s, the Office of Naval Research (ONR) of the US initiated the Advanced Multifunction Radio Frequency (RF) Concept (AMRFC) Program, aiming to design integrated RF front-ends by partitioning multiple antennas into different functional modules, for e.g., radar, communications, and electronic warfare modules [16], [17], respectively. The ISAC research emerged in the 1990s-2000s was largely motivated by the AMRFC and its follow-up projects, such as the Integrated Topside (InTop) program sponsored by the ONR [18]. During that period, various ISAC schemes were proposed by the radar community, where the general idea was to embed communication information into commonly employed radar waveforms. For instance, the pioneering work of [19] proposed combining chirp signals with phase-shift keying (PSK) modulations, which was the first ISAC waveform design to exploit chirp signals. Since then, many research works have begun to focus on modulating communication data by leveraging radar waveforms (such as chirp signals and frequency/phase-coded waveforms) as carriers [20]–[23].

Orthogonal Frequency Division Multiplexing (OFDM), one of the key techniques in wireless networks including 4G and 5G, was found to be useful in radar sensing in the early 2010s [3]. In particular, in OFDM radar, the impact of random communication data can be mitigated in a straightforward manner, and the delay and Doppler processing can be decoupled, via simply performing the Fast Fourier Transform (FFT) and its inverse (IFFT) [3]. The two types of schemes based on chirp and OFDM signals, are examples of "sensing-centric" and "communication-centric" designs, respectively, as will be detailed in later sections.

In 2013, the Defense Advanced Research Projects Agency (DARPA) of the US funded another project named "Shared Spectrum Access for Radar and Communications (SSPARC)", which aimed to release part of the sub-6 GHz spectrum from the radar bands for shared use by radar and communication [24]. This led to another interesting research topic of "radar-communication coexistence (RCC)" within the framework of cognitive radio, where individual radar and communication systems are expected to coexist in the same frequency band, without unduly interfering with each other [25]–[29]. Going beyond the spectral coexistence and interference management involved in RCC, ISAC pursues a deeper integration of the two functionalities through a common infrastructure.

3) Parallel Development of Radar and Communication: In 2010, massive MIMO (mMIMO) was proposed in Marzetta's seminal work [30], which later became one of the core technologies for 5G-and-beyond networks [31]. Three years later, in 2013, NYU WIRELESS published their landmark paper on the feasibility of exploiting millimeter wave (mmWave) signals for mobile communications [32]. From then on, mmWave and mMIMO became a perfect couple that mutually aided each other. Massive MIMO antenna arrays can be made physically much smaller thanks to the reduced signal wavelength, and mmWave signals can be transmitted farther away due to the high beamforming gain provided by the mMIMO array. Nevertheless, a critical challenge preventing the large-scale deployment of mMIMO mmWave technologies is the huge hardware costs and energy consumption imposed due to the large number of required mmWave RF chains. This forced wireless researchers to rethink the RF front-end architecture of mMIMO systems. Among others, the hybrid analog-digital (HAD) structure became a viable promising solution by connecting massive antennas with a small number of RF chains through a well-designed phase-shifter (or even switch) network, thus leading to reduced costs and energy consumption [33]–[35].

Coincidentally, during the same year in which the mMIMO was born, the concept of phased-MIMO radar was proposed in [36], which attempts to achieve a balance between phased-array and MIMO radars. Note that by transmitting individual waveforms at each antenna, the MIMO radar is beneficial for increasing the DoFs at a cost of limited array gains; in contrast, by focusing its transmission power towards a target direction, the phased-array radar is advantageous in terms of achieving higher array gains but with compromised DoFs. Just like the case of HAD structure for communications, a natural idea is to design a system architecture to bridge the gap between the two, by linking multiple antennas with a limited number of RF chains via phase-shifter arrays. By doing so, phased-MIMO radar achieves a flexible tradeoff between phased-array and MIMO radars [36]. In the extreme case when there is only a single RF chain, phased-MIMO radar reduces to phased-array radar. On the other hand, if the number of RF chains equals the number of antennas, phased-MIMO radar is equivalent to MIMO radar. More recently, the advantages of leveraging mMIMO for radar detection were considered in [37], where a target was accurately sensed via a single snapshot in the presence of disturbance with unknown statistics.

Due to the above parallel, yet largely independent developments, there exist duplications in devices, such as those between phased arrays for radar and for communications, and those between MIMO radar and MIMO communications, while multi-static radars can be parallel to cooperative communications. Notably, there are also analogies between the radar and communication signal processing, including between beamforming for communications and for radar, hypothesis

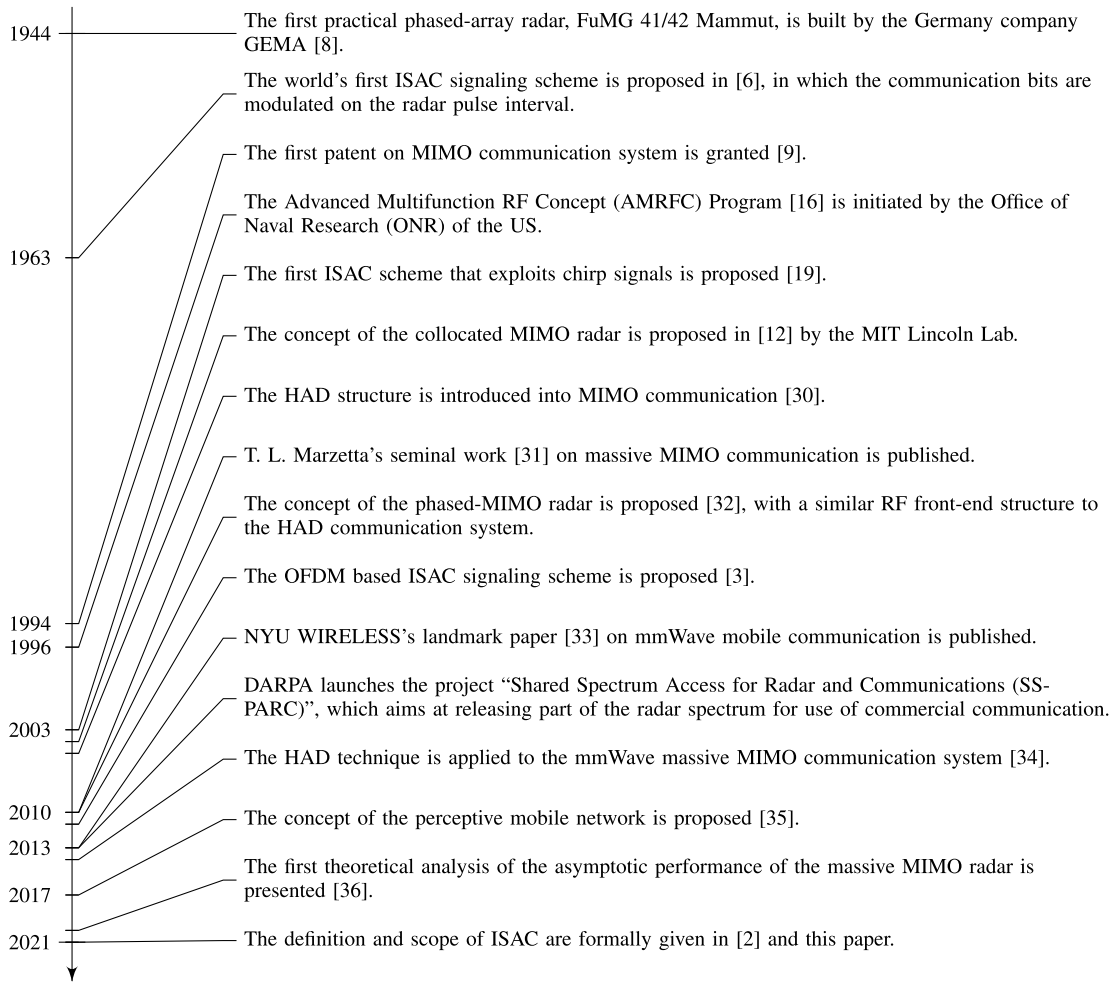

Fig. 2. Interplay between S&C - a historical view.

testing for target detection and symbol detection, mmWave communication channel estimation and radar target estimation, and others that will be detailed later.

4) Convergence of S&C: The above similarities provide a clear opportunity for the convergence of the two technologies into systems and devices, that can serve sensing and communications with a single transmission. Indeed, radar and communication technologies are so deeply interwoven that they have evolved towards the same direction over the last decade. That is, high-frequency bands and large-scale antenna arrays, which are essentially demands for more spectral and spatial resources. From the communication perspective, large bandwidth and antenna arrays boost the communication capacity and provide massive connections. On the other hand, increasing the bandwidth and number of antennas will also considerably improve radar performance in range and angular resolutions, i.e., its ability to more accurately sense more targets, or to map a complex environment.

Radar and communication also tend to be similar with respect to their channel characteristics and signal processing approaches, as their operation frequencies reach to the mmWave band [30]. In particular, the mmWave communication channel is sparse and dominated by Line of Sight (LoS), due to the fact that the available propagation paths are not as rich as those in the sub-6 GHz band. The mmWave channel model thereby aligns better to the physical geometry, which, in conjunction with mMIMO, has triggered the development of beam domain signal processing for mmWave communications [1], [38]. These techniques include but are not limited to, beam training, beam alignment, beam tracking, and beam management, all of which can be based on an HAD structure [39]. It is noteworthy that communication in the beam domain mimics the conventional radar signal processing to a certain degree, where beam training and tracking can be analogously viewed as target searching and tracking [40]. To that end, the boundary between radar and communication turns to be ambiguous, and the sensing functionality is not necessarily restricted to the radar infrastructure. Wireless infrastructures and devices can also perform sensing via radio emission and signaling, which forms the technical foundation and rationale of ISAC [2].

We summarize the historical development of S&C and the interplay of the two technologies in Fig. 2.

C. ISAC: A Paradigm Shift in Wireless Network Design

Given the above technical trends, the wireless community is now witnessing a new paradigm shift that may shape our modern information society in profound ways. While wireless sensors are already ubiquitous, they are expected to be further integrated into wireless networks in the future. More precisely, sensing functionality could be a native capability of next-generation wireless networks, not only as an auxiliary

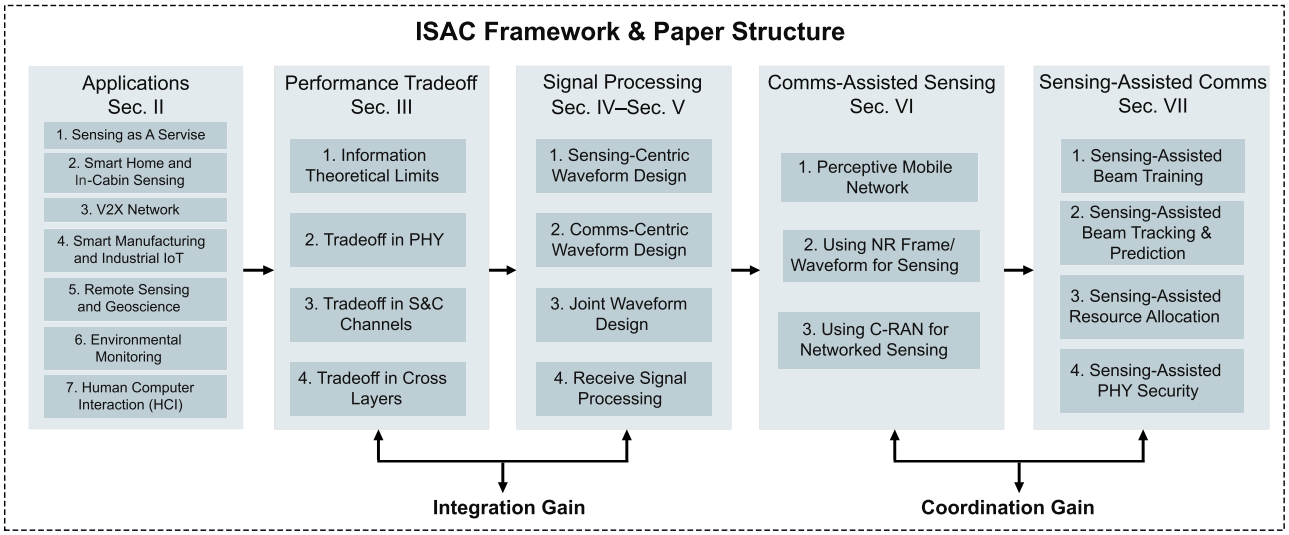

Fig. 3. Framework of ISAC technologies and structure of the paper.

method, but also as a *basic service* provided to a vast number of users [41]. This magnificent picture has provided us a huge space for imagination. Sensory data can be collected and utilized for the purpose of enhancing the communication performance, e.g., sensing aided vehicular beamforming and resource management. Moreover, equipped with sensing functionality, future mobile networks open their "eyes" and become *perceptive networks* [42], [43]. Such networks sense the surrounding environment ubiquitously, providing various services such as urban traffic monitoring, weather observation, and human activity recognition. The wealth of collected data provides the basis for building intelligence both for the ISAC network itself, and for emerging smart home, transportation, and city applications.

We define ISAC as a design methodology and corresponding enabling technologies that integrate sensing and communication functionalities to achieve efficient usage of wireless resources and to mutually benefit each other [2]. Within this definition, we further identify two potential gains of ISAC, namely, i) the *Integration Gain* attained by the shared use of wireless resources for dual purposes of S&C to alleviate duplication of transmissions, devices, and infrastructure, and ii) the *Coordination Gain* attained from the mutual assistance between S&C [2]. By foreseeing that ISAC will play a significant role in B5G/6G cellular systems, the next-generation WLAN, and the V2X network, we overview the applications, use cases, technical approaches, as well as challenges and future directions related to ISAC.

D. Structure of the Paper

In this paper, we provide a comprehensive technical overview on the theoretical framework of ISAC. We first study the use cases and industrial activities related to ISAC in Sec. II. Then, we investigate ISAC theory and performance tradeoffs between S&C in Sec. III, ranging from information theoretical limits, to physical layer (PHY) and ISAC channel tradeoffs, and to the cross-layer tradeoff. We then overview the signal processing aspects of ISAC, such as ISAC waveform design, and receive signal processing in Secs. IV and V, respectively. As a step further, we investigate the mutual assistance between S&C by discussing the design of a perceptive mobile network (PMN) in Secs. VI and VII, and by focusing on communication-assisted sensing, and sensing-assisted communications (including sensing-assisted beam training, beam tracking, generic resource allocation, and security), respectively. In Sec. VIII, we identify the potential interplay between ISAC and other emerging communication technologies. Finally, we conclude the paper in Sec. IX.

As a final remark, we point out that there have been several survey/tutorial papers on ISAC-related topics, e.g., [5] on the general designs of JRC systems, [52] on fundamental limits of ISAC, [53] on the spectral coexistence of radar and communication systems, [54] on sensing-centric DFRC designs, [44] on mmWave JRC, and [45] on DFRC for autonomous vehicles. Unlike previous works that focused on the specific elements of ISAC, this overview demonstrates the panorama of the ISAC theoretical framework, by shedding light on the basic performance tradeoffs, waveform designs, and receiver designs in ISAC systems, as well as the mutual assistance between S&C at a network level. For clarity, we provide a detailed comparison between prior works and this JSAC Special Issue overview in TABLE. I. Our hope is that this paper can provide a reference point for wireless researchers working in the area of ISAC, by offering both bird's eye view and technical details regarding state-of-the-art ISAC innovations.

II. Applications and Industrial Progress

In this section, we first extend the use case studies in [2] to further illustrate our ISAC vision for future wireless networks. In particular, we consider seven potential ISAC application scenarios followed by several key use cases for each of them. Then, we introduce recent ISAC-related industrial activities and research efforts to fill the gap between academia and industry.

A. Case Studies

1) Sensing as a Service: The recent deployment of dense cellular networks as part of 5G provides unique opportunities for sensing. Current communication infrastructures can be

TABLE I
EXISTING OVERVIEW PAPERS ON ISAC

Existing Works	Type	Applications	Fundamental Tradeoff	Signal Processing		Communications and Networking		
				Waveform Design	Transceiver Design	Resource Management	Network Architecture	Network Protocol
[3], [44]–[46]	Tutorial			√	√			
[43], [47]	Survey			√			√	√
[5], [48]	Survey	√	√	√	√			
[49]	Survey			√	√	√	√	√
[50]	Survey					√	√	√
[51]	Survey	√		√		√		√
[52]	Survey		√					
[2]	Survey	√		√	√		√	√
This Paper	Survey	√	√	√	√	√	√	√

reused for sensing with only small modifications in hardware, signaling strategy, and communication standards. In such a case, integrating sensing into current Internet-of-Things (IoT) devices and cellular networks could be performed rapidly and inexpansively, by reusing reference or synchronization signals as sensing waveforms. As a step forward, sensing and communication functionalities can be fully integrated into all radio emissions [55], where both pilot and payload signals can be exploited for sensing. This kind of ISAC strategy is able to achieve better integration and coordination gains; however, more difficulties would be raised in terms of receiver architectures and signaling designs, which will be detailed in Secs. IV, V, and VI.

With the use of ISAC technologies, the role of existing cellular networks will shift to a ubiquitously deployed large-scale sensor network, namely a perceptive network [43], which will trigger a variety of novel applications for the current communication industry. We provide some examples below.

a) Enhanced localization and tracking: Localization has been a key feature for the standardization, implementation, and exploitation of existing cellular networks, from 1G to the future 6G [56]. Due to the low range and angle resolutions that are caused by bandwidth and antenna limitations, respectively, most current cellular networks (e.g., 4G and 5G) only provide measurement data with meter-level accuracy to assist in global navigation satellite systems (GNSS). According to the key parameter indicators (KPIs) of 5G New Radio (NR) Release 17 [57], the highest required localization accuracies are 0.2 m/1 m horizontally/vertically in industrial IoT applications, which are unable to meet the requirement of future applications. Particularly, location resolution requirements for pinpointing the positions of users are higher in indoor environments than that in outdoor environments, e.g., indoor human activity recognition [58] ($\sim$1 cm), autonomous robots and manufacturing [59] ($\sim$5 mm). On the other hand, current wireless localization technologies are mostly implemented in a device-based manner, where wireless equipment (e.g., a smartphone) is attached to the locating object by computing its location through signal interactions and geometrical relationships with other deployed wireless equipment (e.g. a Wi-Fi access point or a base station (BS)). However, this device-based approach limits the choice of locating objects and does not generalize to diverse scenarios.

Benefiting from additional Doppler processing and the exploitation of useful information from multi-path components, ISAC enabled cellular networks are able to achieve higher localization accuracy compared to current localization technologies. On top of that, a cellular network with sensing functionality is not limited to just pinpointing the location of a certain object with a smartphone, but also suits broader scenarios that extract spectroscopic and geometric information from the surrounding environment.

b) Area imaging: RF imaging technology generates high-resolution, day-and-night, and weather-independent images for a multitude of applications ranging from environmental monitoring, climate change research, and security-related applications [60]. Importantly, compared to camera based imaging, RF imaging is less intrusive and allows focusing on the intended information without revealing sensitive information in the surrounding environment. Due to the limited bandwidth used in past-generation cellular systems, the range resolution is roughly at the meter-level which does not support high-resolution services. Thanks to the deployment of mmWave and mMIMO technologies, future BSs could possibly pursue high range and angle resolutions by cooperatively sensing and imaging a specified area. In such a case, a radio access network (RAN) acts as a distributed MIMO radar as elaborated in Sec. VI. Consequently, future cellular networks and user equipment (UE) could "see" the surrounding environment, which would further support high-layer applications such as digital twins, virtual reality, and more [61]. Furthermore, with significantly improved imaging resolutions due to the use of higher frequencies, future cellular networks would also support spectrogram-related and spatial/location-aware services. Finally, cellular BSs and UEs with imaging abilities could provide additional commercial value to traditional telecommunication carriers as a new billing service for civilians.

c) Drone monitoring and management: In recent years, enthusiasm for the use of UAVs in civilian and commercial applications has skyrocketed [62]. However, the civilization of drones is posing new regulatory and management headaches. As aerial platforms that can fly over various terrains, drones have the potential to be employed in no-fly zones and in illegal activities, e.g., unauthorized reconnaissance, and the surveillance of objects and individuals. With merits of low altitudes, small sizes and varying shapes, such non-cooperative UAVs always operate below the LoS of current airborne radars, and are difficult to detect with other surveillance technologies, such as video or thermal sensors. The use of sensing with existing cellular networks would not only provide

an affordable solution to monitor non-cooperative UAVs in low-altitude airspace, but also act as an RAN to manage and control cooperative UAVs with cellular connections, and assist their navigation in swarms. As a result, the ISAC cellular network could develop into a drone infrastructure that provides drone monitoring and management services to secure future low-altitude airspace applications.

2) Smart Home and In-Cabin Sensing: Currently, in most indoor applications, such as in-home and in-cabin scenarios, electronic devices are expected to be interactive and intelligent to fit out comfortable, convenient and safe living conditions. Aiming for this purpose, smart IoT devices should be able to understand the residents both physically and physiologically. With the merits of privacy-preserving, unobtrusive and ubiquitous, standardized wireless signals, e.g., WiFi, LoRa, and 5G NR, have been widely employed to figure out what is occurring in surrounding indoor scenarios [63]–[66].

Recently, the ISAC-enabled IoT has shown great potential in daily activity recognition, daily health care, home security, driver attention monitoring, etc., in which several of them have been implemented into household products [67]. A few of these are described as follows.

a) Human activity recognition: Activity recognition is essential to both humanity and computer science, since it records people's behaviors with data that allow computing systems to monitor, analyze, and assist their daily lives. Over-the-air signals are affected by both static and moving objects, as well as by dynamic human activities. Therefore, amplitude/phase variations in wireless signals could be employed to detect or to recognize human presence/proximity/falls/sleep/breathing/daily activities [68], by extracting range, Doppler, or micro-Doppler features while moving indoors. Moreover, if the sensing resolution is high enough, fatigue driving can be recognized by identifying the driver's blink rate. By integrating sensing functionality into current commercial wireless devices, e.g., Wi-Fi devices, these technologies become able to detect and recognize residents' activities to support a smart and human-centric living environment.

b) Spatial-aware computing: Further exploitation of the geometric relationships among massive IoT devices also potentially enhances residents' well-being and living comfort, which serve as the ultimate goals of spatial-aware computing techniques. The ubiquity of wireless signals with high spatial resolution represents an opportunity to gather all spatial relationships between indoor devices [74], which may be densely and temporarily deployed in a cramped space. For instance, a smartphone with centimeter-level sensing precision is able to pinpoint the location of any electronic device with an angle resolution reaching $\pm 3^{\circ}$. Therefore, by directing the smartphone towards a given device, they can connect and control each other automatically [75].

In addition, knowing where the devices are in space and time promises a deeper understanding of neighbors, networks, and the environment. By considering the spatial relationships between moving devices and access points rather than (signal-to-interference-plus-noise ratio) SINR-only considerations, initial access or cross-network handover operations may be expedited, as will be detailed in Sec. VII-C. Furthermore, spatial-aware computing promises to coordinate household products deployed in a distributed manner to jointly analyze movements, understand mobility patterns, and eventually support augmented virtual reality applications.

3) Vehicle to Everything (V2X): Autonomous vehicles promise the possibility of fundamentally changing the transportation industry, with increases in both highway capacity and traffic flow, less fuel consumption and pollution, and hopefully fewer accidents [76]. To achieve this, vehicles are equipped with communication transceivers as well as various sensors, with the aim of simultaneously extracting environmental information and exchanging information with roadside units (RSUs), other vehicles, or even pedestrians [77]. The combination of sensing and communications has proven to be a viable path, with a reduced number of antennas, a smaller system size, and less weight and power consumption; this combination alleviates electromagnetic compatibility and spectrum congestion concerns [76]. For example, ISAC-aided V2X communications could provide environmental information to support fast vehicle platooning, secure and seamless access, and simultaneous localization and mapping (SLAM). RSU networks can enable sensing services to extend the sensing range of a passing vehicle beyond its own LoS and field-of-view (FoV). We briefly discuss two representative use cases.

a) Vehicle platooning: The presence of autonomous vehicles in tightly spaced, computer-controlled platoons will lead to increased highway capacity and increased passenger comfort. Current vehicle platooning schemes are mostly based on cooperative adaptive cruise control (CACC) through a conventional leader-follower framework [78], [79], which requires multi-hop Vehicle-to-Vehicle (V2V) communications to transfer the state information of each vehicle across all platooned vehicles. However, the high latency of multi-hop communications leads to the out-of-sync problem regarding the situational information of the platooned vehicles, particularly when the platoon is very long and highly dynamic. In this case, platooned vehicles that are unaware of situational changes increase the control risk. RSU, as vehicle infrastructure, offers a more reliable approach to form and maintain a vehicle platoon, as it serves multiple vehicles simultaneously [80], [81]. More importantly, the wireless sensing functionality equipped on the RSU provides an alternative way to acquire vehicles' states in a fast and inexpensive manner, which in turn facilitates the Vehicle-to-Infrastructure (V2I) communications and platooning by significantly reducing the beam training overhead and latency [82], [83], as will be detailed in Sec. VII.

b) Simultaneous localization and mapping (SLAM): Joint localization and mapping can provide vehicles with situational awareness without the need for high-precision maps [84]. Based on the environmental data extracted from various sensors, a vehicle could obtain its current location and its spatial relationships with the objects in a local area, and accordingly perform navigation and path planning. Most previous SLAM studies relied on camera or LiDAR sensors, overlooking the fact that channel propagation characteristics could be utilized to construct 2D or 3D maps of the surrounding environment. In this sense, ISAC-based radio sensing has the potential to become a key component for integration into current SLAM solutions, by endowing communication devices with sensing functionalities while requiring minimal hardware/software modifications [85], [86]. The ISAC receive signal processing

pipeline for SLAM poses a number of challenges, such as the separation of sensing and communication signals, and the reconstruction of high-quality point clouds.

4) Smart Manufacturing and Industrial IoT: The penetration of wireless networks in the hard industries such as construction, car manufacturing, and product lines has given rise to the revolution of Industrial IoT [87], showing orders-of-magnitude increases in automation and production efficiency. Such scenarios often involve network nodes and robots that coordinate to carry out complex and often delicate tasks that require connectivity in large numbers and impose severe latency limitations.

ISAC offers paramount advantages in such smart factory scenarios, where in addition to ultra-fast, low-latency communications that are typical for such scenarios [88], the integration of the sensing functionality enables the factory nodes and robots to seamlessly navigate, coordinate, and map the environment and potentially cut signaling overheads dedicated to such functionalities. The desired technology here involves elements of the above cases such as swarm navigation, platooning, and imaging, but these tasks are completed under the important constraints of ultra reliability, ultra low latency and massive connectivity, which are often encountered in smart factory scenarios [87].

5) Remote Sensing and Geoscience: Radar systems carried by satellites or planes have been widely applied in geoscience and remote sensing to provide high-resolution, all-weather, and day-and-night imaging. Today, more than 15 spaceborne radar systems are operated for innumerous applications, ranging from environmental and Earth system monitoring, change detection, 4D mapping (space and time), and security-related applications to planetary exploration [60]. All these radars are operated in the synthetic aperture radar (SAR) mode, mostly by using chirp or OFDM waveforms. Communication data can be embedded into these waveforms, as will be detailed in Sec. IV, enabling these radar infrastructures to broadcast low-speed data streams to their imaging areas, or provide covert communication services in a battlefield.

Being able to rapidly deploy and linger over a disaster area for hours, drones provide essential emergency response capabilities for addressing many natural disasters. Such response tasks include damage assessment, search-and-rescue operations [89], and emergency communication for disaster areas. To accomplish these tasks, drones should carry various heavy and energy-consuming payloads, including airborne imaging radar systems, communication BSs, and thermal sensors, severely limiting drones' endurance. Benefiting from ISAC, a radio sensing system and an emergency communication system can be merged to achieve higher energy and hardware efficiency by exploiting the integration gain.

More interestingly, a swarm of drones or satellites could exchange sensed information, and therefore cooperatively act as a mobile antenna array by forming a large virtual aperture. In such a case, drone swarm based SAR algorithms may be exploited to implement a high-resolution, low-altitude airborne imaging system.

6) Environmental Monitoring: Environmental information such as humidity and particle concentrations can be indicated by the propagation characteristics of transmitted wireless signals [72]. Wireless signals operating at different frequencies are aware of different environmental changes. For instance, high-frequency mmWave signals are sensitive to humidity because they are closer to the water vapor absorption bands. By analyzing the path-loss data of city-wide mmWave links between BSs and smart phones, it is possible to monitor rainfall or other variations in the atmospheric environment, such as water vapor, air pollutants, and insects. As such, a cellular network with a sensing function serves as a built-in real-time monitoring facility, and therefore, can be utilized as a widely-distributed large-scale atmospheric observation network. Moreover, with the continuous exploitation of higher frequencies, future urban cellular networks could also monitor locusts or other insects, serving as an insect observation network in urban areas.

7) Human Computer Interaction (HCI): An object's characteristics and dynamics can be captured from the time/frequency/Doppler variations in the reflected signal. Therefore, gesture interaction detection via wireless signals is a promising HCI technology. For instance, a virtual keyboard that projects onto a desk could be constructed by recognizing the keystroke gestures at the corresponding position. Another well-known example is the Soli project developed by Google [73], which demonstrated radio sensing with HCI. Based on advanced signal processing via a broad antenna beam, Soli delivers an extremely high temporal resolution instead of focusing on high spatial resolution, i.e., its frame rates range from 100 to 10,000 frames per second, such that high dynamic gesture recognition is feasible. Benefiting from the integration of sensing capability into communication systems of smartphone and other UEs, gesture-based touchless interaction may serve as the harbinger of new HCI applications, which may play key roles in the post COVID-19 era. The main challenges are how to improve micro-Doppler recognition accuracy and how to design a signal processing strategy that provides high temporal resolution.

We summarize the above case studies and the required KPIs for different ISAC use cases in TABLE II, where supplementary information on other potential cases within different scenarios is also provided.

B. Industry Progress and Standardization

As initial research efforts towards 6G are well-underway, ISAC has drawn significant attention from major industrial companies. Recently, Ericsson [90], NTT DOCOMO [91], ZTE [92], China Mobile, China Unicom [92], Intel [93], and Huawei [61] all suggested that sensing will play an important role in their 6G white papers and Wi-Fi 7 visions. In particular, in November 2020 Huawei identified harmonized sensing and communication as one of the three new scenarios in 5.5G (a.k.a. B5G) [94]. The main focus of this new technology is to exploit sensing capabilities of the existing mMIMO BSs, and to support future UAVs and automotive vehicles. Six months later, Huawei further envisioned that 6G new air interface would support simultaneous wireless communication and sensing signaling [61]. This will allow ISAC enabled cellular networks to "see" the physical world, which is one of the unique capabilities of 6G. Nokia has also launched a unified mmWave system as a blueprint for future indoor ISAC technology [95].

TABLE II
CASE STUDIES AND KEY PERFORMANCE INDICATORS

Application	Case	Key Performance Indicators							mmWave
		Max. Range (m)	Max.Velocity (m/s)	Range Resolution	Doppler Resolution	Temporal Resolution	Angular Resolution	Data Rate Per User (Avg. / Peak.)	
Sensing as a Service [69]	• Drone Monitoring and Management	500	40	◉	◉	/	○	Low	/
	• Localization and Tracking in Cellular Network	300	10	◉	●	/	⊙	Low/Very High	/
	• Human Authorization and Identification	300	5	◉	●	/	⊙	Low/Very High	/
	• Human Counting	200	5	◉	●	●	⊙	Low/Very High	/
	• Area Imaging	200	/	⊙	●	●	⊙	Low/Very High	√
	• Mobile Crowd Sensing	300	5	◉	●	/	⊙	Low/Very High	/
	• Channel Knowledge Map Construction	300	5	◉	●	/	⊙	Low/Very High	/
	• Passive Sensing Network	300	30	◉	/	/	●	Low/Very High	/
Smart Home and In-Cabin Sensing [70]	• Human Presence Detection	20	2	◉	⊙	⊙	⊙	High	/
	• Human Proximity Detection	20	4	◉	⊙	●	⊙	High	/
	• Fall Detection	10	3	◉	⊙	◉	⊙	High	/
	• Sleep Monitoring	1	2	◉	⊙	●	◉	High	/
	• Daily Activity Recognition	10	4	◉	⊙	●	◉	High	/
	• Breathing/Heart Rate Estimation	1	2	◉	⊙	⊙	◉	High	/
	• Intruder Detection	20	5	◉	⊙	◉	◉	High	/
	• Location-aware Control	20	3	◉	⊙	/	◉	High	/
	• Sensing Aided Wireless Charging	5	4	◉	⊙	◉	○	High	√
	• Passenger Monitoring	2	/	○	⊙	○	⊙	High	√
	• Driver Attention Monitoring	1	/	○	○	○	○	High	√
Vehicle to Everything [69]	• Raw Data Exchange and High Precision Location	300	30	●	/	/	⊙	High	/
	• Secure Hand-Free Access	300	/	◉	●	/	⊙	Low/Very High	/
	• Vehicle Platooning	100	30	⊙	◉	/	○	High	/
	• Simultaneous Localization and Mapping	300	30	◉	●	/	⊙	Low/Very High	/
	• Extended Sensor	300	30	◉	●	/	○	Low	/
Smart Manufacturing and Industrial IoT [59]	• Employee Localization and Authorization	1000	5	●	◉	/	◉	Low/Very High	/
	• Manufacture Defect Analysis	20	/	●	/	⊙	◉	High	√
	• Automatic Guided Vehicles	500	5	◉	◉	/	⊙	Low	√
	• Predictive Maintenance	100	/	●	/	◉	◉	Low/Very High	√
Remote Sensing and Geoscience [71]	• Drone Swarm SAR Imaging	1000	40	◉	/	/	⊙	Low	√
	• Satellite Imaging and Broadcasting	10000	/	●	/	/	/	Low	√
Environmental Monitoring [72]	• Weather Prediction	500	/	◉	/	/	/	Low/Very High	√
	• Pollution Monitoring	200	/	⊙	/	/	/	Low/Very High	√
	• Rain Monitoring	200	/	◉	/	/	/	Low/Very High	√
	• Insect Monitoring	200	/	◉	/	/	/	Low/Very High	√
Human Computer Interaction [73]	• Gesture Recognition	1	20	○	●	●	/	Low/Very High	√
	• Keystroke Recognition	1	20	○	●	●	/	Low/Very High	√
	• Head Activity Recognition	>2	20	○	◉	◉	/	Low/Very High	√
	• Arm Activity Recognition	>2	10	○	◉	◉	/	Low/Very High	/

(*) In order to indicate different requirements of Range/Doppler/Temporal/Angular resolutions, we artificially categorize these KPI values into four levels, e.g. ○: very low, ⊙: low, ◉: high, ●: very high.
(*) The symbol "/" represents that there are few requirements on this scenario.
(*) KPI specs sources: [59], [69]–[73].

The IEEE Standardization Association (SA) and the Third-Generation Partnership Project (3GPP) have also devoted substantial efforts toward the development of ISAC-related specifications. In particular, IEEE 802.11 formed the WLAN Sensing Topic Interest Group and Study Group in 2019, and created a new official Task Group for IEEE 802.11bf [96] in 2020,[1] intending to define appropriate modifications to existing Wi-Fi standards that could enhance sensing capabilities of Wi-Fi through 802.11-compliant waveforms. On the other hand, in the NR Release 16 specifications, the redefined positioning reference signal (PRS) obtained a more regular signal structure and a much larger bandwidth, allowing for easier signal correlation and parameter estimation (e.g., by estimating the time of arrival (ToA)). Moreover, the measurements of PRSs received from multiple distinct BSs can be shared and fused at either the BS side or the UE side, thereby further enhancing the parameter estimation accuracy to support advanced sensing. Furthermore, to foster research and innovation with respect to the study, design, and development of ISAC, the IEEE Communications Society (ComSoc) established an Emerging Technology Initiative (ETI)[2] and the IEEE Signal Processing Society (SPS) created a Technical Working Group (TWG),[3] both of which focus on ISAC.

[1]https://www.ieee802.org/11/Reports/tgbf_update.htm

III. PERFORMANCE TRADEOFFS IN ISAC

In this section, we identify performance tradeoffs in ISAC, including tradeoffs regarding the information-theoretical limits, PHY performance, propagation channels, and cross-layer metrics. We first introduce basic S&C performance metrics, and then provide some insights into their connections and tradeoffs.

A. S&C Performance Metrics

1) Sensing Performance Metrics: Sensing tasks can be roughly classified into three categories, *detection*, *estimation*, and *recognition*, which are all conducted based on collected

[2]https://isac.committees.comsoc.org/

[3]https://signalprocessingsociety.org/community-involvement/integrated-sensing-and-communication-technical-working-group/integrated

signals/data with respect to the sensed objects [68]. While these terminologies can have varying connotations under different scenarios, and may be performed over different layers, we attempt to define them as follows.

1) **Detection:** Detection refers to making binary/multiple decisions about the state of a sensed object, given noisy and/or interfered observations. Such states typically include: the presence/absence of a target (PHY), and the occurrence of an event (application layer), e.g., motion detection, which can be modeled as binary or multi-hypothesis testing problems. Taking the binary detection problem as an example, we choose from two hypotheses $\mathcal{H}_1$ and $\mathcal{H}_0$, e.g., the target is present or absent, based on the observed signals. Detection metrics include detection probability, which is defined as the probability that $\mathcal{H}_1$ holds true and the detector chooses $\mathcal{H}_1$, and the false-alarm probability, which signifies that $\mathcal{H}_0$ holds true but the detector chooses $\mathcal{H}_1$ [97].
2) **Estimation:** Estimation refers to the extraction of useful parameters of the sensed object from noisy and/or interfered observations. This may include estimating the distance/velocity/angle/quantity/size of the target(s). Estimation performance can be measured by the mean squared error (MSE) and Cramér-Rao Bound (CRB) [98]. In particular, MSE is defined as the mean of the squared error between the true value of a parameter θ and its estimate $\hat{\theta}$. CRB is a lower bound on the variance of any unbiased estimator over θ, which is defined as the inverse of the Fisher Information (FI). FI is the expectation of the curvature (negative second derivative) of the likelihood function with respect to θ, which measures the "sharpness" or the accuracy of the estimator.
3) **Recognition:** Recognition refers to understanding *what* the sensed object is based on noisy and/or interfered observations. This may include target recognition, and human activity/event recognition. Recognition is typically defined as a classification task at the application layer, whose performance is evaluated by the recognition accuracy metric [99].

For sensing tasks over the PHY, detection probability, false-alarm probability, MSE, and CRB are of particular interest. For higher-layer applications, recognition accuracy is at the core of learning based schemes. More advanced sensing tasks, e.g., imaging, require multiple detection and estimation operations to be performed over a complex target.

2) Communication Performance Metrics: Similar to sensing, communication tasks can also be built on different layers. In this section, we consider PHY performance metrics for communications. In general, communication performance can be evaluated from two aspects, i.e., efficiency and reliability, which have the following definitions.

1) **Efficiency:** The successful transmission of the information comes at the cost of wireless resources, e.g., spectrum, spatial, and energy resources. Accordingly, efficiency is a metric that evaluates how much information is successfully delivered from the transmitter to the receiver, given limited available resources [100], [101]. Spectral efficiency and energy efficiency are widely adopted, which are defined as the achievable rate per unit bandwidth/energy, with units of bit/s/Hz or bits/channel use, and bit/s/Joule, respectively. Moreover, channel capacity, coverage, and the maximum number of served users are also important efficiency metrics.
2) **Reliability:** A communication system should have resilience with respect to harmful factors within the communication channel. In other words, we expect communication systems to operate in the presence of noise, interference, and fading effects. Accordingly, reliability measures the ability of a communication system to reduce or even to correct erroneous information bits [100], [101]. Commonly used metrics include the outage probability, bit error rate (BER), symbol error rate (SER) and frame error rate (FER).

In addition to the above, we remark that the SINR plays a key role in that it links to both S&C metrics. While the definition of the SINR may depend on the specific S&C scenario, in most circumstances, an increase in the SINR leads to improved performance for both functionalities. For instance, the detection probability for sensing and the achievable rate for communication both improve as the SINR increases.

B. Information-Theoretical Limits

Information theory is critical for evaluating the fundamental limits of wireless communication systems [102]. However, the performance of sensing, from information theoretical perspectives, is not as clearly defined as that of communications. Therefore, new analytical techniques are needed to evaluate ISAC systems [52]. In this section, we briefly overview the research efforts towards revealing the information-theoretical limits of ISAC. Specifically, we show how to connect the fundamental S&C metrics and achieve their Pareto-optimal boundary by leveraging the information theory.

The most well-known information theoretical result related to ISAC comes from the seminal paper by Guo *et al.* [103], which connected the input-output mutual information, a communication metric, and the minimum mean squared error (MMSE), a sensing metric, via an elegant formula. Given a real-valued Gaussian channel and denoting its received signal-to-noise ratio as snr, the mutual information $I(\mathrm{snr})$ and the MMSE $MMSE(\mathrm{snr})$ of the channel input and output are related by

$$\frac{d}{d\,\mathrm{snr}} I(\mathrm{snr}) = \frac{1}{2} MMSE(\mathrm{snr}). \tag{1}$$

That is, the derivative of the mutual information with respect to snr is equal to half of the MMSE regardless of the input statistics. Eq. (1) highlights a connection between information theory and estimation theory, which play fundamental roles in communication and sensing, respectively. It can be observed from (1) that, while a Gaussian input maximizes the mutual information for Gaussian channels, it also maximizes the MMSE, making it the most favorable for communication yet the least favorable for sensing.

More relevant to ISAC, the classical capacity-distortion tradeoff was first unveiled in [104] by Chiang and Cover. The basic scenario is to consider a communication problem with channel state information [105]–[108]. As shown in Fig. 4 (a), the sender wishes to transmit both pure information, i.e., an

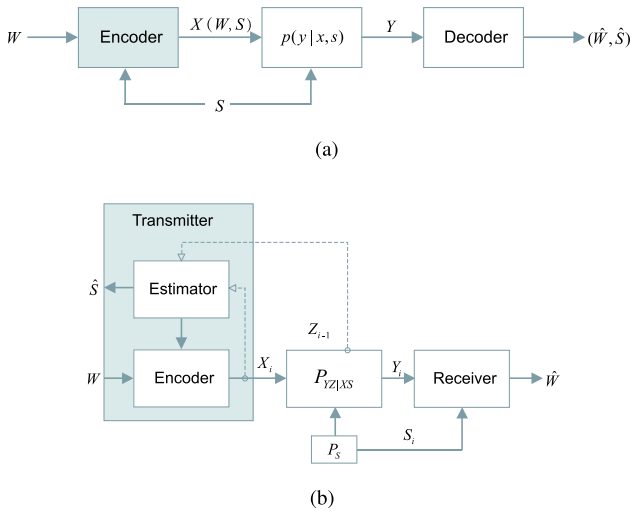

Fig. 4. (a) Information transmission over a state-dependent channel; (b) mono-static ISAC channel: information transmission over a state-dependent channel with generalized feedback.

index $W \in \left\{1, 2, \ldots, 2^{nR}\right\}$, and description $\hat{S}$ of the channel state S to the receiver. Given the information index W and state S, the sender transmits a code $X\left(W, S\right)$ to the receiver, with a rate of R. The receiver observes

$$Y \sim \prod\nolimits_{i=1}^{n} p\left(y_i \left| x_i, s_i \right.\right). \tag{2}$$

The receiver then decodes the information from Y as $\hat{W}\left(Y\right) \in \left\{1, 2, \ldots, 2^{nR}\right\}$, and estimates the state as $\hat{S}\left(Y\right)$. The decoding error probability and state estimation error are defined as

$$\begin{aligned} \mathcal{P}_e^{(n)} &= \frac{1}{2^{nR}} \sum\nolimits_{i=1}^{2^{nR}} \Pr\left\{\hat{W} \neq i \left| W = i \right.\right\}, \\ D &= \mathbb{E}\left\{d\left(S, \hat{S}\right)\right\}, \end{aligned} \tag{3}$$

where $d\left(S, \hat{S}\right)$ is a distortion measure between S and $\hat{S}$. We say that a rate-distortion pair (R, D) is *achievable* if there exists a sequence of $\left(2^{nR}, n\right)$ codes $X\left(W, S\right)$, such that [106]

$$\mathbb{E}\left\{d\left(S, \hat{S}\right)\right\} \leq D, \quad \mathcal{P}_e^{(n)} \to 0, \ n \to \infty. \tag{4}$$

If the distortion function is chosen as the squared state estimation error, then the estimation MSE can be given as

$$\mathbb{E}\left\{d\left(S, \hat{S}\right)\right\} = \frac{1}{n}\mathbb{E}\left\|S - \hat{S}\left(Y\right)\right\|^2. \tag{5}$$

By leveraging the above metric for state estimation, and taking the state-depenedent Gaussian channel $Y = X\left(W, S\right) + S + N$, where $S_i \sim \mathcal{N}\left(0, Q_S\right), N_i \sim \mathcal{N}\left(0, Q_N\right)$, as an example, the Pareto-optimal boundray of the (R, D) pair for $\gamma \in [0, 1]$ is [106]

$$\begin{aligned} (R, D) = \Bigg(& \frac{1}{2}\log\left(1 + \frac{\gamma P}{Q_N}\right), \\ & Q_S \frac{\left(\gamma P + Q_N\right)}{\left(\sqrt{Q_S} + \sqrt{\left(1-\gamma\right)P}\right)^2 + \gamma P + Q_N} \Bigg), \end{aligned} \tag{6}$$

where $\frac{1}{n}\mathbb{E}\left\{\sum_{i=1}^{n} X_i^2\left(W, S\right)\right\} \leq P$ is an expected power constraint on X. It can be shown that the above tradeoff is achieved by the power-sharing strategy, which splits the transmit power into γP and $\left(1-\gamma\right)P$, for transmitting the pure information and a scaled signal of the channel state, respectively [106]. That is, the power resource is shared between pure information delivering and channel state estimation to achieve the optimal tradeoff. This scheme will be analyzed again from the perspective of PHY tradeoff in the next subsection.

The above rate-distortion tradeoff fails to capture an important feature of typical ISAC scenarios, i.e., the estimation of a target from a *reflected echo*. Indeed, in mono-static radar, it is impossible for the transmitter to know the target channel state *a priori*; otherwise, there is no need to sense the target. The work of Kobayashi and Caire proposed to model the target return as a delayed feedback channel [109]. As shown in Fig. 4 (b), the channel state is available at the receiver, but is unknown to the transmitter. During each transmission, the transmitter reconstructs the state estimate $\hat{S}$ from the delayed feedback output $Z \in \mathcal{Z}$ via an estimator. By picking a message W, the transmitter sends a symbol $X \in \mathcal{X}$ via an encoder based on both W and $\hat{S}$. The channel outputs $Y \in \mathcal{Y}$ to the receiver, and feeds back a state to the transmitter. The joint distribution of $SXYZ\hat{S}$ can be expressed by

$$\begin{aligned} & P_{SXYZ\hat{S}}\left(s, x, y, z, \hat{s}\right) \\ & \quad = P_S\left(s\right) P_X\left(x\right) P_{YZ|XS}\left(y, z \left| x, s\right.\right) P_{\hat{S}\left|XZ\right.}\left(\hat{s} \left| x, z\right.\right). \end{aligned} \tag{7}$$

Given a distortion D, the capacity-distortion tradeoff $C\left(D\right)$ is defined as the supremum of the rate R, such that the pair of (R, D) is achievable.

With the above model at hand, by imposing an average power constraint, the capacity-distortion tradeoff is [109]

$$\begin{aligned} C\left(D\right) = \max_{P_X:\, \frac{1}{n}\sum_{i=1}^{n}\mathbb{E}\left\{X_i^2\right\} \leq P} & I\left(X; Y \left| S\right.\right) \\ \text{s.t. } & \mathbb{E}\left\{d\left(S, \hat{S}\right)\right\} \leq D, \end{aligned} \tag{8}$$

where P_X denotes the distribution of the channel input X. The above problem is convex in general, and can be solved via a modified Blahut-Arimoto algorithm. As a step further, multi-user channels are considered under this framework, where the inner and outer bounds of the capacity-distortion region are investigated in terms of both multiple access and broadcast channels. We refer the reader to [109]–[111] for more details.

C. Tradeoff in PHY

When wireless resources are shared between the S&C functionalities, their integration into a common infrastructure allows for the design of scalable tradeoffs between, often contradictory, S&C objectives and metrics. In general, PHY tradeoffs can be analyzed by investigating the relationship between the native performance metrics of S&C, which follows exactly the spirit of the information theoretical framework introduced above. Alternatively, one may also define a new information metric for sensing, which is more convenient to tradeoff with conventional communication metrics. In what follows, we overview recent works focusing on both aspects.

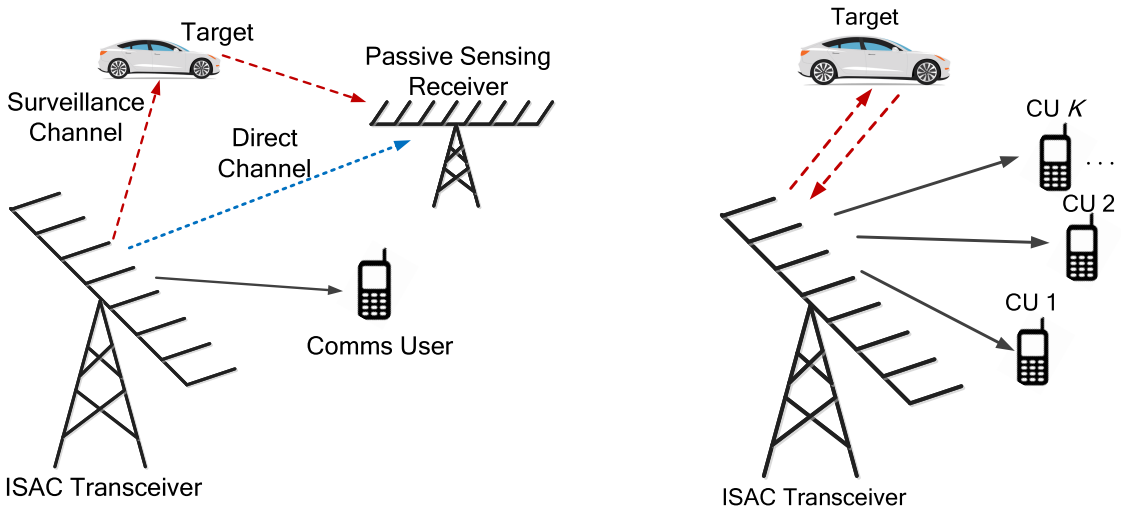

Fig. 5. (a) Joint passive sensing and communication; (b) joint active sensing and multi-user communication.

1) Tradeoff Between Native S&C Metrics: PHY sensing performance is typically measured by the detection probability and the MSE. In the event that a closed-form expression for the MSE is not obtainable, the CRB, which represents the lower bound on the variance of all the unbiased estimators, is an alternative option, as it can often be expressed analytically.

a) Detection vs. communication: We consider a tradeoff example between the detection probability and the achievable communication rate, which was proposed in [112] for a joint communication and passive radar system. As shown in Fig. 5 (a), an ISAC transmitter emits a sensing waveform $s_R(t)$ to detect targets using a portion of its total power budget, and emits a communication waveform $s_C(t)$ using another portion. The two signals are scheduled over orthogonal (time-frequency) resources such that they do not interfere with each other. The sensing receiver (SR) receives $s_R(t)$ from both the direct channel and the surveillance channel, and wishes to detect the presence of a target in the latter. On the other hand, the communication user (CU) receives $s_C(t)$, which contains useful information. The problem is then to optimally allocate power to the S&C functionalities, such that the detection performance can be optimized while ensuring a minimum communication rate. This can be formulated as the following optimization problem

$$\max_{P_R,P_C} \ \mathcal{P}_D \quad \text{s.t. } R \geq R_{th},\ P_R + P_C = P_T, \tag{9}$$

where P_R and P_C represent the transmit power of the radar and communication signals, respectively, and P_T is the total power budget. $\mathcal{P}_D$ denotes the radar detection probability, and $R = \log(1 + P_C\gamma_c)$ is the achievable rate, with γ_c being the communication channel gain normalized by the noise variance. Finally, R_{th} is a rate threshold.

In a passive radar system, the SR detects the target of interest in the surveillance channel by correlating the reflected signal with the reference signal received from the direct channel [113]. By sampling the received signals as L time-domain samples, the detection problem can be modeled as the following binary hypothesis testing problem (ignoring clutter):

$$\mathcal{H}_0: \begin{cases} \mathbf{y}_d = \gamma_d \mathbf{G}_d \mathbf{s}_R + \mathbf{n}_d \\ \mathbf{y}_s = \mathbf{n}_s, \end{cases} \quad \mathcal{H}_1: \begin{cases} \mathbf{y}_d = \gamma_d \mathbf{G}_d \mathbf{s}_R + \mathbf{n}_d \\ \mathbf{y}_s = \gamma_s \mathbf{G}_s \mathbf{s}_R + \mathbf{n}_s, \end{cases} \tag{10}$$

where $\mathcal{H}_0$ and $\mathcal{H}_1$ stand for the hypotheses of target absent (null hypothesis) and target present, $\mathbf{y}_d$ and $\mathbf{y}_s$ are the signals received from the direct and surveillance channels, abd $\mathbf{G}_d$ and $\mathbf{G}_s$ represent the $L \times L$ unitary delay-Doppler operator matrices corresponding to the direct and surveillance channels, respectively, with γ_d and γ_s being the scalar coefficients of the two channels. Finally, $\mathbf{n}_d$ and $\mathbf{n}_s$ are additive white Gaussian noise (AWGN) with variances of σ^2.

Detection is performed via a generalized likelihood ratio test (GLRT), for which the corresponding $\mathcal{P}_D$ can be approximated in cases with high direct-path SNR (D-SNR) as

$$\mathcal{P}_D \approx Q_1\left(\sqrt{\frac{2P_R|\gamma_d|^2}{\sigma^2}}, \sqrt{2\gamma}\right), \tag{11}$$

where $Q_1(a, b)$ denotes the Marcum Q-function of the first order with parameters a and b, and γ is the detection threshold. Using the rate expression, and the relation $P_R + P_C = P_T$, the detection probability can be recast as [112]

$$\mathcal{P}_D \approx Q_1\left(\sqrt{2\left(P_T - \frac{1}{\gamma_c}\left(2^{R_{th}} - 1\right)\right)\frac{|\gamma_d|^2}{\sigma^2}}, \sqrt{2\gamma}\right). \tag{12}$$

In (12), the sensing metric $\mathcal{P}_D$ is related to the communication rate threshold R_{th}, which clearly shows again that a tradeoff exists between S&C if the power resources are shared between them. In [114], the authors further generalized the above power allocation design to a multi-static passive radar-communication system. The approach proposed in [112], [114] can also be extended to active and monostatic ISAC/radar-communication systems.

b) Estimation vs. communication: While the assumption of non-overlapping resources makes the analysis more tractable, this results in low efficiency, and does not address more challenging scenarios where resources must be reused by S&C. To this end, the authors of [115] considered optimizing the estimation performance of an ISAC system via the use of a common waveform, where the temporal, spectral, power, and signaling resources were fully reused for S&C, thus achieving the maximum integration gain. Consider a multi-antenna ISAC transceiver with N_t transmit and $N_r \geq N_t$ receive antennas, which serves K single-antenna users, and in the meantime detects target(s), as shown in Fig. 5 (b). This forms a multi-user multi-input single-output (MU-MISO) downlink communication system as well as a monostatic/active MIMO radar. By transmitting an ISAC waveform matrix $\mathbf{X} \in \mathbb{C}^{N_t \times L}$, which is constrained by a power budget P_T, the BS receives the following echo signal

$$\mathbf{Y}_R = \mathbf{G}\mathbf{X} + \mathbf{N}_R, \tag{13}$$

where $\mathbf{G} \in \mathbb{C}^{N_r \times N_t}$ represents the target response matrix (TRM), which can possess different forms for different target models, and $\mathbf{N}_R$ is an AWGN matrix with a variance of σ_R^2. The receive signal model for multi-user communication is

$$\mathbf{Y}_C = \mathbf{H}\mathbf{X} + \mathbf{N}_C, \tag{14}$$

where $\mathbf{H} = [\mathbf{h}_1, \mathbf{h}_2, \ldots, \mathbf{h}_K]^H \in \mathbb{C}^{K \times N_t}$ is the communication channel matrix, which is assumed to be known to the BS, and again, $\mathbf{N}_C$ is an AWGN matrix with variance σ_C^2.

The maximum likelihood estimation (MLE) of $\mathbf{G}$ is known to be $\hat{\mathbf{G}}_{MLE} = \mathbf{Y}_R\mathbf{X}^H\left(\mathbf{X}\mathbf{X}^H\right)^{-1}$ [98]. Accordingly, the MSE of estimating $\mathbf{G}$ can be computed as [98]

$$\mathbb{E}\left\{\left\|\mathbf{G} - \hat{\mathbf{G}}_{MLE}\right\|^2\right\} = \frac{\sigma_R^2 N_r}{L}\,\mathrm{tr}\left(\mathbf{R}_X^{-1}\right), \tag{15}$$

where $\mathbf{R}_X = \frac{1}{L}\mathbf{X}\mathbf{X}^H$ is the sample covariance matrix of $\mathbf{X}$. Note that since the MLE problem reduces to a linear estimation problem in the presence of i.i.d. Gaussian noise, its CRB is achieved by the above MSE. To design an ISAC waveform $\mathbf{X}$ that is favorable for both target estimation and information delivery, one can formulate an optimization problem as

$$\min_{\mathbf{X}} \;\; \mathrm{tr}\left(\mathbf{R}_X^{-1}\right) \quad \text{s.t.} \;\; \|\mathbf{X}\|_F^2 \leq LP_T, \; c_i\left(\mathbf{X}\right) \trianglelefteq C_i, \quad \forall i, \tag{16}$$

where $\trianglelefteq$ can represent either $\geq$, $\leq$, or $=$, and $c_i\left(\mathbf{X}\right)$ is a communication utility function constrained by C_i, e.g., per-user SINR, sum-rate, and SER. In (16), an S&C tradeoff exists due to the reuse of a single waveform $\mathbf{X}$ to achieve conflicting objectives.

Note that in (16) the existence of $\mathbf{R}_X^{-1}$ implies that $\mathbf{X}$ is of full rank. Otherwise, an unbiased estimator and the MLE do not exist [116]. This can be interpreted as follows. To estimate a rank-N_t matrix $\mathbf{G}$, the ISAC transmitter should utilize all the available DoFs in the system, and thus transmit a rank-N_t waveform for sensing. This, however, leads to an interesting conflict between S&C. In conventional MU-MISO downlink, the number of DoFs is limited by $\min\left(N_t, K\right)$, where $K \leq N_t$ is almost always the case, especially for mMIMO scenarios. That is, during each transmission, K individual data streams should be communicated from the BS to K users, which is typically implemented by precoding a rank-K data matrix $\mathbf{S}_C \in \mathbb{C}^{K \times L}$ into $\mathbf{X}$. In the event that a linear precoder is employed, i.e., $\mathbf{X} = \mathbf{W}_C\mathbf{S}_C, \mathbf{W}_C = [\mathbf{w}_1, \mathbf{w}_2, \ldots, \mathbf{w}_K] \in \mathbb{C}^{N_t \times K}$, $\mathbf{X}$ should have a rank of K, which means that $\mathbf{R}_X \in \mathbb{C}^{N_t \times N_t}$ is rank-deficient and thereby non-invertible.

To resolve the above issue, a possible method is to augment the data matrix $\mathbf{S}_C$ by adding at least $N_t - K$ dedicated sensing streams $\mathbf{S}_A$, which contain no useful information and are orthogonal to the data streams $\mathbf{S}_C$ [115], [117]. Accordingly, the precoding matrix $\mathbf{W}_C$ should also be augmented by an additional precoder $\mathbf{W}_A$. This suggests that

$$\mathbf{X} = [\mathbf{W}_C, \mathbf{W}_A]\begin{bmatrix}\mathbf{S}_C \\ \mathbf{S}_A\end{bmatrix} = \mathbf{W}_C\mathbf{S}_C + \mathbf{W}_A\mathbf{S}_A. \tag{17}$$

By doing so, $\mathbf{X}$ is of full rank. It can be observed at the receiver that the communication data are corrupted by the dedicated sensing streams $\mathbf{S}_A$, in which case the per-user SINR is expressed as follows (assuming white Gaussian signaling for $\mathbf{S}_C$ and $\mathbf{S}_A$).

$$\gamma_k = \frac{\left|\mathbf{h}_k^H\mathbf{w}_k\right|^2}{\sum_{i=1, i\neq k}^{K}\left|\mathbf{h}_k^H\mathbf{w}_i\right|^2 + \left\|\mathbf{h}_k^H\mathbf{W}_A\right\|^2 + \sigma_C^2}, \quad \forall k, \tag{18}$$

where the first item in the denominator is the multi-user interference, and the second item is the interference imposed by dedicated sensing streams. On the other hand, both $\mathbf{W}_C\mathbf{S}_C$ and $\mathbf{W}_A\mathbf{S}_A$ can be used for monostatic sensing, which suggests that communication will not interfere with sensing. Instead, it will facilitate target estimation.[4] By substituting (18) into (16) as communication utility function, problem (16) minimizes the estimation MSE subject to per-user SINR constraints, which can be optimally solved via semidefinite relaxation (SDR) [119].

On top of improving the sensing performance, the addition of a dedicated sensing waveform $\mathbf{W}_A\mathbf{S}_A$ also benefits the MIMO radar beampattern design. As discussed in [117], the extra DoFs provided by the dedicated sensing signals enable the formation of a better MIMO radar beampattern with guaranteed SINR of CUs; this is superior to the conventional ISAC scheme that exploits $\mathbf{W}_C\mathbf{S}_C$ only [120]. We refer readers to [115], [117], [118] for more details on the use of dedicated sensing signals.

2) Tradeoff Between Capacity Metrics of Sensing and Communication: In addition to the tradeoff between the native S&C metrics, research efforts have also focused on defining a new measure of "capacity" for sensing, particularly for radar sensing. In light of this, a basic question is how much information is gained from a sensing operation.

Guerci *et al.* [121] studied radar capacity from a resolution point of view. As shown in Fig. 6, a resolution unit/cell in radar signal processing can be defined in three dimensions, i.e., delay, Doppler, and angle. Each unit accommodates only one point target. If there is more than one target in the same resolution unit, the radar is unable to identify them and regards them as a single target. In this sense, each resolution unit can be considered as a binary information storage unit in which a

[4]The dedicated sensing signals $\mathbf{W}_A\mathbf{S}_A$ can be *a-priori* designed, and thus known at the communication receivers prior to transmission. In this case, the communication receivers can pre-cancel the interference caused by the sensing signals before decoding the communication signal, thus leading to an increased SINR [118].

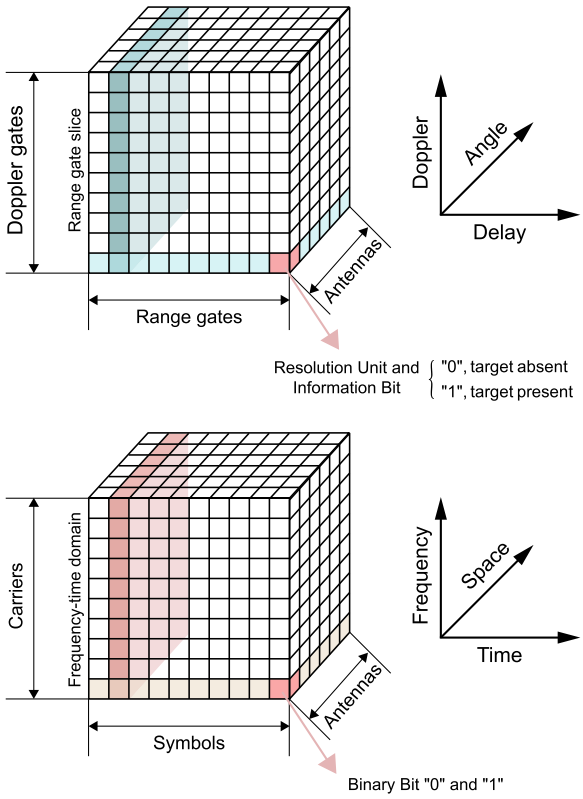

Fig. 6. Radar sensing resolution unit.

binary decision is made for target detection, i.e., "0" = target absent, and "1" = target present. The maximum "capacity" of a moving target indication (MTI) radar can be expressed by the Hartley capacity measure as [121]

$$C_R = \log N_u. \tag{19}$$

In (19), N_u is the total number of resolution cells, which satisfies

$$N_u \propto \left(\frac{D_{\max}}{\Delta D}\right)\left(\frac{2\pi}{\Delta\theta}\right)\left(\frac{PRF}{\Delta f_D}\right), \tag{20}$$

where ΔD, $\Delta\theta$, and Δf_D stand for the range resolution, angular resolution, and Doppler resolution of the radar, and $D_{\max}$ and PRF denote the maximum detectable range and the pulse repetition frequency (PRF), respectively.

The capacity in (19) is simply a noiseless measure of how many point targets can be distinguished by the radar system. Consider an N_t-antenna pulsed radar whose antenna array is uniformly and linearly placed. Its range, velocity, and angular resolutions can be calculated by

$$\Delta D = \frac{c}{2B}, \quad \Delta f_D = \frac{1}{T_d}, \ \Delta\theta \approx \frac{2}{N_t}, \tag{21}$$

where B is the bandwidth, and T_d represents the dwell time, i.e., the duration that a target stays within the area illuminated by the radar. The resolution of a radar is determined by its physical limit, or the maximum amount of available temporal, spectral, and spatial resources. Again, we observe an interesting parallel between S&C, as the information bits for communications can also be embedded in the time-frequency-space domain via a classical MIMO-OFDM architecture, as shown in Fig. 6. This being the case, it is still not straightforward to see how the "sensing capacity" in (19) trades off with the fundamental communication metrics, as it is specifically restricted to the identifiability of targets.

Inspired by the classical rate-distortion theory,[5] the authors of [122], [123] proposed the "estimation rate" as a sensing metric. Consider the range estimation problem in radar sensing. By transmitting a radar pulse $s_R(t)$ with a bandwidth B and pulse duration T, a single target is sensed with a delay of τ and an amplitude h_R, yielding the following echo signal

$$y_R(t) = h_R\sqrt{P_R}s_R(t-\tau) + n_R(t), \tag{22}$$

where $n_R(t)$ is the AWGN with a variance of σ_R^2. The CRB for delay estimation is given by

$$CRB(\tau) \triangleq \sigma_{\tau,est}^2 = \frac{\sigma_R^2}{8\pi^2 h_R^2 B_{rms}^2 BTP_R}, \tag{23}$$

where B_{rms} is the root-mean-square (RMS) bandwidth of $s_R(t)$.

Suppose that the radar is operating in tracking mode, and prior knowledge on the range of the target is available, subject to some random fluctuations. The radar can then predict the delay of the target of interest by leveraging a prediction function, which we denote as τ_{pre}. The true delay for the target can then be expressed as

$$\tau = \tau_{pre} + n_{pre}, \tag{24}$$

where $n_{pre} \sim \mathcal{N}\left(0, \sigma_{\tau,pre}^2\right)$ represents the range fluctuation.

The radar estimation rate is defined as the cancellation of the uncertainty in the target parameters per second, with the unit of bits/s, and is upper-bounded by [123]

$$R_{est} \le \frac{H_{\tau,rr} - H_{\tau,est}}{T_{PRI}}, \tag{25}$$

where T_{PRI} is the pulse repetition interval, and

$$\begin{aligned} H_{\tau,rr} &= \frac{1}{2}\log\left(2\pi e\left(\sigma_{\tau,pre}^2 + \sigma_{\tau,est}^2\right)\right), \\ H_{\tau,est} &= \frac{1}{2}\log\left(2\pi e\sigma_{\tau,est}^2\right) \end{aligned} \tag{26}$$

are the received signal entropy and the estimation entropy, respectively. Using (23), the estimation rate bound is expressed as [123]

$$R_{est} \le \frac{1}{2T_{PRI}}\log\left(1 + \frac{8\pi^2 h_R^2 \sigma_{\tau,pre}^2 B_{rms}^2 BTP_R}{\sigma_R^2}\right). \tag{27}$$

This estimation rate can then be employed to form a tradeoff with the communication rate. Let us consider an ISAC receiver, which receives both communication signals from the user(s) and echo signals reflected from the target, yielding

$$y(t) = h_C\sqrt{P_C}s_C(t) + h_R\sqrt{P_R}s_R(t-\tau) + n(t), \tag{28}$$

where h_C, P_C and $s_C(t)$ are the communication channel coefficient, transmit power and communication signal, respectively. Such a scenario can be modeled as a multi-access channel, where the target is viewed as a virtual user that unwillingly communicates information with the ISAC receiver on its parameters [123]. Different inner bounds between the

[5]Note that the rate-distortion theory is distinctly different from the rate-distortion tradeoff discussed above.

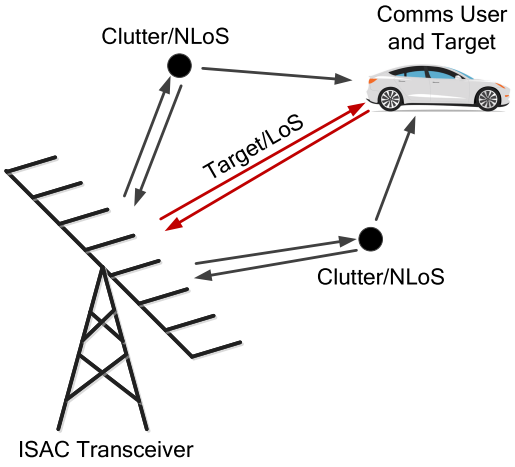

Fig. 7. Tradeoff in S&C channels: NLoS reduction or exploitation?

communication rate and estimation rate can be achieved via schemes of isolated sub-band allocation, successive interference cancellation (SIC), water filling, and Fisher Information optimization schemes [123].

D. Tradeoff in S&C Spatial DoFs

Another fundamental tradeoff naturally arises in ISAC systems due to the different treatments employed for the spatial resources in S&C. In a generic communication system, one needs to "exploit all the available degrees of freedom (DoFs) in the channel" [101] to enhance the communication performance. For example, Non-LoS (NLoS) propagation was initially considered harmful to wireless systems, as it results in channel fading. With the development of the multi-antenna technology, surprisingly, a common sense is condensed, that NLoS paths and fading effects can be exploited to provide diversity and DoFs for MIMO communications. For sensing, on the contrary, not all paths are useful, and some of them may have negative impacts on the sensing performance. In most cases, sensing requires the existence of an explicit LoS path between the sensor and the object to be sensed. In typical radar applications, signals reflected by objects other than the targets of interest are referred to as "clutter", which are regarded as harmful and need to be mitigated. NLoS components fall into this category in general. Accordingly, a specific propagation path can be useful for both functionalities, as long as it contains information of the target of interest. Otherwise, this path is useful only for communication, and is harmful to sensing. This again reflects the contradictory needs in S&C.

To see this more clearly, consider the simple scenario shown in Fig. 7, where a mmWave BS also acts as a monostatic radar equipped with N_t and N_r transmit and receive antennas. The ISAC BS serves an N_v-antenna vehicle while tracking its movements, which suggests that the vehicle is both a CU and a target. By transmitting an ISAC signal matrix $\mathbf{X} \in \mathbb{C}^{N_t \times L}$, the received signal at the vehicle is expressed as

$$\begin{aligned}\mathbf{Y}_C &= \underbrace{\alpha_0 \mathbf{b}_v(\phi_0)\mathbf{a}_t^H(\theta_0)\mathbf{X}}_{\text{LoS}} + \underbrace{\sum_{i=1}^{I}\alpha_i \mathbf{b}_v(\phi_i)\mathbf{a}_t^H(\theta_i)\mathbf{X}}_{\text{NLoS}} \\ &\quad + \underbrace{\mathbf{Z}_C}_{\text{Noise}} \\ &\triangleq \mathbf{H}\mathbf{X} + \mathbf{Z}_C, \end{aligned} \tag{29}$$

where α_i, θ_i and ϕ_i represents the channel coefficient, the angle of departure (AoD) and the angle of arrival (AoA) of the ith path, respectively, with $i = 0$ and $i \geq 1$ being the indices of the LoS path and NLoS paths, $\mathbf{a}_t(\theta) \in \mathbb{C}^{N_t \times 1}$ and $\mathbf{b}_v(\phi) \in \mathbb{C}^{N_v \times 1}$ being the steering vectors for the transmit antenna array of the BS and the receive antenna array of the vehicle, and I being the total number of available paths in the channel. Note that we omit the delay and Doppler of each path without loss of generality.

By assuming each NLoS path corresponds to a clutter source, the ISAC BS receives the reflected echo from the vehicle as

$$\begin{aligned}\mathbf{Y}_R = \underbrace{\beta_0 \mathbf{a}_r(\theta_0)\mathbf{a}_t^H(\theta_0)\mathbf{X}}_{\text{Target}} + \underbrace{\sum_{i=1}^{I}\beta_i \mathbf{a}_r(\theta_i)\mathbf{a}_t^H(\theta_i)\mathbf{X}}_{\text{Clutter}} \\ + \underbrace{\mathbf{Z}_R}_{\text{Noise}}, \end{aligned} \tag{30}$$

where β_i is the reflection coefficient of the ith clutter, and $\mathbf{a}_r(\theta) \in \mathbb{C}^{N_r \times 1}$ is the steering vector of the receive antenna array of the ISAC BS. From (29), we see that the receive SNR of the vehicle is given by

$$\text{SNR}_C = \frac{\|\mathbf{H}\mathbf{X}\|_F^2}{L\sigma_C^2}, \tag{31}$$

where all the propagation paths contribute to the receive power. From (30), on the other hand, the signal-to-clutter-plus-noise ratio (SCNR) of the target return is expressed as [124]

$$\text{SCNR}_R = \frac{\left\|\beta_0 \mathbf{a}_r(\theta_0)\mathbf{a}_t^H(\theta_0)\mathbf{X}\right\|_F^2}{\left\|\sum_{i=1}^{I}\beta_i \mathbf{a}_r(\theta_i)\mathbf{a}_t^H(\theta_0)\mathbf{X}\right\|_F^2 + \sigma_R^2}. \tag{32}$$

To balance the S&C performance, an ISAC waveform $\mathbf{X}$ should be carefully designed to allocate power and other resources to each of the propagation paths, such that both S&C performance can be guaranteed, where convex optimization techniques may be employed to solve the problem. The tradeoff discussed above can be extended to generic ISAC scenarios with multiple targets/CUs of interest, or even simultaneous imaging and communications [125], where multiple paths are seen as useful to sensing.

E. Cross-Layer Tradeoff

As discussed in Sec. II, S&C operations can be performed at different layers, instead of being restricted to the PHY only. An interesting example is mobile sensing or wireless sensing, where commercial wireless devices are employed for the dual purposes of communication and higher-layer sensing tasks, e.g., human motion recognition, which is typically realized by training a deep neural network (DNN) using the sensory data. Accordingly, the performance tradeoff of S&C may no longer be analyzed through conventional framework built upon the PHY, where cross-layer designs are required. In wireless sensing, a commonly employed sensing metric is the recognition accuracy rate, i.e., the probability that the mobile sensor correctly recognizes the human activities/events. Nonetheless, the exploitation of a DNN for such sensing tasks makes the resource allocation between S&C challenging, given that the relationship between the accuracy rate and the

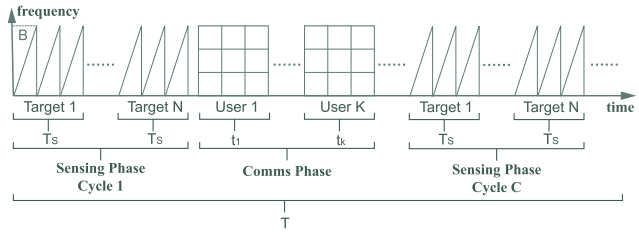

Fig. 8. Target recognition and communication in a time-division manner.

amount of allocated wireless resources could be mathematically intractable for DNN based recognition tasks.

To reveal the above cross-layer tradeoff, [126] considered the ISAC scenario shown in Fig. 8, where the time budget T is divided into interleaved sensing and communication cycles. In each sensing cycle, N targets are sensed, each of which is allocated a sensing duration t_S. On the other hand, for each communication cycle, K users are scheduled through a round-robin protocol, by allocating a communication duration $t_1, t_2, \ldots, t_K$ to each of them. By assuming constant-power transmission, the following multi-objective optimization problem is formulated to allocate time slots to S&C [126]:

$$\begin{aligned} \max_{A,R,C,t_k} \quad & (A, R) \\ \text{s.t. } & A = \Theta(C), \\ & R = \min_{k=1,2..,K} \frac{t_k}{T} B \log\left(1 + \frac{h_k P}{\sigma_C^2}\right), \\ & CNt_S + \sum\nolimits_{k=1}^{K} t_k = T, \end{aligned} \tag{33}$$

where A is the sensing accuracy rate of a well-trained DNN, R is the minimum achievable rate among K users, C stands for the number of sensing cycles, and h_k is the channel coefficient of the kth user. In particular, the relationship between the accuracy rate and the number of allocated sensing cycles is represented by $A = \Theta(C)$, which may be an unknown nonlinear function. The authors proposed employing the classical nonlinear model $\Theta(C) \approx 1 - \alpha C^{-\beta}$ to approximately capture the shape of $\Theta(C)$, and to find (α, β) by least-squares fitting using training data. Problem (33) can then be solved via the Lagrangian multiplier method.

By solving the problem in (33), an optimal time allocation strategy is obtained, such that the sensing accuracy rate and communication rate are maximized simultaneously in the sense of Pareto optimality. We remark that in addition to the cross-layer tradeoff in terms of time allocation, one may also consider various other types of tradeoffs achieved by spectral, power, and spatial resource allocation for the cross-layer ISAC design.

F. Summary and Open Challenges

In this section, we have overviewed various types of performance tradeoffs between S&C, from the information-theoretical limits, to the tradeoff in PHY, and to that in ISAC channels and cross-layer designs. These tradeoffs are resulting from the shared use of wireless resources and the contradictory design objectives of S&C. While the tradeoff issues have been addressed to a certain degree in the prior art, there are still challenges that remain open, which we list in the following.

1) Efficiency Metrics for Sensing: One may notice from Sec. III-A that most of the sensing metrics are reliability metrics, namely, detection probability and MSE, which measure how reliable the detection/estimation operation is. While there are initial efforts towards defining the "capacity" of sensing [121], [123], the efficiency aspect of sensing, however, still remains widely unexplored, This, to a large extent, is because that the information gained from the sensing process cannot be straightforwardly measured in *bits*. Therefore, a fundamental and insightful metric should be properly defined to measure the resource utilization efficiency for sensing.

2) Quantative Description of Integration Gain: While the shared use of wireless resources between S&C may potentially increase the efficiency and thus to achieve the integration gain, it is unclear how to measure this gain in a quantative manner. This accounts for the reason why we need a meaningful metric to measure the resource efficiency of sensing. Together with the spectral/energy efficiencies of communications, one may readily see how much efficiency improvement is achieved by using the ISAC transmission over that of individual S&C designs.

3) Performance Bounds and Achievable Strategies: A natural question resulting from the above discussion is what is the maximum integration gain that can be achieved from ISAC design. In other words, what is the Pareto-optimal boundray between S&C performance in terms of the resource efficiencies. More importantly, given such an optimal boundary, how to design a practical ISAC transmission strategy/resource allocation scheme to reach to it.

IV. Waveform Design for ISAC

Waveform design plays a key role in ISAC systems, which mainly focuses on designing a dual-functional waveform that is capable of S&C by the shared use of signaling resources, such that the integration gain can be achieved. Depending on the integration level, ISAC waveforms can be conceived from the most loosely coupled approach (time-/frequency-/spatial-/code-division), to the most tightly coupled approach (fully unified waveform). In this section, we first overview the ISAC waveform design with non-overlapped resource allocation, and then discuss approaches for fully unified waveform design.

A. Non-Overlapped Resource Allocation

It is straightforward to see that S&C can be scheduled on orthogonal/non-overlapped wireless resources, such that they do not interfere with each other. This can be realized over temporal, spectral, spatial, or even code domains, which are known as time-, frequency-, spatial-, and code-division ISAC, respectively.

1) Time-Division ISAC: Time-division ISAC is the most loosely coupled waveform design, which can be conveniently implemented into the existing commercial systems, where a straightforward example has been shown in Sec. III-E. In [22], a joint radar-communication waveform design was proposed, where the transmission duration was split into radar cycles and radio cycles. In particular, a frequency-modulated continuous waveform (FMCW) with up- and down-chirp modulations is used for radar sensing, while various modulation schemes, e.g., BPSK, PPM, and OOK can be flexibly leveraged for communication. More recently, time-division

ISAC has been realized in a number of commercial wireless standards, such as IEEE 802.11p and IEEE 802.11ad, where the channel estimation field (CEF)/pilot signals, originally designed for channel estimation, are exploited for radar sensing [127]–[131].

2) Frequency-Division ISAC: Frequency-division ISAC is another simple option, which is typically constructed on the basis of an OFDM waveform. In this sense, it is not as flexible as its time-division counterpart, where any S&C waveforms may be employed. To be specific, S&C functionalities are allocated to different subcarriers given the channel conditions, the required KPIs for S&C, and the power budget of the transmitter [132], [133]. For instance, in [133], a power allocation and subcarrier selection scheme is designed to minimize the transmit power, while guaranteeing both mutual information and achievable data rate constraints for radar sensing and communications, respectively.

3) Spatial-Division ISAC: Spatial-division ISAC has recently gained attentions due to research progress regarding MIMO and mMIMO technologies [134]. In such methods, S&C are performed over orthogonal spatial resources, e.g., different antenna groups [120]. In the event that the communication channel is dominated by a LoS component, the S&C waveforms can be transmitted over different spatial beams, which show strong orthogonality in the mMIMO regime [27]. On the other hand, if the communication channel is composed of rich scattering paths, the sensing waveform may be projected into its null space to avoid interfering with the communication functionality [26], [135].

4) Code-Division ISAC: In addition to the time, frequency and spatial division regimes, code-division designs are also considered viable ISAC solutions, where sensing and communication signals are carried by orthogonal/quasi-orthogonal sequences [136], [137]. As an example, a novel code-division ISAC scheme was proposed in [138], where the code-division OFDM ISAC signal and a corresponding SIC based receiver design were considered to achieve the code-division multiplexing (CDM) gain and improve the reliability of both S&C.

Although being easy to implement on hardware platforms, the above designs suffer from poor spectral and energy efficiency. To maximize the integration gain, it is favorable to design a fully unified ISAC waveform, where the temporal, sepectral, spatial, and signaling resources are utilized in a shared manner between S&C [28], [29].

B. Fully Unified Waveforms

Fully unified ISAC waveforms are generally designed following three philosophies, namely, sensing-centric design (SCD), communication-centric design (CCD), and joint design (JD) approaches [45], [49], which we elaborate on as follows.

1) Sensing-Centric Design: SCD aims to incorporate the communication functionality into existing sensing waveforms/infrastructures. In other words, the sensing performance needs to be primarily guaranteed. Nevertheless, a pure radar sensing waveform cannot be directly exploited for communication, as it contains no signaling information. The essence of SCD is to embed information data into a sensing waveform, without unduly degrading the sensing performance. To provide insight into such an operation, consider a radar waveform matrix $\mathbf{S}_R$, and a communication data matrix $\mathbf{D}$. The sensing-centric waveform can be designed by [139]

$$\mathbf{X} = \mathcal{C}\left(\mathbf{S}_R, \mathbf{D}\right), \tag{34}$$

where $\mathcal{C}\left(\cdot\right)$ represents the embedding operation. Similar to the case in Sec. IV-A, the communication data can be embedded into different domains of the sensing signal, in order to formulate an ISAC waveform.

a) Chirp-based waveform design (time-frequency domain embedding): Early SCD schemes typically focused on time-frequency domain embedding, where chirp signals, which are widely employed in various radar applications, acted as information carriers [19], [20]. Chirp signals possess large time-bandwidth product, and are capable of generating narrow pulse with high peak power from long-duration pulse with low peak power via pulse compression/matched filtering method, thus offering superior range estimation performance.

A generic chirp signal is given by

$$s_{\text{chirp}}\left(t\right) = A\exp\left(j2\pi\left(f_0 t + \frac{1}{2}kt^2\right) + \phi_0\right), \quad t \in [0, T_0], \tag{35}$$

where A, f_0, k, ϕ_0, and T_0 stand for the amplitude, start frequency, chirp slope, initial phase, and duration of the chirp signal, respectively. The derivative of the overall phase of (35) with respect to time t is a linear function. This suggests that the frequency of the chirp signal linearly increases with time, resulting in a bandwidth $B = kT_0$, and a large time-bandwidth product $BT_0 = kT_0^2$. Given the design DoFs available in (35), one may represent communication symbols using variations in the parameters A, f_0, and ϕ_0. Accordingly, a wide variety of modulation formats, e.g., amplitude-shift keying (ASK), frequency-shift keying (FSK) and PSK, can be straightforwardly applied by using chirp signals as carriers. Note that it is also possible to modulate communication symbols onto the chirp slope k.

b) Sidelobe control approach (spatial domain embedding): To equip an MIMO radar system with communication functionality, recent SCD schemes considered embedding useful data into the radar's spatial domain [140], [145], [146]. One classical approach is to represent each communication symbol by the sidelobe level of the MIMO radar beampattern, where the main beam is used solely for target sensing [140]. Suppose that an N_t-antenna MIMO radar transmits information to an N_r-antenna CU located at angle θ_C. Within each radar pulse, a Q-bit message is represented by a binary sequence $B_q, q = 1, \ldots, Q$. Let $\mathbf{S}_R = \left[\mathbf{s}_{R,1}, \ldots, \mathbf{s}_{R,Q}\right]^H \in \mathbb{C}^{Q\times L}$ be Q orthogonal radar waveforms. The transmitted ISAC signal can be represented by

$$\mathbf{X} = \mathbf{W}\mathbf{S}_R, \tag{36}$$

where $\mathbf{W} \in \mathbb{C}^{N_t\times Q}$ is an ISAC beamforming matrix, which is expressed as [140]

$$\mathbf{W} = \left[B_1\mathbf{w}_1 + \left(1 - B_1\right)\mathbf{w}_0, \ldots, B_Q\mathbf{w}_1 + \left(1 - B_Q\right)\mathbf{w}_0\right], \tag{37}$$

where $\mathbf{w}_0$ and $\mathbf{w}_1$ are beamforming vectors associated with "0" and "1" data, respectively, which are designed offline to satisfy certain radar beamforming constraints. For example,

$\mathbf{w}_i, i = 0, 1$, may be designed by solving the following optimization problem [140]

$$\begin{aligned} &\min_{\mathbf{w}_i} \max_{\theta} \ \left|G(\theta) - \left|\mathbf{w}_i^H \mathbf{a}(\theta)\right|\right|, \quad \theta \in \Theta \\ &\text{s.t.} \ \left|\mathbf{w}_i^H \mathbf{a}(\theta)\right| \le \varepsilon, \theta \in \bar{\Theta}, \quad \mathbf{w}_i^H \mathbf{a}(\theta_C) = \delta_i, \end{aligned} \tag{38}$$

where $\mathbf{a}(\theta)$ is the transmit steering vector of the MIMO radar. The objective function is to approximate the desired beampattern magnitude $G(\theta)$ within the mainlobe region Θ. The first constraint is imposed to control the sidelobe level within the sidelobe regin $\bar{\Theta}$. The second constraint is to ensure that the sidelobe level at the direction of the CU equals to a given value δ_i, where $\delta_0 < \delta_1$.

When transmitting $\mathbf{X}$, the CU receives

$$\begin{aligned} \mathbf{Y}_C &= \beta \mathbf{b}(\phi_C) \mathbf{a}^H(\theta_C) \mathbf{W} \mathbf{S}_R + \mathbf{Z}_C \\ &= \alpha \mathbf{b}(\phi_C) \mathbf{a}^H(\theta_C) \sum_{q=1}^{Q} \left(B_q \mathbf{w}_1 \mathbf{s}_{R,q}^H + (1 - B_q) \mathbf{w}_0 \mathbf{s}_{R,q}^H\right) \\ &\quad + \mathbf{Z}_C, \end{aligned} \tag{39}$$

where α is the channel coefficient, $\mathbf{b}(\phi)$ is the receive steering vector at the communication receiver, and ϕ_C is the AoA of the ISAC signal, which can be readily estimated at the receiver's side via various algorithms, e.g., the multiple signal classification (MUSIC) and estimation of signal parameters via rotational invariance techniques (ESPRIT).

Matched-filtering $\mathbf{Y}_C$ with the qth waveform yields the signal vector

$$\mathbf{y}_{C,q} = \begin{cases} \alpha \mathbf{b}(\phi_C) \mathbf{a}^H(\theta_C) \mathbf{w}_0 + \mathbf{z}_{C,q}, & B_q = 0, \\ \alpha \mathbf{b}(\phi_C) \mathbf{a}^H(\theta_C) \mathbf{w}_1 + \mathbf{z}_{C,q}, & B_q = 1, \end{cases} \tag{40}$$

where $\mathbf{z}_{C,q}$ is the output noise of the q-th matched filter. Note that $\mathbf{w}_0^H \mathbf{a}(\theta_C) = \delta_0 < \delta_1 = \mathbf{w}_1^H \mathbf{a}(\theta_C)$. By multiplying (40) with a receive beamformer $\mathbf{b}^H(\phi_C)$, B_q can be simply detected as [140]

$$\hat{B}_q = \begin{cases} 0, & \left|\mathbf{b}^H(\phi_C) \mathbf{y}_{C,q}\right| < \lambda, \\ 1, & \left|\mathbf{b}^H(\phi_C) \mathbf{y}_{C,q}\right| > \lambda, \end{cases} \tag{41}$$

where λ is a pre-defined threshold. The above scheme can also be extended to M-ary modulation by designing M beamforming vectors $\mathbf{w}_i, i = 1, \ldots, M$, while maintaining a desired MIMO radar beampattern.

We show a numerical example of the sidelobe control scheme in Fig. 9, where a 10-antenna MIMO radar serves a single CU while formulating a wide radar beam towards $\Theta \in [-10^\circ, 10^\circ]$. The CU is located at -50°. The overall sidelobe level is controlled to be less than $\varepsilon = -20$dB. Accordingly, the sidelobe level radiated towards the CU's direction alternates between $\delta_0 = -40$ dB and $\delta_1 = -20$ dB, which represent the "0" and "1" data, respectively. It can be observed in the figure that the -50° sidelobe is indeed exploited to transmit communication bits, and that the two beamforming vectors generate almost the same pattern at the main beam.

We note that while the main beam shape for target detection can be kept unchanged by the sidelobe control scheme, this approach may not ensure 100% radar performance, as the frequent fluctuation in the sidelobe of the radar beampattern may lead to a high false alarm rate, which is particularly pronounced when the communication channel changes rapidly.

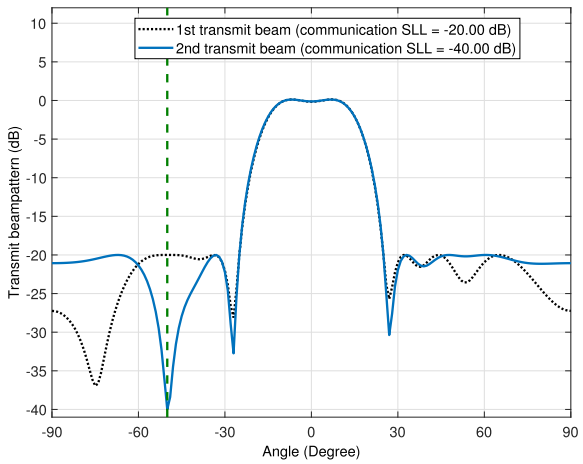

Fig. 9. ISAC beamforming based on sidelobe control.

c) Index modulation: To fully guarantee radar sensing performance, a more promising SCD approach is to realize ISAC via *index modulation*. Pioneered by [146], when N_t orthogonal waveforms are transmitted by an N_t-antenna MIMO radar, the communication functionality can be implemented by shuffling the waveforms across multiple antennas. In this case, the communication codeword is represented by a permutation matrix, resulting in a maximum bit rate of $f_{\text{PRF}} \cdot \log_2 N_t!$, where f_{PRF} is the radar's PRF.

As a further study, an index modulation scheme based on carrier agile phased array radar (CAESAR) was proposed to enable ISAC capability, namely, the multi-carrier agile joint radar-communication (MAJoRCom) system [141], [147]. In particular, this system randomly changes the carrier frequencies pulse by pulse, and randomly allocates these frequencies to each antenna element, thus introducing agility to both the spatial and frequency domains. Suppose that the available carrier frequencies form the following set with a cardinality of M_f:

$$\mathcal{F} := \{f_c + m\Delta f \,|m = 0, 1, \ldots, M_f - 1\}, \tag{42}$$

where f_c is the initial carrier frequency, and Δf is the frequency step. During each pulse, the radar randomly chooses K_f frequencies from $\mathcal{F}$. The resultant number of possible selections is

$$N_1 = \binom{M_f}{K_f} = \frac{M_f!}{K_f!(M_f - K_f)!}. \tag{43}$$

Once K_f frequencies are selected, each antenna is allocated a carrier frequency to transmit a monotone waveform. All N_t antennas are arranged into $L_K = \frac{N_t}{K_f}$ with L_K being an integer, where antennas in one group share the same carrier frequency. By doing so, the number of possible allocation patterns is

$$N_2 = \frac{N_t!}{(L_K!)^{K_f}}. \tag{44}$$

Accordingly, the total number of bits that can be represented by varying the selections of carrier frequencies and allocation

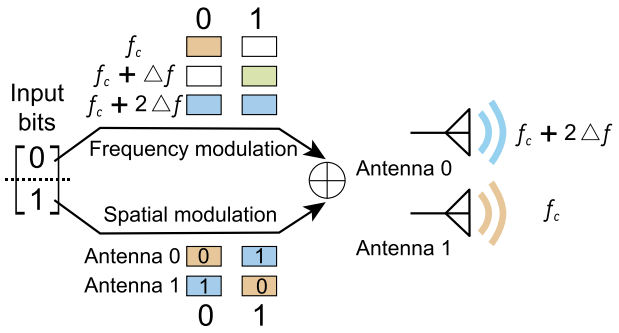

Fig. 10. ISAC signaling based on index modulation.

patterns is calculated as

$$\log_2 N_1 + \log_2 N_2 = \log_2 \frac{M_f!}{K_f!\,(M_f - K_f)!} + \log_2 \frac{N_t!}{(L_K!)^{K_f}} \approx K_f \log_2 M_f + N_t \log_2 K_f, \tag{45}$$

where the approximation is based on the Stirling's formula. The maximum bit rate is therefore $f_{\text{PRF}} \cdot (K_f \log_2 M_f + N_t \log_2 K_f)$. For clarity, a simple example with 2 transmit antennas is illustrated in Fig. 10, where the input bits are mapped to selected carrier frequencies and antennas using index modulation.

We note that the sensing performance of MAJoRCom is almost unaffected by the transmission of communication bits, since communication codewords are random and equally distributed over different pulses, just as in a standard CAESAR radar [147]. This allows for the use of random sensing matrices for range-Doppler reconstruction with guaranteed estimation performance. In addition to pulsed radar, the index modulation technique can also be applied in conjunction with FMCW signaling, leading to an FMCW-based radar-communication system (FRaC) [143]. FRaC achieves a higher bit rate than that of MAJoRCom, through an extra level of phase modulation for the ISAC signal.

Note that most SCD schemes employ slow-time coding, i.e., inter-pulse modulations rather than inner-pulse approaches, resulting in a bit rate that is tied to the PRF of the radar. Consequently, while SCD provides a favorable sensing performance, its application is limited in scenarios requiring low/moderate data rates only.

2) Communication-Centric Design: In contrast to SCD, communication-centric design implements the sensing functionality over an existing communication waveform/system, i.e., communication is the primary functionality to be guaranteed. In principle, any communication waveform can be utilized for mono-static sensing, as the waveform is fully known to the transmitter. Nevertheless, the randomness brought by the communication data may considerably degrade the sensing performance of the system.

As a representative CCD strategy, the use of OFDM waveforms for radar sensing has recently received growing attention [148], [149], thanks to their compatibility with the state-of-the-art 4G and 5G standards [3]. A baseband OFDM communication signal, in its simplest form, is analytically given by

$$s_{\text{OFDM}}(t) = \sum_{m=1}^{N_s} \sum_{n=1}^{N_c} d_{m,n} e^{j2\pi f_n t} \,\text{rect}\left(\frac{t - (m-1)\,T_{\text{OFDM}}}{T_{\text{OFDM}}}\right), \tag{46}$$

where N_s and N_c are the number of OFDM symbols and subcarriers within a signal frame, respectively, $d_{m,n}$ is the m-th data symbol at the n-th subcarrier, $f_n = (n-1)\,\Delta f$ is the n-th subcarrier frequency with a subcarrier interval Δf, $T_{\text{OFDM}} = T_s + T_g$ is the overall OFDM symbol duration, with T_s and T_g being the durations of an elementary symbol and a cyclic prefix (CP), and $\text{rect}\,(t/T)$ depicts a rectangular window with a duration T.

At the ISAC BS, (46) is transmitted to sense a point target with a Doppler frequency f_D and delay τ. The noiseless echo signal received at the BS is then

$$y_R(t) = \sum_{m=1}^{N_s} e^{j2\pi f_D t} \cdot \sum_{n=1}^{N_c} \alpha_{m,n} \left(d_{m,n} e^{-j2\pi f_n \tau}\right) e^{j2\pi f_n t} \times \text{rect}\left(\frac{t - (m-1)\,T_s - \tau}{T_s}\right), \tag{47}$$

where $\alpha_{m,n}$ is the channel coefficient at the mth OFDM symbol and the nth subcarrier. By assuming that the guard interval T_g is properly chosen, the time shift on the rectangular function can be neglected. Through sampling at each OFDM symbol, and performing block-wise FFT, the received discrete signal can be arranged into a matrix, with the (m,n)th entry being

$$y_{m,n} = \alpha_{m,n} d_{m,n} e^{-j2\pi(n-1)\Delta f \tau} e^{j2\pi f_D (m-1) T_{\text{OFDM}}}, \tag{48}$$

where the noise is again omitted for simplicity. We first observe that, the random communication data $d_{m,n}$ can be mitigated by simple element-wise division, which yields

$$\tilde{y}_{m,n} = \frac{y_{m,n}}{d_{m,n}} = \alpha_{m,n} e^{-j2\pi(n-1)\Delta f \tau} e^{j2\pi f_D (m-1) T_{\text{OFDM}}}. \tag{49}$$

Furthermore, (49) can be recast into a matrix form as

$$\tilde{\mathbf{Y}} = \mathbf{A} \odot \mathbf{v}_\tau \mathbf{v}_f^H, \tag{50}$$

where $\left(\tilde{\mathbf{Y}}\right)_{m,n} = \tilde{y}_{m,n}$, $(\mathbf{A})_{m,n} = \alpha_{m,n}$, and

$$\mathbf{v}_\tau = \left[1, e^{-j2\pi\Delta f \tau}, \ldots, e^{-j2\pi(N_c-1)\Delta f \tau}\right]^T, \quad \mathbf{v}_f = \left[1, e^{-j2\pi f_D T_{\text{OFDM}}}, \ldots, e^{-j2\pi f_D (N_s-1) T_{\text{OFDM}}}\right]^T. \tag{51}$$

To sense the target of interest, we compute the FFT for each column of $\tilde{\mathbf{Y}}$ to obtain the Doppler estimate, and then compute the IFFT for each row to obtain the delay estimate. This can be represented as [3]

$$\bar{\mathbf{Y}} = \mathbf{F}_{N_s} \tilde{\mathbf{Y}} \mathbf{F}_{N_c}^H, \tag{52}$$

where $\mathbf{F}_N$ is the N-dimensional Discrete Fourier Transform (DFT) matrix. The resultant $\bar{\mathbf{Y}}$ forms a 2-dimensional delay-Doppler profile, where a peak is detected at the corresponding delay-Doppler grid that contains the target. Unlike with conventional chirp signals, delay and Doppler processing

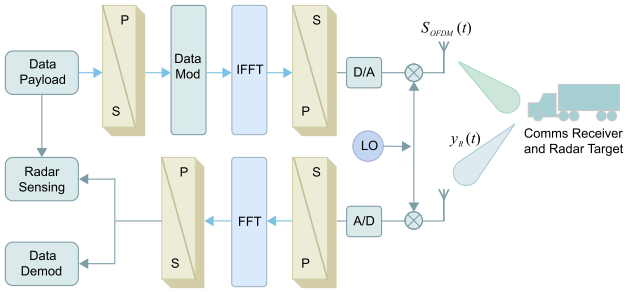

Fig. 11. Signal processing flow chart for OFDM based ISAC signaling.

are decoupled in OFDM waveforms, which is favorable for radar applications.

Although the above OFDM-based ISAC waveform is able to fully guarantee the communication performance, its sensing performance is rather restricted, since many desired properties for sensing are not addressed. First, constant envelope is typically needed for a radar system to transmit at the maximum available power budget without signal distortion, such that the SNR of the received echo signal is maximized. Second, the reliance to clutter interference, a key requirement in radar sensing, is rarely considered in CCD schemes. Finally, the sensing waveform should possess good correlation properties, so that the temporal/spectral/angular sidelobes are reduced to the lowest level to avoid false target detection. To achieve improved sensing performance, the CCD ISAC waveform needs to be effectively shaped subject to the above sensing-specific constraints.

3) Joint Design: As mentioned above, while the SCD and CCD schemes realize ISAC to a certain extent, they fail to formulate a scalable tradeoff between S&C. That is to say, SCD and CCD are two extreme cases in ISAC waveform design, where the communication/sensing functionality is implemented in a rather restricted manner provided that the sensing/communication performance is fully guaranteed. To address this issue, JD is regarded as a promising methodology. Unlike its SCD and CCD counterparts, JD aims at conceiving an ISAC waveform from the ground-up, instead of relying on existing sensing and communication waveforms [5], [55], [117], [120], [144], [150], [151]. This offers extra DoFs and flexibility, and thereby improves the S&C performance levels simultaneously. In what follows, we overview a state-of-the-art JD scheme in detail [55].

We consider an N_t-antenna ISAC BS that serves K single-antenna users in an MU-MISO downlink while sensing targets. Suppose that an ISAC signal matrix $\mathbf{X} \in \mathbb{C}^{N_t \times L}$ is transmitted, with L being the length of the radar pulse/communication block. The received signal at the users can be modeled as [55], [152]

$$\mathbf{Y}_C = \mathbf{H}\mathbf{X} + \mathbf{Z}_C = \mathbf{S}_C + \underbrace{(\mathbf{H}\mathbf{X} - \mathbf{S}_C)}_{\text{MUI}} + \mathbf{Z}_C, \tag{53}$$

where $\mathbf{H} \in \mathbb{C}^{K \times N}$ is the MU-MISO communication channel matrix, and $\mathbf{Z}_C \in \mathbb{C}^{K \times L}$ is again an AWGN noise matrix with variance σ_C^2. Finally, $\mathbf{S}_C \in \mathbb{C}^{K \times L}$ contains communication data streams intended for K users, with each entry being a communication symbol drawn from some pre-defined constellations, e.g., QPSK or 16-QAM. Here, $(\mathbf{H}\mathbf{X} - \mathbf{S}_C)$ denotes the multi-user interference (MUI). By zero-forcing the MUI, the channel $\mathbf{H}$ vanishes, and the MU-MISO channel becomes a standard AWGN channel.

The reduction in the MUI term leads to a higher communication sum-rate [152], which motivates the use of MUI as a cost function for communications. In addition to bearing the information matrix $\mathbf{S}_C$, the ISAC signal $\mathbf{X}$ should possess a number of aforementioned features that are favorable for sensing, which are quite challenging to be implemented simultaneously in a single waveform. Therefore, an alternative option is to approximate a well-designed pure sensing waveform $\mathbf{X}_0$, e.g., an orthogonal chirp waveform, which is known to have superior sensing performance. With the above consideration, we formulate the following ISAC waveform design problem.

$$\begin{aligned} \min_{\mathbf{X}} \ & \rho \left\| \mathbf{H}\mathbf{X} - \mathbf{S}_C \right\|_F^2 + (1-\rho) \left\| \mathbf{X} - \mathbf{X}_0 \right\|_F^2 \\ \text{s.t.} \ & f_n(\mathbf{X}) \preceq C_n, \quad \forall n, \end{aligned} \tag{54}$$

where we use a weighting factor $\rho \in [0,1]$ to control the weight assigned to S&C functionalities, i.e., ρ and $1-\rho$ represent the priority/preference for the communication and sensing performance in the ISAC system, respectively. In addition to minimizing the weighted cost function, N waveform shaping constraints are imposed on $\mathbf{X}$, which may include the overall power budget constraint, per-antenna power budget constraint, constant-modulus (CM) constraint (in order to enable the full-power and distortionless signal emission for radar sensing), and range/Doppler/angle sidelobe control constraints. For instance, by imposing a total transmit power constraint P_T, (54) can be reformulated into

$$\begin{aligned} \min_{\mathbf{X}} \ & \rho \left\| \mathbf{H}\mathbf{X} - \mathbf{S}_C \right\|_F^2 + (1-\rho) \left\| \mathbf{X} - \mathbf{X}_0 \right\|_F^2 \\ \text{s.t.} \ & \left\| \mathbf{X} \right\|_F^2 = LP_T. \end{aligned} \tag{55}$$

Note that if $\rho = 1$, communication is given the full priority, and solving problem (55) yields a zero-forcing (ZF) precoded signal with respect to the channel $\mathbf{H}$. In contrast, if $\rho = 1$, sensing is given the full priority, and the optimal solution is exactly $\mathbf{X} = \mathbf{X}_0$, provided that $\mathbf{X}_0$ is also constrained by the same power budget P_T. When ρ varies from 0 to 1, a favorable S&C performance tradeoff can be obtained via solving (55). It is worth highlighting that while (55) is non-convex, the globally optimal solution can be obtained by solving the corresponding Karush-Kuhn-Tucker (KKT) equations [55].

We show a numerical example of the JD in (54) for $N_t = 16, K = 4, 6, 8$, by using an orthogonal waveform $\mathbf{X}_0$ as a benchmark, which is known to have superior sensing performance for MIMO radar. We consider a scenario in which a point-like target located at the angle of 36° is to be sensed via the constant false-alarm rate (CFAR) detection approach, where the false-alarm probability and receive SNR are fixed at 10^{-7} and -6 dB, respectively. The tradeoff between the detection probability $\mathcal{P}_D$ and the average achievable rate per user is investigated in Fig. 12 by varying ρ from 0 to 1, under both total and per-antenna (perAnt) power constraints. Accordingly, the ISAC performance varies smoothly from sensing-optimal to communication-optimal, which suggests that the performances of SCD and CCD are the two end-points on the JD tradeoff curve. Another tradeoff that can be observed from Fig. 12 is that, as the number of communication users decreases, the detection probability rises. When $K = 4$,

TABLE III
ISAC WAVEFORM DESIGNS

Waveform Designs	Methodologies	Representative Techniques	Pros	Cons
Non-overlapped Resource Allocation	Time-Division	• TD between FMCW and comms modulations [22] • Using CEF of IEEE 802.11ad frame for sensing [128]	Easy to implement	Low efficiency
	Frequency-Division	• Subcarrier allocation between S&C in OFDM [133]		
	Spatial-Division	• Antenna separation between S&C [120]		
Fully Unified Waveform	Sensing-Centric	• Using chirp signals as information carriers [20] • MIMO radar sidelobe embedding approach [140] • Index modulation [141]–[143]	Guaranteed sensing performance	Low infomation rate/ spectral efficiency
	Communication-Centric	• Using OFDM for sensing [3]	Guaranteed comms performance	Unreliable sensing performance
	Joint Design	• Waveform design based on optimization [55], [117], [120], [144]	Scalable S&C performance tradeoff	High complexity

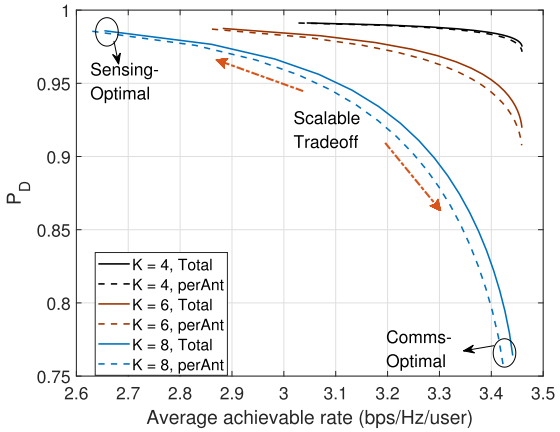

Fig. 12. Performance tradeoff between S&C by the joint design, $N_t = 16$ radar SNR $= -6$ dB, $P_{FA} = 10^{-7}$.

the achievable rate is increased without sacrificing too much sensing performance.

Despite the higher computational complexity of the JD scheme, it often outperforms conventional schemes in many aspects, as elaborated below.

1) While most SCD waveforms are based on inter-pulse modulation (slow-time coding), the JD waveform in (54) modulates communication data in an inner-pulse manner (fast-time coding), where each fast-time snapshot represents a communication symbol. This significantly improves the data rate.
2) While the classical sidelobe control scheme in (36)-(41) serves communication users in LoS channels only, the JD waveform in (54) is not conditional on any specific channel. In fact, any MIMO channel matrix $\mathbf{H}$ can be inserted into (54) to design the JD waveform.
3) Problem (54) takes sensing-specific constraints, such as constant modulus and waveform similarity, into account, which improves the sensing quality of JD over that of CCD schemes, such as OFDM-based designs.

C. Summary and Open Challenges

In this section, we have overviewed numerous ISAC waveform design methodologies, including non-overlapped resource allocation based designs and fully unified waveforms. In particular, the fully unified waveforms can be conceived in the spirit of three types of philosophies, namely, SCD, CCD, and JD. We further discuss representative examples as well as the pros and cons for different waveform designs, which are summarized in TABLE. III. Accordingly, the open challenges in ISAC waveform design include, but are not limited to:

1) SCD Waveforms With High Communication Rate: SCD waveforms are typically built upon existing radar signaling strategies, which implement certain communication functionality on a radar infrastructure. To avoid unduly affect the radar sensing performance, SCD waveforms can only accommodate limited amount of communication bits; this typically results in a low data rate at a level of radar pulse repetition frequency (PRF), e.g., ∼kbits per second. In order to support practical communication applications, it is of particular importance to conceive SCD waveforms that deliver information at a high data rate.

2) CCD Waveforms With Reliable Sensing Performance: CCD approaches implement sensing functionality over existing wireless communication waveforms, which may possess unreliable sensing performance, e.g., poor auto- and cross-correlation properties. This is partially because of the randomness in the communication data, and is also because of the lack of flexibility of the signal structure, which is often required to be compatible with communication standards. Therefore, CCD waveforms with reliable sensing performance should be pursued in ISAC waveform design.

3) Efficient Implementation of JD Waveforms: While JD waveforms may realize a scalable tradeoff between sensing-optimal and communication-optimal performance. They typically suffer from higher design complexity, and are thus difficult to be efficiently implemented in real-time platforms. To address this issue, low-complexity and real-time design methodologies towards JD waveforms are strongly pursued.

V. RECEIVE SIGNAL PROCESSING

The requirement for simultaneously accomplishing S&C tasks poses unique challenges in receive signal processing. In general, an ISAC receiver should be able to decode useful information from the communication signal, and at the same time detect/estimate targets from the echoes. In the event that the two signals do not overlap, conventional signal processing can be applied unalterably, as both S&C are interference

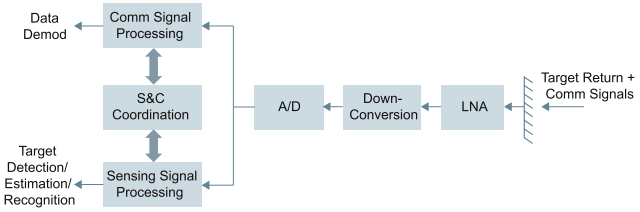

Fig. 13. General structure of an ISAC receiver.

free. However, mutual interference occurs if the two signals are fully/partially overlapped on both temporal and frequency domains, which is the price to pay for acquiring the integration gain.

We demonstrate a generic ISAC receiver structure in Fig. 13, where the mixed communication and echo signals are received from the same antenna array, and are amplified, down-converted, and sampled from an RF chain. The sampled signals are then fed into communication and sensing processors for the purpose of information decoding and target detection/estimation/recognition, where cooperation between S&C is required to facilitate mutual interference cancellation. Within this framework, below we overview state-of-the-art ISAC receive signal processing techniques.

A. Fundamental Insights From a Toy Model

Let us first examine a toy model in an AWGN channel that was considered in [153], [154], where a transmitter wishes to communicate with a receiver in the presence of strong radar interference. The radar signal is modeled as a short-duration pulse with large amplitude, while the communication signal is assumed to possess a small bandwidth and considerably lower power with a 100% duty cycle. From the communication point of view, the radar interference can be approximated as a constant modulus signal, whose amplitude is accurately estimated, but the phase shift randomly fluctuates and thus is difficult to track. In this case, the received signal at the communication receiver is given as [153]

$$y = \underbrace{\sqrt{P_C} s_C}_{\text{Comms Signal}} + \underbrace{\sqrt{P_R} e^{j\theta}}_{\text{Radar Interference}} + \underbrace{z}_{\text{Noise}}, \tag{56}$$

where P_C and P_R represent the received power levels of the communication and radar signals, respectively, which are assumed to be known to the receiver. Moreover, s_C is a communication symbol to be detected, which is drawn from a constellation $\mathcal{S} = \{s_1, s_2, \ldots, s_M\}$, and θ is an unknown phase shift randomly distributed over $[0, 2\pi]$. Finally, z is the Gaussian noise with zero mean and unit variance. Note that we adopt this toy model to simply illustrate the basic problems in ISAC receive signal processing, and thus omit the nonlinearity of the amplifier and assume an ideal RF front-end.

Two fundamental problems arise from the model in (56). The first involves determining the optimal decision region for a given constellation in accordance with the maximum likelihood (ML) criterion. The second is how to design a self-adaptive constellation that optimizes communication metrics, e.g., the communication rate and the SER.

To answer the first question, one may form an ML decoder by averaging over all the possible phases θ, which yields

$$\hat{m}^{opt} = \underset{m\in[1:M]}{\arg\min} \left(\left| y - \sqrt{P_C} s_m \right|^2 - \ln I_0 \left(2\sqrt{P_R} \left| y - \sqrt{P_C} s_m \right| \right) \right), \tag{57}$$

where $I_0(\cdot)$ is the zero-order modified Bessel function of the first kind. For low interference-to-noise (INR) regime, i.e., $\alpha_R\sqrt{P_R} \ll \alpha_C\sqrt{P_C}$, the ML decoder reduces to a Treat-Interference-as-Noise (TIN) decoder, i.e., the radar interference is regarded as noise. This can be approximated by

$$\hat{m}^{opt} = \underset{m\in[1:M]}{\arg\min} \left| y - \sqrt{P_C} s_m \right|^2. \tag{58}$$

In contrast, when $\alpha_C\sqrt{P_C} \ll \alpha_R\sqrt{P_R}$, i.e., the INR is high, the ML decoder can be approximately expressed as

$$\hat{m}^{opt} = \underset{m\in[1:M]}{\arg\min} \left(\left| y - \sqrt{P_C} s_m \right| - \sqrt{P_R} \right)^2, \tag{59}$$

which is known as Interference-Cancellation (IC) receiver, where the radar interference is pre-canceled before communication symbols are decoded. By taking low-, mid-, and high-INR regimes into consideration, the authors analyzed the SER for commonly-employed constellations in detail, including PAM, QAM, and PSK.

Based on the above analysis, one may answer the second question by employing optimization techniques to design interference-aware constellations. The first design, which optimizes the communication rate, i.e., the cardinality of the constellation, can be formulated as [153]

$$\begin{aligned} \max_{\mathcal{S}} \ & M \\ \text{s.t. } & \mathcal{S} = \{s_1, s_2, \ldots, s_M\}, \\ & \mathcal{P}_e(\mathcal{S}) \le \varepsilon, \\ & \frac{1}{M}\sum\nolimits_{m=1}^{M} |s_m|^2 \le 1, \quad s_m \in \mathbb{C}, \end{aligned} \tag{60}$$

where $\mathcal{P}_e(\mathcal{S})$ in the second constraint is the SER of the constellation, which is required to be smaller than a given threshold ε, and the third constraint is imposed as a normalized power constraint. Accordingly, the SER minimization problem can be formulated into [153]

$$\begin{aligned} \min_{\mathcal{S}} \ & \mathcal{P}_e(\mathcal{S}) \\ \text{s.t. } & \mathcal{S} = \{s_1, s_2, \ldots, s_M\}, \\ & \frac{1}{M}\sum\nolimits_{m=1}^{M} |s_m|^2 \le 1, \quad s_m \in \mathbb{C}. \end{aligned} \tag{61}$$

The above two optimization problems are non-convex in general, which can be sub-optimally solved via the MATLAB Global Optimization Toolbox using the Global Search (GS) method. The numerical results show that for both design criteria, the optimal constellation has a concentric hexagonal shape for low-INR regime, and an unequally spaced PAM shape for its high-INR counterpart.

The study of the toy model (56) shows that, in regimes with mid/high radar INRs, one may consider recovering/estimating the radar interference first, and pre-canceling it from the mixed reception y. More importantly, *a good ISAC receiver design should exploit the structural information of the S&C signals*. For instance, the constant modulus of the radar signal is

considered when developing the optimal decoder. In the next subsection, we will show that the hidden sparsity of S&C signals can also be employed for receiver design.

B. ISAC Receiver Design Based on Sparsity

In accordance with the above spirit, a practical receiver design was proposed in [155], where an ISAC receiver received communication signals from a single user, as well as interference from J radar/sensing systems. The aim was to correctly demodulate the encountered communication data while recovering the radar signals. The generic form of the received coded signal can be given as

$$\begin{aligned} y(t) &= y_C(t) + y_R(t) + z(t) \\ &= \underbrace{\sum_{n=0}^{N-1} x(n)\,\varepsilon(t-nT)}_{\text{Comms Signal}} \\ &\quad + \underbrace{\sum_{j=1}^{J}\sum_{n=0}^{N-1} c_j g_j(n)\,\varepsilon(t-nT-\tau_j)}_{\text{Radar Interference}} + \underbrace{z(t)}_{\text{Noise}} \end{aligned} \tag{62}$$

where $y_C(t)$, $y_R(t)$, and $z(t)$ stand for the communication signal, coded radar signal, and noise in the time domain, respectively, $\varepsilon(t)$ is a basic pulse satisfying the Nyquist criterion with respect to its length T, N is the code length for both communication and radar, τ_j and c_j denote the delay and complex channel coefficient between the jth radar interference and the communication receiver, $g_j(n)$ is the nth code for the jth radar signal, and finally, $x(n)$ is the nth communication signal sample. It is assumed that the radar code $\mathbf{g}_j = [g_j(1), g_j(2), \ldots, g_j(N)]^T$ lies in a low-dimensional subspace, spanned by the columns of a known matrix $\mathbf{D}$, such that $\mathbf{g}_j = \mathbf{D}\mathbf{h}_j$. This can be interpreted as an implementation scheme of radar waveform diversity, where radar copes with different situations, e.g., interference, clutter, spectrum sharing, by varying the transmit waveforms via selecting from a given waveform dictionary. Moreover, we have $\mathbf{x} = [x(0), x(1), \ldots, x(N-1)]^T = \mathbf{H}_C\mathbf{b}$, where $\mathbf{H}_C$ and $\mathbf{b} \in \mathcal{B}$ are communication channel and data symbols, respectively, with $\mathcal{B}$ being a communication alphabet. After completing standard signal processing, the received signal can be arranged into a discrete form as

$$\mathbf{r} = \mathbf{H}_C\mathbf{b} + \mathbf{H}_R\boldsymbol{\alpha} + \mathbf{z}, \tag{63}$$

where $\mathbf{H}_R$ is a matrix function of an overcomplete dictionary/grid formed by time delays $\tilde{\tau}_1, \tilde{\tau}_2, \ldots, \tilde{\tau}_{\tilde{J}}$, $\tilde{J} \geq N$ and the known matrix $\mathbf{D}$, and $\boldsymbol{\alpha} = \left[c_1\mathbf{h}_1^T, c_2\mathbf{h}_2^T, \ldots, c_{\tilde{J}}\mathbf{h}_{\tilde{J}}^T\right]^T$. The sparsity-based receiver design is implemented in an iterative manner. To proceed, an initial symbol demodulation is operated over $\mathbf{r}$, yielding an incorrectly detected symbol vector $\hat{\mathbf{b}}^{(0)}$ due to the presence of strong radar interference. One may recover the communication signal by computing $\mathbf{H}_C\hat{\mathbf{b}}^{(0)}$, and subtracting it from $\mathbf{r}$, leading to

$$\begin{aligned} \mathbf{r}^{(1)} &= \mathbf{H}_C\left(\mathbf{b} - \widehat{\mathbf{b}}^{(0)}\right) + \mathbf{H}_R\boldsymbol{\alpha} + \mathbf{z} \\ &\triangleq \mathbf{H}_C\mathbf{v}^{(1)} + \mathbf{H}_R\boldsymbol{\alpha} + \mathbf{z}, \end{aligned} \tag{64}$$

where $\mathbf{v}^{(1)} = \mathbf{b} - \widehat{\mathbf{b}}^{(0)}$ is the demodulation error.

Then, during each iteration we reconstruct $\mathbf{v}$ for communication and $\boldsymbol{\alpha}$ for radar simultaneously (e.g., from $\mathbf{r}^{(1)}$ in (64) in the first iteration), and refine the demodulation process. Given $J \ll N \leq \tilde{J}$, $\boldsymbol{\alpha}$ should be a sparse vector. Furthermore, to minimize the SER, we need $\mathbf{v}$ to be as sparse as possible, i.e., the number of zero elements in $\mathbf{v}$ should be maximized. With these two observations in mind, an iterative on-grid compressed sensing (CS) problem is formulated. For the lth iteration, we have

$$\begin{aligned} \left(\hat{\boldsymbol{\alpha}}^{(l)}, \hat{\mathbf{v}}^{(l)}\right) = \arg\min_{\alpha, \mathbf{v}^{(l)}} \; & \frac{1}{2}\left\|\mathbf{r}^{(l)} - \mathbf{H}_C\mathbf{v}^{(l)} - \mathbf{H}_R\boldsymbol{\alpha}\right\|_2^2 \\ & + \lambda\left\|\mathbf{v}^{(l)}\right\|_1 + \gamma\|\boldsymbol{\alpha}\|_1, \end{aligned} \tag{65}$$

where l_1 norm penalties are imposed to replace the non-convex l_0 norm. Moreover, λ and γ are weights that determine the sparsity of the reconstruction process. After solving the convex problem (65), we obtain the demodulation error $\hat{\mathbf{v}}^{(l)}$. By combining $\hat{\mathbf{v}}^{(l)}$ and $\widehat{\mathbf{b}}^{(l-1)}$, the data symbols can be re-demodulated as

$$\hat{\mathbf{b}}^{(l)} = \arg\min_{\mathbf{b}\in\mathcal{B}} \; \left\|\mathbf{b} - \widehat{\mathbf{b}}^{(l-1)} - \mathbf{v}^{(l)}\right\|_2^2, \tag{66}$$

and we update $\mathbf{v}^{(l+1)}$ and $\boldsymbol{\alpha}$ as

$$\mathbf{v}^{(l+1)} = \mathbf{r}^{(l)} - \mathbf{H}_C\widehat{\mathbf{b}}^{(l)}, \boldsymbol{\alpha} = \hat{\boldsymbol{\alpha}}^{(l)}. \tag{67}$$

The algorithm terminates if $\hat{\mathbf{b}}^{(l)} = \hat{\mathbf{b}}^{(l-1)}$, or if the maximum number of iterations is reached. To further boost the performance, an off-grid CS algorithm can also be developed, where the atomic norm is used instead of the l_1 norm [155].

C. Summary and Open Challenges

In this section, we have discussed the general receive signal processing framework for ISAC systems. We started from a toy model to reveal the fundamental issues emerged in ISAC receive signal processing, i.e., simultaneous target sensing and communication data decoding. Then, we briefly introduced a practical ISAC receiver design based on the sparsity in radar target echoes and communication decoding errors. The relevant open challenges are listed as follows.

1) S&C Signals Classification/Recognition: As discussed above, state-of-the-art ISAC receivers typically process the mixed reception of S&C signals via SIC-type algorithms. To further improve the performance and reduce the receiver complexity, it would be beneficial to directly perform signal classification/recognition by exploiting machine learning techniques. In particular, since the receiver may have prior knowledge of S&C signals, namely, modulation schemes (e.g., QPSK) and sensing waveform formats (e.g., chirp), it is possible to leverage these features to enhance the recognition accuracy.

2) Clutter Suppression: In contrast to communication-only scenarios, clutter is emerged as a new type of interference for ISAC applications, which is generated by the reflection of unwanted targets. In fact, even the targets of interest will interfere with each other, namely the inter-target interference. Therefore, ISAC receiver should be carefully designed to cope with different interference, including conventional communication interference and clutter.

VI. Communication-Assisted Sensing: Perceptive Network

As discussed in Secs. I and II, the sensing functionality is expected to be integrated into the future wireless network to form a perceptive network [43], [156], [157], such that it becomes a native capability that provides various sensing services to users, e.g., localization, recognition, and imaging. In this sense, communication can assist sensing with the following two levels of design methodologies:

1) **Frame-Level ISAC:** Sensing supported by default communication frame structures and protocols, such as Wi-Fi 7 and 5G NR.
2) **Network-Level ISAC:** Distributed/Networked sensing supported by state-of-the-art wireless network architectures, such as Cloud-RAN (C-RAN).

Below we overview the basic framework of the perceptive network and the technical issues raised. Without loss of generality, our discussion is based on a general cellular network, namely a perceptive mobile network (PMN). We refer readers to [2] for a detailed examination on other types of perceptive networks, such as Wi-Fi and the IoT.

A. General Framework

Before presenting the basic framework, we first investigate and classify the objects to be sensed, i.e., the targets, in a PMN. A target to be sensed can either be a communication or non-communication object. The first case often emerges in high-mobility scenarios, where a BS/UE wishes to communicate with a mobile terminal while tracking its movement, which is quite typical in V2X or UAV networks. This will be discussed in Sec. VII in detail, where we show that the V2X beamforming performance can be significantly improved with the aid of downlink active sensing. In the second case, the target usually belongs to the surrounding environment, which needs to be localized, recognized or even imaged for further applications, e.g., high-precision mapping. In this subsection, we do not differentiate between these two types of targets, but instead focus on the technical challenges on realizing sensing using 5G-and-beyond communication infrastructures.

In a PMN, sensing can be performed in ways that are similar to communication links. That is, it can be implemented by using downlink or uplink signals, which are transmitted from a BS or UE, respectively. This accordingly defines downlink and uplink sensing operations. Furthermore, one may define mono-static, bi-static, and distributed/networked sensing operation modes, which are determined by the locations of the transmitter(s) and receiver(s). For clarity, we split the sensing operations in a PMN into the following categories [156]:

1) **Downlink Mono-static Sensing:** Downlink signals transmitted from the BS to the UE are exploited for sensing, while the BS receives the echo signals reflected from targets by its own receiver. In this case, the BS acts as a mono-static radar, for which the transmitter and the receiver are collocated.
2) **Uplink Mono-static Sensing:** Uplink signals transmitted from the UE to the BS are exploited for sensing, and the UE receives the signals reflected from targets by itself.
3) **Downlink Bi-static Sensing:** Downlink signals are exploited for sensing, as they hit the target(s) and are reflected to another BS. This is deemed to be similar to a bi-static radar, where the transmitter and receiver are well-separated.
4) **Uplink Bi-static Sensing:** Uplink signals transmitted from the UE to the BS are exploited for sensing, and the BS receives the uplink signals scattered from the targets. This is again a bi-static radar architecture.
5) **Distributed/Networked Sensing:** Sensing signals can be emitted from multiple transmitters, and are received by multiple receivers after hitting the target. Both BSs and UEs can act as transmitters and receivers. This corresponds to a multi-static radar system, where a certain level of cooperation is required among the transceivers.

Note that uplink mono-static sensing is rarely considered, due to the fact that UEs with small size normally possess limited sensing capability when acting as sensing receiver, which is the general case for small-size UE devices. Nevertheless, we note that for specific UEs with high computational capacity, e.g., vehicles, uplink mono-static sensing could also be possible.

B. Using 5G-and-Beyond Waveforms for Sensing

In this subsection, we provide our insights into the feasibility of using 5G-and-beyond waveform for sensing, and the challenges and opportunities therein.

1) Feasibility: For any sensing operation mode in ISAC systems, a known reference signal is indispensable, either for matched-filtering the received echo signal and thereby to extract the target information, or simply for mitigating the impact of the random communication data. In both 4G LTE and 5G NR, OFDM is the default waveform format, which can be exploited for sensing in the PMN by following the general signal processing pipeline overviewed in Sec. IV-B. Recall that in (49), the dependence of the data is removed from the echo signal via element-wise division. This requires that the communication signal sent from the transmitter is known to the receiver before the target is sensed, which motivates examining the signal resources that are available for sensing within a communication frame.

Let us investigate a standard frame structure for NR, which is based on 3GPP Technical Specification 38.211, Release 15 [158], as shown in Fig. 14. A 5G NR frame lasts for 10 ms, consisting of 10 subframes, each with a duration of 1 ms. Each subframe contains 2^μ time slots, where μ is a numerology ranging from 0 to 5, referring to a subcarrier spacing of $2^\mu \cdot 15$ kHz. Each slot occupies 14 or 12 OFDM symbols, determined by whether normal or extended CP is used.

Fig. 14 (b) shows the structures of 2 time slots for $\mu = 4$, i.e., 28 OFDM symbols. It can be seen that in addition to the data payload, there are 4 signal synchronization blocks (SSBs), each of which occupies 4 OFDM symbols. The components of an SSB include a Primary Synchronization Signal (PSS), a Secondary Synchronization Signal (SSS), Physical Broadcast Channel (PBCH), and its Demodulation Reference Signal (PBCH-DMRS). An SSB is broadcasted periodically for channel estimation and synchronization. Under certain circumstances, multiple SSBs can be transmitted within a localized burst to support possible beam sweeping operations.

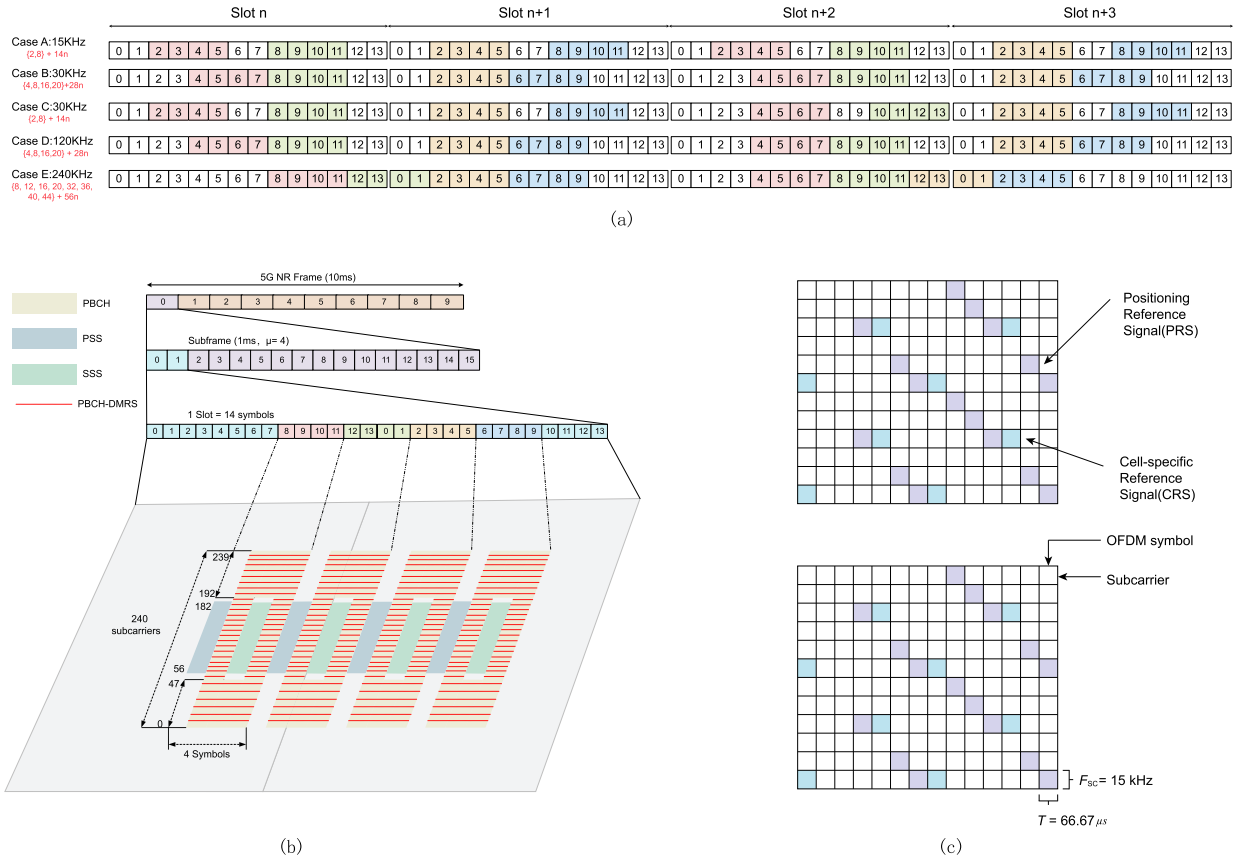

Fig. 14. (a) Five SSB patterns defined in 3GPP 38.211. Their pulse repetition intervals (PRIs) are different such that the time resolution is also different for sensing usage. (b) A signal structure of SSB within a 5G NR frame, where the numerology $\mu = 4$. (c) The time and frequency location of PRS and CRS in a $\mu = 1$ NR frame.

Signals accommodated in an SSB are known to both the BS and UE, and can be easily exploited for sensing. In particular, synchronization signals, i.e., PSS and SSS, are typically with fixed structures, while the PBCH and its DMRS are more flexible and could be optimized for both S&C, through specifically tailored precoding and scheduling schemes. Further to that, the PRS defined in Release 16 of NR can also be readily utilized for localization. These designs fall into the scope of the time-frequency division ISAC approach discussed in Sec. IV-A, where only part of a frame structure is exploited for sensing. In line with the design philosophy of the fully unified waveform, one may further employ the data payload available in the frame for sensing, which would significantly improve the matched filtering gain and the sensing SNR.

2) Challenges and Opportunities: As per the analysis above, we next discuss the critical challenges encountered in waveform-level ISAC design using 5G NR, as well as their potential solutions.

a) Limited bandwidth for high-precision sensing: 3GPP has defined 2 frequency range (FR) types for NR. FR1 (sub-6 GHz) ranges from 450 MHz to 6 GHz, and FR2 (mmWave) ranges from 24.25 GHz to 52.6 GHz. The channel bandwidth is up to 100 MHz in FR1, and 400 MHz in FR 2, which correspond to range resolutions of 1.5 m and 0.375 m, respectively, as per (20). While these resolutions may be sufficient for basic sensing services, they are unable to fulfill the demand of high-precision localization applications, e.g., autonomous vehicles that require sensing resolution at the level of 0.1 m. One possible way to improve the range resolution is to leverage the carrier aggregation (CA) technique, which is able to boost the data rate by assigning multiple frequency blocks to the same user. In this spirit, one may also assign multiple frequency blocks to sense the same target. For example, if 16 carriers are aggregated within the sub-6 GHz band, the overall bandwidth can be up to 1.6 GHz, leading to a range resolution of 0.094 m. However, if the aggregated bandwidths are discontinued, high range sidelobes may occur, possibly resulting in a high false-alarm probability. To that end, proper measures should be taken to reduce the sidelobes.

b) Self-interference in mono-static sensing: For mono-static sensing operation, while both the SSB and the data payload are known and can thus be used for target probing, self-interference (SI) is a problem that cannot be bypassed. Let us take the case with $\mu = 4$ frames as an example, for which the subcarrier spacing is 240 kHz, and the corresponding OFDM symbol plus CP last for 4.46 μs. Such a duration translates to a target at a distance of 670 m. That is, if a target is within the range of 670 m, its echo signal is reflected back to the BS within the duration of one OFDM symbol, while the BS is still transmitting. The signal leaked from the transmitter to the receiver results in strong SI, which saturates the receiver's amplifiers and masks the target return. For a moving target, the SI could be less harmful as long as the BS can distinguish it on the Doppler spectrum. Nevertheless, for static targets, this leads to a "black zone" at the level of 100-1000 m, even if only a single OFDM symbol is

employed, not to mention the use of both the SSB and the data payload, which combine to generate an even larger black zone. In fact, a large signal dynamic range is required to resolve both types of targets, which practical analog-to-digital converters (ADCs) are unable to handle. To address this issue, full-duplex and SI cancellation techniques are necessary [159], [160], or at least a certain degree of isolation between transmit and receive antennas is required. Fortunately, recent research has reported that by leveraging both RF and digital cancelers, a 100 dB SI suppression can be reached for OFDM signaling, which is sufficient for a BS to identify a static drone at a distance of 40 m [161].

c) Unknown data payload in bi-static sensing: For bi-static sensing where the transmitter and receiver are separated, SI is no longer an issue, and known SSB signals can be readily leveraged as sensing waveforms. Nevertheless, the data payload is unable to be straightforwardly utilized, as it may be unknown to the receiver side when there are no direct channels/links in between. To tackle this problem, the receiver may first estimate the channel matrix by using the PBCH available in the SSB, and demodulate the data symbols using the estimated channel. By doing so, the demodulated symbols can be used in conjunction with the SSB for estimating the target parameters of interest.

For clarity, let us revisit the OFDM model presented in (47) by taking the spatial channel into account. Through transmitting a symbol vector $\mathbf{x}_{m,n} \in \mathbb{C}^{N_t \times 1}$ at the n-th subcarrier and the m-th OFDM symbol to sense L targets, which correspond to L propagation paths from the transmitter to the receiver, the received N_r-dimensional signal vector at the same subcarrier and OFDM symbol can be expressed as

$$\mathbf{y}_{m,n} = \sum_{l=1}^{L} \alpha_l e^{-j2\pi(n-1)\Delta f \tau_l} e^{j2\pi f_{D,l}(m-1)T_{\mathrm{OFDM}}} \cdot \mathbf{b}\left(\phi_l\right) \mathbf{a}^H\left(\theta_l\right) \mathbf{x}_{m,n} + \mathbf{z}_{m,n}, \quad (68)$$

where $\alpha_l, \tau_l, f_{D,l}, \phi_l$ and θ_l represent the amplitude, delay, Doppler frequency, AoA and AoD of the l-th target/path, respectively, and $\mathbf{z}_{m,n}$ is a Gaussian noise vector. By letting

$$\begin{aligned} \mathbf{B}(\Phi) &= \left[\mathbf{b}\left(\phi_1\right), \ldots, \mathbf{b}\left(\phi_L\right)\right], \\ \mathbf{A}\left(\Theta\right) &= \left[\mathbf{a}\left(\theta_1\right), \ldots, \mathbf{a}\left(\theta_L\right)\right], \\ \mathbf{C}_n &= \operatorname{diag}\left\{\left[\alpha_1 e^{-j2\pi(n-1)\Delta f \tau_1}, \ldots, \alpha_L e^{-j2\pi(n-1)\Delta f \tau_L}\right]\right\}, \\ \mathbf{D}_m &= \operatorname{diag}\left\{\left[e^{j2\pi f_{D,1}(m-1)T_{\mathrm{OFDM}}}, \ldots, e^{j2\pi f_{D,L}(m-1)T_{\mathrm{OFDM}}}\right]\right\}, \end{aligned} \quad (69)$$

the relation (68) can be written in compact form as

$$\begin{aligned} \mathbf{y}_{m,n} &= \mathbf{B}\left(\Phi\right) \mathbf{C}_n \mathbf{D}_m \mathbf{A}^H\left(\Theta\right) \mathbf{x}_{m,n} + \mathbf{z}_{m,n} \\ &\triangleq \mathbf{H}_{m,n} \mathbf{x}_{m,n} + \mathbf{z}_{m,n}. \end{aligned} \quad (70)$$

For communication purposes, the ISAC channel matrix $\mathbf{H}_{m,n}$ can be estimated via the known pilots in the NR frame, without the need of knowing its inner structure. On the other hand, for sensing purposes, the target parameters $\alpha_l, \tau_l, f_{D,l}, \phi_l$, and θ_l need to be estimated. To proceed, one can either extract these parameters from the estimated channel $\hat{\mathbf{H}}_{m,n}$ directly, or first demodulate the data symbols and reconstruct $\mathbf{x}_{m,n}$ by using $\hat{\mathbf{H}}_{m,n}$, and then estimate the target parameters by further exploiting the reconstructed signal $\hat{\mathbf{x}}_{m,n}$ as a reference signal [156]. With the latter design, not only the target can be more accurately estimated, but also the communication channel estimate can be further refined, which is an example of attaining the coordination gain.

The feasibility of using a 5G waveform for sensing was proven by both system-level simulations [162], and hardware testbed [163]. In [163], a novel smart time and frequency resource filling (STFRF) algorithm was designed to support flexible S&C time-frequency resource configuration. Field test results verified that by leveraging the NR frame structure, an ISAC system could achieve an acceptable target detection performance as well as a stable data rate for communication, at the 28 GHz mmWave frequency band for the autonomous driving vehicle (ADV) scenario [164].

C. Using 5G-and-Beyond Network Architectures for Sensing

In this subsection, we show how 5G-and-beyond network architectures can be utilized for sensing.

1) Feasibility: Over the past several decades, networked sensing has been well-studied for a variety of sensing systems, including wireless sensor network (WSN), multi-static radar, and distributed MIMO radar (a.k.a. MIMO radar with widely separated antennas) [15], [165], [166]. Among these sensing systems, a common structure is that the sensing operation is performed by multiple sensing nodes, and the sensed results are collected by a centralized unit for further processing, e.g., data fusion. By doing so, better sensing performance can be achieved over that of a single-node sensing operation.

Depending on the processing pipeline at the centralized unit, networked sensing can be generally split into the following two categories.

1) **Information-Level Fusion:** Each sensing node performs individual sensing according to its own observations. The sensed parameters are collected and fused at the centralized unit. A conventional WSN that localizes an agent (target) using measurements of received signal strength (RSS), ToA, AoA, and time difference of arrival (TDoA) from anchors (sensing nodes), is a representative system that utilizes information-level fusion [167], [168].
2) **Signal-Level Fusion:** Each sensing node observes the signals reflected/scattered from the target, which can be transmitted from other nodes. The signals, instead of the sensed parameters, are collected and fused at the centralized unit, where an important application of such techniques is distributed MIMO radar [15], [169]. Signal-level fusion is known to be superior to information-level fusion, as the latter may discard important information relevant for sensing by individually processing the sensing signals at each node [165].

While it is plausible that signal-level fusion provides performance gains over its information-level counterpart, it suffers from much higher computational and signaling overheads, as well as increased hardware costs. This is particularly pronounced for distributed MIMO radar, in which case a massive amount of sensed data needs to be communicated to a fusion center with strong computational power.

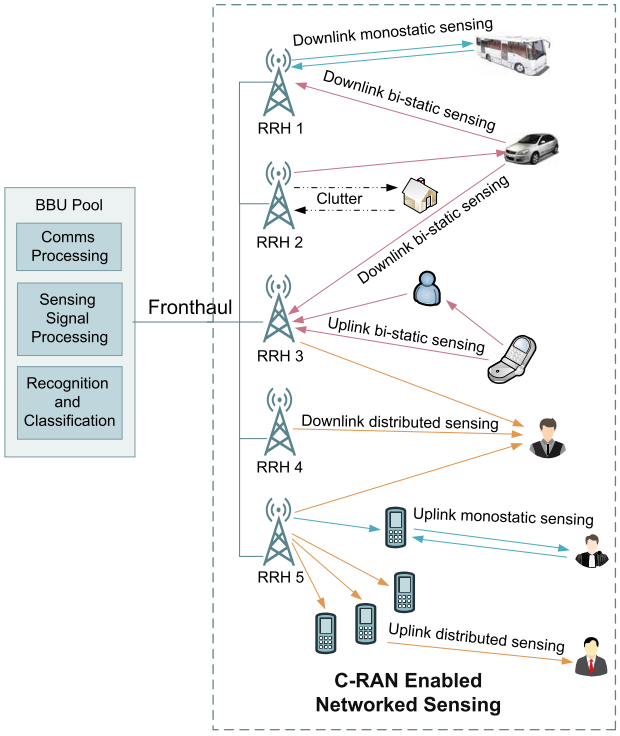

Fig. 15. C-RAN architecture for networked sensing.

Fortunately, the C-RAN architecture designed for 5G-and-beyond communications provides a flexible and reconfigurable framework that enables a variety of the sensing modes discussed above [170], [171]. As shown in Fig. 15, a typical C-RAN consists of a pool of base band units (BBUs), a large number of remote radio heads (RRHs), and a Fronthaul network that connects RRHs to BBUs. The BBU pool is deployed at a centralized site, where software-defined BBUs process the baseband signals and coordinate the wireless resource allocation. Eventually, the BBU pool can act as a centralized signal processing unit for networked sensing. The RRHs are in charge of RF amplification, up/down-conversion, filtering, analog-to-digital/digital-to-analog conversion, and interface adaption, which can be leveraged as radar sensors supported by the NR waveform and relevant ISAC signaling techniques. Finally, the Fronthaul link is typically realized by optical fiber communication technologies with high capacity and low latency, which can be exploited to transmit both S&C data with high reliability [172].

2) Challenges and Opportunities: We end this subsection by identifying the unique challenges and opportunities imposed in C-RAN based ISAC, from a networked sensing perspective.

a) Is inter-cell interference a friend or foe?: In most cases, inter-cell interference in communication networks is recognized as a harmful factor that needs to be reduced. In fact, C-RAN is able to effectively mitigate the inter-RRH interference by using interference management approaches, e.g., coordinated multi-point (CoMP) or soft fractional frequency reuse (S-FFR) techniques [170], [173]. For perceptive networks, however, inter-RRH interference may contain useful information with respect to targets of interest, which needs to be exploited to enhance the sensing performance of the system, rather than being cancelled. More specifically, in addition to receiving the echo signal originating from the mono-static sensing operation, each RRH may also receive the target return generated from the ISAC signals transmitted by other RRHs or UEs, thus to acquire additional coordination gain.

Assuming that there are Q RRHs connected to a BBU pool, and recalling (70), the sensing signals received at the qth RRH, the mth OFDM symbol, and the nth subcarrier can be modeled as [43]

$$\mathbf{y}_{q,m,n} = \mathbf{H}_{q,m,n}\mathbf{x}_{q,m,n} + \sum_{\substack{q'=1 \\ q'\neq q}}^{Q} \mathbf{H}_{q',m,n}\mathbf{x}_{q',m,n} + \mathbf{z}_{q,m,n}, \tag{71}$$

where $\mathbf{H}_{q,m,n}$ represents the ISAC channel matrix for mono-static sensing, $\mathbf{H}_{q',m,n}$ is the ISAC channel matrix for bi-static sensing between the q'th and the qth RRHs, and $\mathbf{x}_{q,m,n}$ and $\mathbf{x}_{q',m,n}$ stand for the OFDM ISAC signals transmitted from the q'th and the qth RRHs, respectively, and finally $\mathbf{z}_{q,m,n}$ is the noise. While the qth RRH may be interested in recovering the target information from the mono-static channel matrix $\mathbf{H}_{q,m,n}$, bi-static channel matrices $\mathbf{H}_{q',m,n}, \forall q' \neq q$ may also contain useful information with respect to the same target, which need to be estimated and recovered. By doing so, the fluctuation in the radar cross section (RCS) of the target can be easily compensated for, since the same target may be sensed from different looking directions [15]. This provides coordination gains to the sensing performance, which is similar to the diversity gain in MIMO communications.

b) Target return as an outlier in C-RAN scheduling: On top of the interference management, sensing operations also impose resource scheduling challenges in a PMN. In the control plane of a C-RAN system, the resource management module is composed of three functions: the context-aware function (CAFun), the resource scheduling function (RSFun), and the reconfiguration function (RFun). The CAFun collects context information, e.g., Channel State Information (CSI), Quality-of-Service (QoS) requirements, and battery consumption levels, from the network and forwards it to the RSFun. The RSFun then generates the scheduling strategy given the context information, and communicates it to the RFun, which executes a scheduling decision for RANs and UEs [172]. In a communication-only C-RAN, the above framework is sufficient to coordinate resource allocation for RRHs and UEs, as they are generally controllable in terms of their transmission and reception operations. Nevertheless, for PMNs, the target return tends to be an outlier, as it can randomly appear in the time, frequency, and spatial domains. To this end, novel scheduling approaches are needed to incorporate the prediction of target echoes into the control plane.

c) Network synchronization: A more critical challenge occurs in the sensing scenario between multiple UEs and RRHs. While RRHs can be precisely synchronized at a clock level since they are connected to the centralized BBU via fronthaul links, UEs and RRHs are unlikely to be clock-synchronized due to the wireless channel in between. This leads to severe phase noise in terms of the timing offset (TO) and carrier frequency offset (CFO) between the sensing transmitter and receiver, thereby causing ambiguity

TABLE IV
FEASIBLE TECHNIQUES AND CHALLENGES IN PERCEPTIVE MOBILE NETWORK

Sensing Operation Modes	Feasible Techniques	Challenges
Downlink Mono-static (RRH mono-static sensing)	Using both SSB and data for sensing	• SI cancellation • transmitter/receiver isolation
Downlink Bi-static (RRH-RRH bi-static sensing)	Using both SSB and data for sensing	• Interference management
Uplink Bi-static (UE-RRH bi-static sensing)	Using SSB only for sensing	• Low matched-filtering gain • Synchronization issue
	Using both SSB and data for sensing	• Unknown data payload • Synchronization issue
Networked Sensing	Using C-RAN architecture for sensing	• Interference management • Scheduling with target return • Network synchronization issue

when estimating the delay and Doppler frequency of the target. As an example, a clock stability of 20 parts per million (PPM) may generate a TO of 20 ns over 1 ms, which leads to a ranging error of 6 m [49]. For typical coherent radar signal processing across packets/pulses, the sensing performance will be seriously degraded due to the accumulation of the TO and CFO. To overcome this challenge, a cross-antenna cross-correlation method was proposed for passive Wi-Fi sensing [174]. A more recent work addressing this issue for uplink sensing between a UE and an RRH is [157], where MUSIC-like algorithms were developed to further enhance the performance of the method proposed in [174].

D. Summary

This section has considered the general framework for PMN, which is able to perform large-scale networked sensing supported by 5G-and-Beyond waveforms and network architectures, namely, frame-level ISAC and network-level ISAC. We first categorized sensing operations in a PMN into downlink/uplink mono-static sensing, downlink/uplink bi-static sensing, and distributed sensing, and then provided a detailed discussion on the feasibility and challenges of two levels of ISAC designs under above sensing deployments.

In light of the discussion above, we summarize the feasible techniques and challenges of PMNs in TABLE. IV. Among all the sensing operation modes, we highlight that downlink bi-static sensing between RRHs is the most promising technique. Since RRHs are connected via fronthaul links to the BBU pool, both the SSB and the data payload transmitted from one RRH can be straightforwardly known by another RRH through coordination, and can thus be exploited for sensing. This also removes the necessity of complicated phase noise compensation and synchronization algorithms thanks to the high-capacity and low-latency optical fiber fronthaul.

VII. SENSING-ASSISTED COMMUNICATION

Despite being rarely discussed in an explicit manner, communication systems are often assisted by sensing in a general setting. An example is the estimation of CSI before data transmission by sending pilots from the transmitter to the receiver. Another example for sensing-assisted communication is spectrum sensing in the context of cognitive radio, where the secondary user detects the presence of the primary user over a frequency band of interest, and then utilizes the spectrum to transmit information if the band is not occupied [175]–[177]. While sensing techniques have indeed been employed to assist with communication in the aforementioned applications, we underline that conventional sensing-assisted communication schemes generally rely on device-based and cooperative sensing, i.e., a sensing device should be attached to the sensed target, where device-free techniques such as radar sensing remain widely unexplored for improving the communication performance.

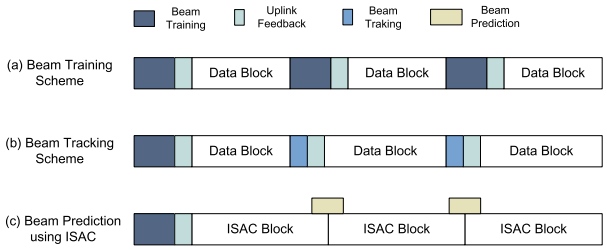

Fig. 16. Frame structures for feedback based beam training and tracking, and ISAC based beam prediction.

In what follows, we take the sensing-assisted V2X network as an example, to shed light on how sensing, especially device-free sensing, can be employed to enhance mmWave communication performance, thus pursuing the coordination gain. For convenience, we consider mono-static sensing with the assumption that the SI is fully cancelled.

A. Sensing-Assisted Beam Training

In mmWave communication systems, a communication link is configured via classical *beam training* protocols [178], [179]. As illustrated in Fig. 16, the transmitter sends pilots to the receiver over different spatial beams. The receiver measures the SNR of the received pilots by leveraging different receive combiners/beamformers, and feeds back the indices of the beam pair that yields the highest SNR to the transmitter. In this way, the transmit and receive beams are aligned with each other. Nevertheless, an exhaustive search of the optimal pair requires a large number of pilots as well as frequent uplink feedback, which leads to large overheads and high latency.

To guarantee the communication QoS for latency-critical applications such as V2X networks, the beam training overhead needs to be reduced to the minimum, which motivates research on sensor-aided beam alignment. Indeed, by leveraging the prior information provided by the sensors, such as GNSS, radar, lidar, and cameras, the search space of the beams can be narrowed down [180]. It has been shown in [181] that,

for a V2I communication system with $64\times16 = 1024$ beam pairs, the search space can be reduced to 475 beam pairs through the use of the positioning information generated by the GPS, and to 32 beam pairs with the help of radar-based positioning, both of which attain the same accuracy compared to the exhaustive search method. In addition, it is also possible to use a hierarchical beam search method in conjunction with the positioning information obtained from the sensors, which further reduces overheads.

A more interesting example can be found in [182], where an MIMO radar mounted on an RSU is exploited to sense the vehicle. By assuming that the radar and communication channels share the same dominant paths, the covariance matrix of the communication channel can be estimated by relying on echo signals. Based on this information, the RSU can further design a precoder and send pilots to the vehicle to facilitate its receive beamforming. In this case, feedback between the vehicle and the RSU is no longer needed, as the channel reciprocity is employed.

B. Sensing-Assisted Beam Tracking and Prediction

Once the communication link is established, i.e., the initial access is accomplished by beam training, both the transmitter and receiver are required to keep tracking the variation of the optimal beam pairs for the purpose of preserving the communication quality, which is known as *beam tracking* [183], [184]. Beam tracking schemes exploit the temporal correlation between adjacent signal blocks, i.e., the previously estimated beams are utilized as prior information for the current epoch. By doing so, the search space of the beams can be maintained within a small interval centered around the previous beam, thus avoiding the transmission of redundant pilots. Nonetheless, the receiver still needs to feed the optimal beam index back to the transmitter in each of beam tracking cycles. Again, it is possible to remove the feedback loop by using a radar sensor mounted on the transmitter.

By taking a closer look at the above radar-aided beam training and tracking schemes, we see that an S&C coordination gain is achieved by reducing the training overhead, but this comes at the cost of extra radar hardware, i.e., with the loss of integration gain [181], [182]. Moreover, in high-mobility communication channels, e.g., V2X channels, it is necessary to have the capability of *beam prediction*, as beam tracking may not be sufficient to adapt to fast-changing channels. To address these issues, the authors of [82], [83] consider employing ISAC signaling in V2I beam tracking and prediction, which demands no dedicated sensors and hence realizes both integration and coordination gains.

Consider an ISAC-enabled V2I downlink shown in Fig. 17, where an RSU equipped with N_t transmit and N_r receive antennas is serving a single-antenna vehicle in the LoS channel. An ISAC signal is transmitted on a block-by-block basis. At the nth transmission block, the vehicle's state is represented by $\mathbf{x}_n = [d_n, v_n, \theta_n]^T$, where d_n, v_n, and θ_n are the distance, velocity, and azimuth angle of the vehicle relative to the RSU, respectively, which are assumed to be constant within a single block. Suppose that the initial access is achieved via radar-aided beam training method upon the arrival of the vehicle, based on which the RSU acquires the parameter estimates $\hat{\mathbf{x}}_0 = \left[\hat{d}_0, \hat{v}_0, \hat{\theta}_0\right]^T$. The RSU then tracks and predicts the vehicle's state by following the steps below.

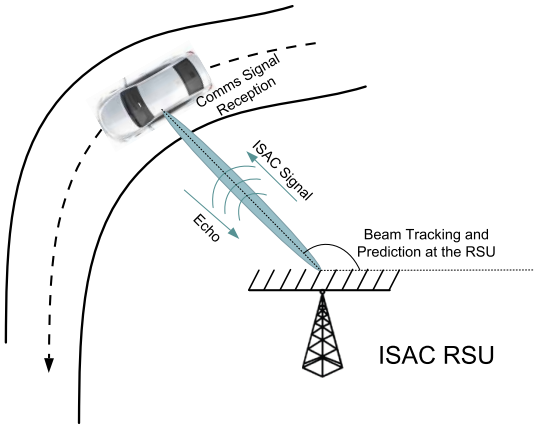

Fig. 17. ISAC-enabled V2I downlink system.

1) State Prediction: At the $(n-1)$th epoch, the RSU predicts the vehicle's state at the nth epoch as

$$\hat{\mathbf{x}}_{n|n-1} \triangleq \left[\hat{d}_{n|n-1}, \hat{v}_{n|n-1}, \hat{\theta}_{n|n-1}\right]^T = \mathcal{P}\left(\hat{\mathbf{x}}_{n-1}\right), \quad (72)$$

where $\hat{\mathbf{x}}_{n|n-1}$ stands for the nth predicted state based on the $(n-1)$th estimate, and $\mathcal{P}(\cdot)$ is a predictor, which can be designed either through model-based or model-free methods. While the model-based prediction typically relies on the vehicle's kinetic model, model-free approaches can be built upon machine learning frameworks, which is particularly useful in the case of complex traffic environment and channel conditions.

2) Beamforming: With the predicted angle $\hat{\theta}_{n|n-1}$ at hand, the RSU transmits the following ISAC signal to the vehicle at the nth epoch

$$\tilde{\mathbf{s}}_n(t) = \mathbf{f}_n^H s_n(t), \quad (73)$$

where $\mathbf{f}_n$ and $s_n(t)$ are the predictive beamformer and the unit-power data stream intended for the vehicle at epoch n, respectively. The beamformer $\mathbf{f}_n$ is given by

$$\mathbf{f}_n = \mathbf{a}\left(\hat{\theta}_{n|n-1}\right), \quad (74)$$

where $\mathbf{a}(\theta) \in \mathbb{C}^{N_t\times1}$ is again the transmit steering vector. Accordingly, the received signal at the vehicle can be expressed as

$$y_{C,n}(t) = \alpha_n \mathbf{a}^H(\theta_n)\mathbf{f}_n s_n(t) + z_{C,n}(t), \quad (75)$$

where α_n and $z_C(t)$ represents the channel coefficient and the AWGN with zero mean and variance σ_C^2, respectively. The achievable rate can be computed as

$$R_n = \log\left(1 + \frac{\left|\alpha_n \mathbf{a}^H(\theta_n)\mathbf{f}_n\right|^2}{\sigma_{C,n}^2}\right). \quad (76)$$

If the predicted angle is sufficiently accurate, i.e., $\left|\hat{\theta}_{n|n-1} - \theta_n\right| \approx 0$, then the resulting high beamforming gain $\mathbf{a}^H(\theta_n)\mathbf{f}_n$ is able to support reliable V2I communications.

3) State Tracking: Once the ISAC signal hits the vehicle, it is partially recived by the vehicle's receiver, and is also partially reflected back to the RSU. The received echo signal at the RSU can be modeled as

$$\mathbf{y}_{R,n}(t) = \beta_n e^{j2\pi f_{D,n} t} \mathbf{b}(\theta_n) \mathbf{a}^H(\theta_n) \times \mathbf{f}_n s_n(t-\tau_n) + z_{R,n}(t), \quad (77)$$

where β_n is the reflection coefficient, $f_{D,n} = \frac{2v_n f_c}{c}$ is the Doppler frequency, with f_c and c being the carrier frequency and the speed of the light, respectively. Again, $\mathbf{b}(\theta)$ denotes the receive steering vector. $\tau_n = \frac{2d_n}{c}$ stands for the round-trip delay. Finally, $z_{R,n}(t)$ is the AWGN with zero mean and variance of σ_R^2. By inputing (77) into the estimator $\mathcal{F}(\cdot)$, the nth state can be estimated as

$$\hat{\mathbf{x}}_n = \mathcal{F}(\mathbf{y}_{R,n}). \quad (78)$$

Alternatively, by taking the prediction $\hat{\mathbf{x}}_{n|n-1}$ into account, one can use a Bayesian filter $\mathcal{F}_B(\cdot)$, e.g., Kalman filter, to improve the estimation precision. This can be expressed as

$$\hat{\mathbf{x}}_n = \mathcal{F}_B\left(\mathbf{y}_{R,n}, \hat{\mathbf{x}}_{n|n-1}\right). \quad (79)$$

The estimate $\hat{\mathbf{x}}_n$ is then served as the input of the predictor for the $(n+1)$th epoch.

By iteratively performing state/beam prediction and tracking, the RSU is able to keep up with the movement of the vehicle, while preserving a high-quality V2I downlink. As observed from the ISAC frame structure shown in Fig. 16, ISAC based beam tracking /prediction schemes outperform communication-only protocols in the following aspects [185].

1) **No downlink pilots are needed:** The entire ISAC signal block is exploited for both V2I communication and vehicle sensing, where dedicated downlink pilots are no longer needed. This reduces downlink overheads, while simultaneously improving radar estimation performance.
2) **No uplink feedbacks are needed:** The uplink feedback signal is replaced with the echo signal reflected by the vehicle, which reduces the uplink overheads.
3) **No quantization errors:** The communication-only scheme requires quantizing the estimated angle before feeding it back to the RSU. In contrast to that, the ISAC scheme performs continuous angle estimation by relying on the echoes received by the RSU, which improves the resulting estimation accuracy.
4) **Significant matched-filtering gain:** The use of the entire ISAC signal block for radar sensing benefits from the matched-filtering gain, which is equal to the ISAC block length. In general, the matched filtering gain that spans the whole communication block, is much more significant than that of the feedback based scheme, where only a limited number of pilots are used for beam tracking. As a result, the estimation accuracy is improved.

In Fig. 18, we consider a scenario where a 64-antenna RSU serves a vehicle on a straight road, where the vehicle drives from one side at a distance of 25 m and a speed of 18 m/s, passing by the RSU to another side. Since the RSU transmits at a fixed power, the communication rate firstly increases and then decreases. We compare the achievable rate of the ISAC scheme using extended Kalman filtering (EKF), with that of a feedback-based communication-only scheme, namely the auxiliary beam pair (ABP) tracking method proposed in [184]. It can be observed that while the ISAC scheme maintains a relatively stable rate, the achievable rate of the ABP technique drastically decreases to zero at 1040 ms, as it loses the track of the vehicle's angle. This further proves the superiority of ISAC signaling for V2I beam tracking and prediction.

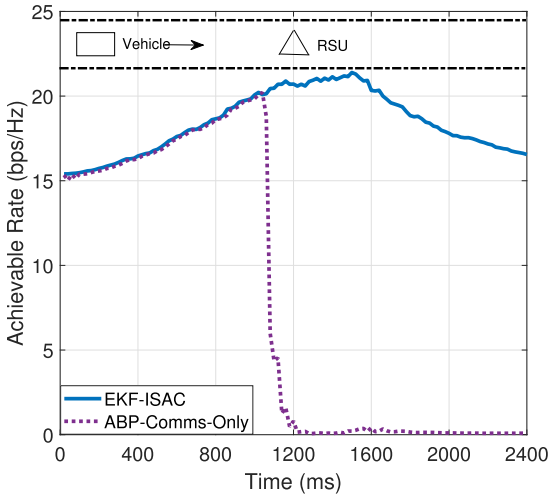

Fig. 18. Achievable rates comparison of the ISAC based and communication-only beam tracking schemes.

While the above study mainly focuses on V2I communications, it can be generalized to the V2V scenairo in a straightforward manner, for which the above features still hold. In addition, it is worth highlighting that the feasibility of sensing-assisted beam tracking was verified in [186] by using the PSS slot in a 5G NR communication frame structure for sensing, where the novel smart weighted grid searching (SWGS) based fast beam alignment and beam tracking algorithms were designed for the ISAC enabled ADV scenario, and field test results were provided.

C. Sensing-Assisted Resource Allocation

Apart from assisting in mmWave beamforming, sensing can also be a powerful tool for supporting the efficient allocation of more general wireless resources.

1) Sensing-Assisted Cell Handover: Let us consider again a V2I downlink, where a vehicle drives from one cell into another. In order to provide continuous communication service, handover is typically needed between the RSUs. The conventional handover protocol is built upon dual-connection techniques [187], in which the vehicle is connected simultaneously with a serving RSU and an idle RSU. The QoS of the two links is measured by their receive SINR, i.e., $\text{SINR}_{\text{serve}}$ and $\text{SINR}_{\text{idle}}$. If $\text{SINR}_{\text{serve}} < \text{SINR}_{\text{idle}}$ due to blockage or large distance, then the serving RSU hands over and forwards the buffered data to the idle RSU. Given the high mobility of the vehicle, frequent handovers and re-connections, which consume extra wireless resources, are needed. In view of that, a more efficient approach is to equip RSUs with the ISAC ability, such that the idle RSU can actively monitor the vehicle's state, including its distance, velocity, azimuth angle, and heading direction, by sending ISAC signals and hearing their echoes. These results are then exploited to estimate the

time and location at which the vehicle enters into the idle RSU's coverage. Accordingly, the RSU then prepares the resources and data intended for the vehicle in advance, such that seamless high-quality service can be provided in an almost handover-free mode.

Under the framework above, it would be even more interesting to consider V2X scenarios where multiple vehicles are served simultaneously. Resource allocation can again be designed based on sensing the kinematic states, driving environments, and geometrical relationship of vehicles, where both S&C performance should be considered. Below we list some potential allocation strategies for different resources.

2) Bandwidth Allocation: Bandwidth allocation for communications aims to maximize the spectral efficiency, or to satisfy the individual QoS requirement of users. In the case that the spectrum is reused among multiple users, bandwidth allocation should also take the avoidance/mitigation of mutual interference [188], [189] into account. While bandwidth is key to increasing the communication rate, one may recall from (21) that it also determines the range resolution achievable for sensing. In ISAC-powered V2X networks, different vehicles may demand different S&C services, and hence have various needs for communication rate and sensing resolution. All these requirements can be imposed as constraints in bandwidth allocation designs given the overall available spectrum [190].

3) Beamwidth Allocation: Beamwidth plays an important role in both S&C [191]. For faraway vehicles that are deemed to be point-like targets, the transmit beam can be made as narrow as possible, thus providing both high beamforming gain for communication and superior angular resolution for sensing. For nearby vehicles, however, the situation becomes distinctly different, as the vehicle is no longer viewed as a point target but rather as an extended target. To sense the vehicle, a wide beam should be employed to cover the vehicle's body. On the other hand, a narrow beam is still preferred for communication, since the RSU should accurately steer the beam towards the receive antennas mounted on the vehicle. Moreover, it is readily seen that velocity also affects beamwidth allocation, where narrow and wide beams are preferred for low- and high-speed vehicles, respectively [192].

4) Power Allocation: Power allocation affects almost all aspects of S&C, as it is involved in all the related performance metrics. For multi-user communications, while the classical water-filling power allocation design is able to maximize the communication rate, it is not able to address the issue of minimizing estimation errors. In V2X scenarios where both high-throughput communication and high-accuracy localization services are required, S&C performance metrics including the CRB and communication rate, should be considered simultaneously in the problem formulation. For instance, ISAC power allocation designs were proposed in [82], [193], where the CRB for vehicle tracking was minimized, subject to the sum-rate constraints of multiple vehicles.

While Sec. VII mainly concentrates on vehicular communications served by radar, we remark that sensing, not only mono-static sensing, can indeed assist in a wide variety of communication applications that require low overhead and latency, as well as efficient resource allocation [194].

D. Sensing-Assisted PHY Security

The compelling applications emerging with 5G and beyond such as remote-Health, V2X communications, are expected to carry confidential personal data. Ensuring security and privacy is of key importance, and traditional cryptographic techniques developed at the network layer [195] face a number of issues, most importantly an increasing vulnerability with the relentless growth of computational power. Critically, cyber threats start from the acquisition of access to wireless traffic, and this has motivated decades-long research regarding security solutions at the PHY.

Furthermore, ISAC transmission poses unique security challenges. The inclusion of data into the probing signal, used to illuminate targets, makes it prone to eavesdropping by potentially malicious radar targets [196]. Even if the data itself is protected with higher layer encryption, the existence of a communication link can still be detected by a malicious target that can jeopardize the communication privacy, reveal the AP's location and ID and make it prone to cyberattacks [197]–[199]. Classical communication-only PHY security solutions often involve reducing the signal power in the direction of the eavesdropper (target), which would severely deteriorate the sensing performance of ISAC. There is an abundance of communication-only PHY layer security approaches, ranging from secure beamforming, jamming, and artificial noise design, to cooperative security designs [200], that could be adopted to address this challenge. Recent work has focused on addressing this vulnerability of ISAC by designing secure ISAC transmission methods [196], [201]. This aims to address the conflicting objectives of illuminating signal energy to the radar target, while at the same time constraining the useful signal energy (SNR) towards the same direction of the sensed target, to inhibit its capability to eavesdrop the information signal sent to the communication users.

In addition to the unique security challenges encountered by ISAC, it provides key opportunities to address the limitations of PHY security solutions. Importantly, the sensing functionality offers new opportunities with respect to making PHY security solutions practical [202]. The major limitation of a large class of PHY security solutions stems from the need to know the eavesdroppers' (Eves) channels, or direction as a minimum. The sensing capability has been an enabling role for PHY security, where the detected targets' (Eves') AoAs can be used to enable null steering and secure beamforming, and provides new ground for the development of sensing-assisted secure communications.

The provision of security is an additional requirement in the wireless network of the future, that gives rise to new and unexplored tradeoffs at the cross-domain among communications, sensing, and security.

E. Summary and Open Challenges

In this section, we overviewed (device-free) sensing-assisted communication techniques under the scenario of V2X networks. We have shown that sensing facilitates efficient beam management in terms of beam training, tracking, and prediction. More interestingly, in addition to beam resouces, sensing can also be useful in allocating and managing more general wireless resources, e.g., bandwidth and power, in a high-mobility network. Finally, we ended this section by a

brief prospect on sensing-assisted PHY security designs. The relevant open challenges are listed as follows.

1) Correlation Model Between S&C Channels: It can be noted from the above that sensing-assisted communication designs generally leverge the correlation between S&C channels to reduce the communication overheads and thus improving the efficiency. For instance, sensing-assisted V2X beam training, tracking and prediction approaches are based on the fact that a vehicle is both a communication receiver and a radar target, such that the S&C channels are closely correlated. Nevertheless, it is still unclear how to accurately model this correlation in a practical channel environment, which is key to developing efficient ISAC transmission schemes.

2) Quantative Description of Coordination Gain: In most of the state-of-the-art ISAC literature, the mutual performance gain between S&C is analyzed in a qualitative way, and is typically scenario-specific. Currently, there is no effective approach to describe the ISAC coordination gain neither quantatively nor in a unified manner. A deeper investigation into this issue will bring forward fruitful and promising theoretical breakthroughs within the area of ISAC.

VIII. Interplay Between ISAC and Other Emerging Technologies

In this section, we speculate on the potential interplay and connections between ISAC and other emerging communication technologies.

A. ISAC Meets Edge Intelligence

Edge intelligence has been recognized as another key technology for next-generation wireless networks such as 6G (see, e.g., [203]). Driven by the recent success of mobile edge computing (MEC) [204], [205], edge intelligence pushes computation-intensive artificial intelligence (AI) tasks from the centralized cloud to distributed BSs at the wireless network edge, to efficiently utilize the massive data generated at a large number of edge devices. Integration with edge intelligence is important for unlocking the full potential of ISAC [206]. In particular, ISAC is expected to generate a large volume of data at distributed wireless transceivers, which need to be properly processed (potentially jointly processed with sensed data from other sensors such as camera and lidar) via AI algorithms in a swift manner (e.g., for recognition), in order to support applications with ultralow-latency sensing, communication, computation, and control requirements [206], [207]. Towards this end, federated edge learning has emerged as a promising solution, where sensing devices can iteratively exchange their locally trained AI models to update the desired global AI model in a distributed manner, while preserving data privacy at each sensing device, as shown in Fig. 19 [208], [209].

The integration between ISAC and edge intelligence poses new technical challenges [210]. First, due to the scarcity of spectrum resources, the wireless communication for the exchange of AI models between sensing devices and edge servers is recognized as the performance bottleneck for federated edge learning. With the integration of ISAC, this issue will become even more severe, as the limited spectrum resources need to be further reused to support the radio sensing functionality. To resolve this problem, a new multiple access

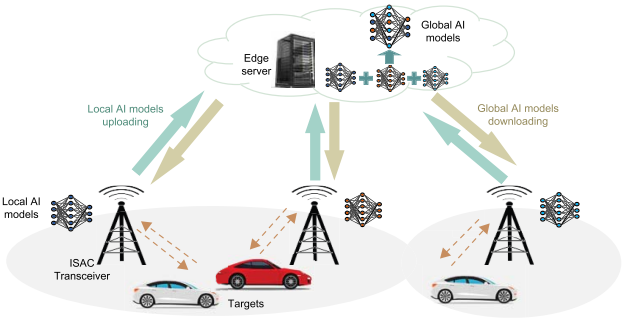

Fig. 19. ISAC meets edge intelligence.

technique, namely over-the-air computation (AirComp) [211], has been utilized to enhance the communication efficiency of federated edge learning (see, e.g., [212]), in which the sensing devices can simultaneously transmit their local AI models over the same frequency band for global aggregation, by exploiting the wireless signal superposition at the edge server. It becomes an interesting new research direction to coordinate the integration of AirComp with ISAC. How to optimize the power control (see, e.g., [213]) and wireless resource allocation schemes to balance the AirComp and sensing performances, and how to properly control the multi-cell sensing and AirComp interference (see, e.g., [214]) are interesting problems to be investigated. Proper precoding design may also play an important role (see, e.g., [215]).

Furthermore, the integration of ISAC and edge intelligence introduces more complicated tradeoffs among the sensing, communication, and computation. In particular, the demand for higher sensing accuracy and resolution in ISAC may lead to more data needing to be processed, which thus will induce higher communication and computational burdens. To deal with such tradeoffs, the joint design over the sensing-communication-computation flow is crucial, in which the ultimate goals of the AI tasks (e.g., recognition accuracy) should be adopted as new optimization objectives (instead of considering conventional sensing/communication metrics). For instance, adaptive AI-task-aware ISAC may be an interesting direction worth pursuing, where the sensing devices can adaptively adjust their sensing area/accuracy/resolution based on the requirements of AI tasks subject to wireless and computational resource constraints.

B. ISAC Supported By Reconfigurable Intelligent Surface (RIS)

Reconfigurable intelligent surface (RIS), also known as intelligent reflecting surface (IRS) and large intelligent surface (LIS), is a new type of passive metamaterial device consisting of a large number of reflecting elements whose reflecting amplitudes and phases can be independently controlled to reconfigure the wireless environment [216], [217]. While RISs have shown great potential in increasing the spectrum and energy efficiency of wireless communications, they are also expected to benefit the ISAC by providing better sensing coverage, accuracy and resolution. First, in conventional ISAC systems, sensing generally depends on the LoS link between the ISAC transmitter and the target of interest. How to sense targets without LoS connections is quite challenging. To resolve this issue, an RIS can serve as a viable new solution

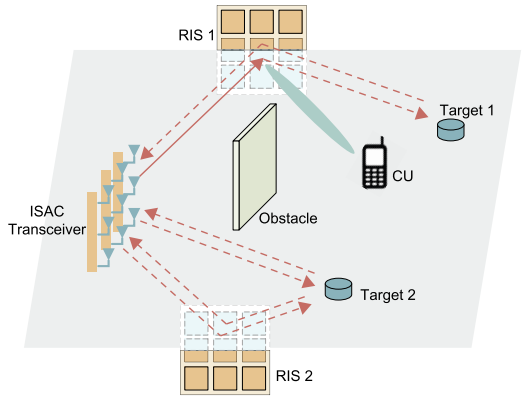

Fig. 20. ISAC served by reconfigurable intelligent surface.

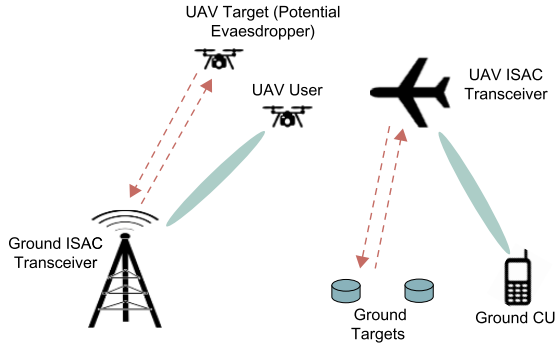

Fig. 21. ISAC with unmanned aerial vehicles.

by potentially providing additional LoS links with targets in those conventionally NLoS covered areas, as shown in Fig. 20. Next, RIS is also beneficial for facilitating the sensing of targets with LoS links, via providing an additional link to see the targets from a different angle, thus potentially enhancing the sensing and localization accuracy and resolution [218], [219]. To fully reap these benefits, it is important to properly design the deployment locations of RISs based on the new sensing requirements, and optimize their reflecting amplitudes and phases in real time by taking into account the new sensing performance metrics and new co-channel sensing-communication interference. This is a challenging task, especially when there are many RISs deployed in a distributed manner and when the RIS-related network information is only partially available due to its passive nature.

On the other hand, ISAC in return can also be useful for enhancing wireless communication performance with RISs. One of the key technical challenges faced in RIS-enabled wireless communications is that the RIS-related CSI is difficult and costly to obtain due to the lack of signal processing capability at the RIS, thus making beam tracking and beam alignment difficult. In this case, by employing the sensing function to measure the parameters related to communication users (e.g., the AoA/AoD parameters), ISAC provides an alternative approach for acquiring the CSI to facilitate the passive RIS beamforming.

C. ISAC With UAVs

With recent technical advances, UAVs have found abundant applications in wireless networks, e.g., as aerial users, relays, BSs, or APs. In this case, wireless networks are experiencing a paradigm shift from conventional terrestrial networks to terrestrial-and-aerial integration (see, e.g., [220] and the references therein). As a result, the interplay between UAVs and ISAC is becoming another interesting research topic, in which UAVs may act as sensing targets, communication users, and aerial ISAC platforms, depending on the different application scenarios discussed in Sec. II.

First, similar to conventional radar, ISAC enabled cellular networks can be used to detect and monitor undesirable or suspicious UAV targets in the sky to protect cyber and physical security. Next, when UAVs are connected to wireless networks as communication users, the on-ground BSs can send ISAC signals to localize these UAVs during communications, and measure the related channel parameters [221]. Such information may be utilized to facilitate the transmit beam tracking and wireless resource allocation, thus increasing the communication data rate and reliability, mitigating severe ground-air interference, and enhancing data security with reduced signaling overhead. Finally, UAVs can act as mobile aerial platforms to perform ISAC with on-ground targets and communication users [222]. This is appealing for both sensing and communication, as UAVs are highly likely to have strong LoS links towards users. Due to their fully controllable mobility, UAVs are able to maneuver towards desired locations to provide ISAC services on demand, and their maneuver control provides a new DoF for optimizing ISAC performance. The proper design of the ISAC signal processing and resource allocation, together with the UAVs' deployment or trajectory optimization, is an interesting but challenging problem. Moreover, as discussed in Sec. VII-D, the security of ISAC transmission should be guaranteed in the event that an unauthorized UAV eavesdrops on the information intended for a legitimate UAV user.

D. Others

In addition to the above research directions, ISAC may also find potential usages in conjunction with other emerging and important technologies, e.g., low-earth-orbit (LEO) satellite networks [223], [224], Terahertz (THz) communications and sensing [225], [226], digital twins [227], [228], orthogonal time frequency space (OTFS) modulation [229]–[231], and more. Given the page limit, we will not elaborate on these aspects.

IX. Conclusion

In this paper, we provided our vision of future dual-functional wireless networks supported by integrated sensing and communications (ISAC) technologies. To begin with, we overviewed the historical development of radar and communications systems, based on which a formal definition and rationale for ISAC was given, followed by the definition of two types of gains in ISAC, namely, integration gain and coordination gain. On top of that, we discussed various applications and use cases supported by ISAC, including sensing as a service, smart home and in-cabin sensing, V2X, smart manufacturing, remote sensing and geoscience, environmental monitoring, and human-computer interaction, and then elaborated on the industrial progress and relevant standardization activities of ISAC.

We further investigated the technical foundation of ISAC, from the performance tradeoff between S&C, to the ISAC

waveform design, and to the ISAC receiver design. First, we showed that due to the shared use of wireless resources and contradictory design objectives, S&C tradeoffs generally emerge at numerous domains, including tradeoffs in information-theoretical limits, physical layer metrics, S&C channel DoFs and cross-layer designs. Second, we discussed several ISAC waveform design methodologies, ranging from non-overlapped resource allocation based design, sensing-centric design, communication-centric design, and joint design. Finally, we motivated the basic problems in ISAC receiver design from a toy model, and introduced an SIC-type signal processing approach based on the sparse structure of S&C signals.

As a step forward, we demonstrated the great benefits achieved by communication-assisted sensing and sensing-assisted communication, which pave the way towards future perceptive networks. We commenced by introducing the general framework of perceptive mobile network (PMN), and then discussed the feasibility and challenges of using 5G-and-beyond waveforms and networking architectures to support frame-level and network-level ISAC in a PMN, respectively. On this basis, we considered the sensing-assisted communication designs under typical V2X scenarios, including but are not limited to, sensing-assisted beam management, resource allocation, and PHY security.

As a final remark and a prospect, we examined the potential interplay between ISAC and other emerging communication technologies, including ISAC with edge intelligence, RIS, and UAV.

While there are still quite a lot of technical challenges remain open in the fundamental theory, signal processing, and networking aspects of ISAC, tremendous research efforts from both academia and industry are well-underway to make ISAC a reality in the next-generation wireless network. We firmly believe that ISAC will not only serve as the foundation of the new air interface for the 6G network, but will also act as the bond to bridge the physical and cyber worlds, where *everything is sensed, everything is connected, and everything is intelligent.*

REFERENCES

[1] W. Saad, M. Bennis, and M. Chen, "A vision of 6G wireless systems: Applications, trends, technologies, and open research problems," *IEEE Netw.*, vol. 34, no. 3, pp. 134–142, 2019.

[2] Y. Cui, F. Liu, X. Jing, and J. Mu, "Integrating sensing and communications for ubiquitous IoT: Applications, trends, and challenges," *IEEE Netw.*, vol. 35, no. 5, pp. 158–167, Sep. 2021.

[3] C. Sturm and W. Wiesbeck, "Waveform design and signal processing aspects for fusion of wireless communications and radar sensing," *Proc. IEEE*, vol. 99, no. 7, pp. 1236–1259, Jul. 2011.

[4] P. Kumari, A. Mezghani, and R. W. Heath, "JCR70: A low-complexity millimeter-wave proof-of-concept platform for a fully-digital SIMO joint communication-radar," *IEEE Open J. Veh. Technol.*, vol. 2, pp. 218–234, 2021.

[5] F. Liu, C. Masouros, A. P. Petropulu, H. Griffiths, and L. Hanzo, "Joint radar and communication design: Applications, state-of-the-art, and the road ahead," *IEEE Trans. Commun.*, vol. 68, no. 6, pp. 3834–3862, Jun. 2020.

[6] R. M. Mealey, "A method for calculating error probabilities in a radar communication system," *IEEE Trans. Space Electron. Telemetry*, vol. SET-9, no. 2, pp. 37–42, Jun. 1963.

[7] A. J. Fenn, D. H. Temme, W. P. Delaney, and W. E. Courtney, "The development of phased-array radar technology," *Lincoln Lab. J.*, vol. 12, no. 2, pp. 321–340, 2000.

[8] H. Griffiths, "The MAMMUT phased array radar: Compulsive hoarding," in *Proc. Int. Radar Conf. (RADAR)*, Sep. 2019, pp. 23–27.

[9] A. J. Paulraj and T. Kailath, "Increasing capacity in wireless broadcast systems using distributed transmission/directional reception (DTDR)," U.S. Patent 5 345 599, Sep. 6, 1994.

[10] G. J. Foschini and M. J. Gans, "On limits of wireless communications in a fading environment when using multiple antennas," *Wireless Pers. Commun.*, vol. 6, no. 3, pp. 311–335, Mar. 1998.

[11] İ. E. Telatar, "Capacity of multi-antenna Gaussian channels," *Eur. Trans. Telecommun.*, vol. 10, no. 6, pp. 585–595, 1999.

[12] E. Fishler, A. Haimovich, R. Blum, D. Chizhik, L. Cimini, and R. Valenzuela, "MIMO radar: An idea whose time has come," in *Proc. IEEE Radar Conf.*, Philadelphia, PA, USA, Apr. 2004, pp. 71–78.

[13] D. Cohen, D. Cohen, and Y. C. Eldar, "High resolution FDMA MIMO radar," *IEEE Trans. Aerosp. Electron. Syst.*, vol. 56, no. 4, pp. 2806–2822, Aug. 2020.

[14] J. Li and P. Stoica, "MIMO radar with colocated antennas," *IEEE Signal Process. Mag.*, vol. 24, no. 5, pp. 106–114, Sep. 2007.

[15] A. M. Haimovich, R. S. Blum, and L. J. Cimini, "MIMO radar with widely separated antennas," *IEEE Signal Process. Mag.*, vol. 25, no. 1, pp. 116–129, Dec. 2007.

[16] P. K. Hughes and J. Y. Choe, "Overview of advanced multifunction RF system (AMRFS)," in *Proc. IEEE Int. Conf. Phased Array Syst. Technol.*, May 2000, pp. 21–24.

[17] G. C. Tavik *et al.*, "The advanced multifunction RF concept," *IEEE Trans. Microw. Theory Techn.*, vol. 53, no. 3, pp. 1009–1020, Mar. 2005.

[18] J. A. Molnar, I. Corretjer, and G. Tavik, "Integrated topside–integration of narrowband and wideband array antennas for shipboard communications," in *Proc. MILCOM Mil. Commun. Conf.*, Nov. 2011, pp. 1802–1807.

[19] M. Roberton and E. R. Brown, "Integrated radar and communications based on chirped spread-spectrum techniques," in *IEEE MTT-S Int. Microw. Symp. Dig.*, vol. 1, Oct. 2003, pp. 611–614.

[20] G. N. Saddik, R. S. Singh, and E. R. Brown, "Ultra-wideband multifunctional communications/radar system," *IEEE Trans. Microw. Theory Techn.*, vol. 55, no. 7, pp. 1431–1437, Jul. 2007.

[21] M. Jamil, H. J. Zepernick, and M. I. Pettersson, "On integrated radar and communication systems using oppermann sequences," in *Proc. IEEE Military Commun. Conf.*, San Diego, CA, USA, Nov. 2008, pp. 1–6.

[22] L. Han and K. Wu, "Joint wireless communication and radar sensing systems-state of the art and future prospects," *IET Microw., Antennas Propag.*, vol. 7, no. 11, pp. 876–885, Aug. 2013.

[23] D. Garmatyuk, J. Schuerger, and K. Kauffman, "Multifunctional software-defined radar sensor and data communication system," *IEEE Sensors J.*, vol. 11, no. 1, pp. 99–106, Jan. 2011.

[24] DARPA. (2016). *Shared Spectrum Access for Radar and Communications (SSPARC)*. [Online]. Available: https://www.darpa.mil/program/shared-spectrum-access-for-radar-and-communications

[25] B. Li and A. P. Petropulu, "Joint transmit designs for coexistence of MIMO wireless communications and sparse sensing radars in clutter," *IEEE Trans. Aerosp. Electron. Syst.*, vol. 53, no. 6, pp. 2846–2864, Dec. 2017.

[26] J. A. Mahal, A. Khawar, A. Abdelhadi, and T. C. Clancy, "Spectral coexistence of MIMO radar and MIMO cellular system," *IEEE Trans. Aerosp. Electron. Syst.*, vol. 53, no. 2, pp. 655–668, Apr. 2017.

[27] C. D'Andrea, S. Buzzi, and M. Lops, "Communications and radar coexistence in the massive MIMO regime: Uplink analysis," *IEEE Trans. Wireless Commun.*, vol. 19, no. 1, pp. 19–33, Jan. 2020.

[28] K. V. Mishra, Y. C. Eldar, E. Shoshan, M. Namer, and M. Meltsin, "A cognitive sub-Nyquist MIMO radar prototype," *IEEE Trans. Aerosp. Electron. Syst.*, vol. 56, no. 2, pp. 937–955, Apr. 2020.

[29] D. Cohen, K. V. Mishra, and Y. C. Eldar, "Spectrum sharing radar: Coexistence via Xampling," *IEEE Trans. Aerosp. Electron. Syst.*, vol. 54, no. 3, pp. 1279–1296, Jun. 2018.

[30] J. G. Andrews *et al.*, "What will 5G be?" *IEEE J. Sel. Areas Commun.*, vol. 32, no. 6, pp. 1065–1082, Jun. 2014.

[31] T. L. Marzetta, "Noncooperative cellular wireless with unlimited numbers of base station antennas," *IEEE Trans. Wireless Commun.*, vol. 9, no. 11, pp. 3590–3600, Nov. 2010.

[32] T. S. Rappaport *et al.*, "Millimeter wave mobile communications for 5G cellular: It will work!" *IEEE Access*, vol. 1, pp. 335–349, 2013.

[33] X. Zhang, A. F. Molisch, and S.-Y. Kung, "Variable-phase-shift-based RF-baseband codesign for MIMO antenna selection," *IEEE Trans. Signal Process.*, vol. 53, no. 11, pp. 4091–4103, Nov. 2005.

[34] O. El Ayach, S. Rajagopal, S. Abu-Surra, Z. Pi, and R. W. Heath, Jr., "Spatially sparse precoding in millimeter wave MIMO systems," *IEEE Trans. Wireless Commun.*, vol. 13, no. 3, pp. 1499–1513, Mar. 2014.

[35] T. Gong, N. Shlezinger, S. S. Ioushua, M. Namer, Z. Yang, and Y. C. Eldar, "RF chain reduction for MIMO systems: A hardware prototype," *IEEE Syst. J.*, vol. 14, no. 4, pp. 5296–5307, Dec. 2020.

[36] A. Hassanien and S. A. Vorobyov, "Phased-MIMO radar: A tradeoff between phased-array and MIMO radars," *IEEE Trans. Signal Process.*, vol. 58, no. 6, pp. 3137–3151, Jun. 2010.

[37] S. Fortunati, L. Sanguinetti, F. Gini, M. S. Greco, and B. Himed, "Massive MIMO radar for target detection," *IEEE Trans. Signal Process.*, vol. 68, pp. 859–871, 2020.

[38] R. W. Heath, N. González-Prelcic, S. Rangan, W. Roh, and A. M. Sayeed, "An overview of signal processing techniques for millimeter wave MIMO systems," *IEEE J. Sel. Topics Signal Process.*, vol. 10, no. 3, pp. 436–453, Apr. 2016.

[39] X. Yu, J.-C. Shen, J. Zhang, and K. B. Letaief, "Alternating minimization algorithms for hybrid precoding in millimeter wave MIMO systems," *IEEE J. Sel. Topics Signal Process.*, vol. 10, no. 3, pp. 485–500, May 2016.

[40] Z. Cheng and B. Liao, "QoS-aware hybrid beamforming and DOA estimation in multi-carrier dual-function radar-communication systems," *IEEE J. Sel. Areas Commun.*, vol. 40, no. 6.

[41] D. K. P. Tan *et al.*, "Integrated sensing and communication in 6G: Motivations, use cases, requirements, challenges and future directions," in *Proc. 1st IEEE Int. Online Symp. Joint Commun. Sens. (JC&S)*, Feb. 2021, pp. 1–6.

[42] J. A. Zhang, A. Cantoni, X. Huang, Y. J. Guo, and R. W. Heath, "Framework for an innovative perceptive mobile network using joint communication and sensing," in *Proc. IEEE 85th Veh. Technol. Conf. (VTC Spring)*, Jun. 2017, pp. 1–5.

[43] A. Zhang, M. L. Rahman, X. Huang, Y. J. Guo, S. Chen, and R. W. Heath, "Perceptive mobile networks: Cellular networks with radio vision via joint communication and radar sensing," *IEEE Veh. Technol. Mag.*, vol. 16, no. 2, pp. 20–30, Jun. 2021.

[44] K. V. Mishra, M. R. B. Shankar, V. Koivunen, B. Ottersten, and S. A. Vorobyov, "Toward millimeter-wave joint radar communications: A signal processing perspective," *IEEE Signal Process. Mag.*, vol. 36, no. 5, pp. 100–114, Sep. 2019.

[45] D. Ma, N. Shlezinger, T. Huang, Y. Liu, and Y. C. Eldar, "Joint radar-communication strategies for autonomous vehicles: Combining two key automotive technologies," *IEEE Signal Process. Mag.*, vol. 37, no. 4, pp. 85–97, Jul. 2020.

[46] A. Hassanien, M. G. Amin, Y. D. Zhang, and F. Ahmad, "Signaling strategies for dual-function radar communications: An overview," *IEEE Aerosp. Electron. Syst. Mag.*, vol. 31, no. 10, pp. 36–45, Oct. 2016.

[47] J. A. Zhang *et al.*, "Enabling joint communication and radar sensing in mobile networks—A survey," *IEEE Commun. Surveys Tuts.*, vol. 24, no. 1, pp. 306–345, 1st Quart., 2022.

[48] B. Paul, A. R. Chiriyath, and D. W. Bliss, "Survey of RF communications and sensing convergence research," *IEEE Access*, vol. 5, pp. 252–270, 2016.

[49] J. A. Zhang *et al.*, "An overview of signal processing techniques for joint communication and radar sensing," *IEEE J. Sel. Topics Signal Process.*, vol. 15, no. 6, pp. 1295–1315, Nov. 2021.

[50] T. Wild, V. Braun, and H. Viswanathan, "Joint design of communication and sensing for beyond 5G and 6G systems," *IEEE Access*, vol. 9, pp. 30845–30857, 2021.

[51] Z. Feng *et al.*, "Joint radar and communication: A survey," *China Commun.*, vol. 17, no. 1, pp. 1–27, Jan. 2020.

[52] A. Liu *et al.*, "A survey on fundamental limits of integrated sensing and communication," *IEEE Commun. Surveys Tuts.*, early access, doi: 10.1109/COMST.2022.3149272.

[53] L. Zheng, M. Lops, Y. C. Eldar, and X. Wang, "Radar and communication coexistence: An overview: A review of recent methods," *IEEE Signal Process. Mag.*, vol. 36, no. 5, pp. 85–99, Sep. 2019.

[54] A. Hassanien, M. G. Amin, E. Aboutanios, and B. Himed, "Dual-function radar communication systems: A solution to the spectrum congestion problem," *IEEE Signal Process. Mag.*, vol. 36, no. 5, pp. 115–126, Sep. 2019.

[55] F. Liu, L. Zhou, C. Masouros, A. Li, W. Luo, and A. Petropulu, "Toward dual-functional radar-communication systems: Optimal waveform design," *IEEE Trans. Signal Process.*, vol. 66, no. 16, pp. 4264–4279, Aug. 2018.

[56] J. A. del Peral-Rosado, R. Raulefs, J. A. López-Salcedo, and G. Seco-Granados, "Survey of cellular mobile radio localization methods: From 1G to 5G," *IEEE Commun. Surveys Tuts.*, vol. 20, no. 2, pp. 1124–1148, 2nd Quart., 2017.

[57] *Study on NR Positioning Support*, Standard TR 38.855 16.0.0, 3GPP, 2019.

[58] K. Chen, D. Zhang, L. Yao, B. Guo, Z. Yu, and Y. Liu, "Deep learning for sensor-based human activity recognition: Overview, challenges, and opportunities," *ACM Comput. Surveys*, vol. 54, no. 4, pp. 1–40, May 2022, doi: 10.1145/3447744.

[59] H. Lasi, P. Fettke, H. G. Kemper, T. Feld, and M. Hoffmann, "Industry 4.0," *Bus. Inf. Syst. Eng.*, vol. 6, no. 4, pp. 239–242, 2014.

[60] A. Moreira, P. Prats-Iraola, M. Younis, G. Krieger, I. Hajnsek, and K. P. Papathanassiou, "A tutorial on synthetic aperture radar," *IEEE Geosci. Remote Sens. Mag.*, vol. 1, no. 1, pp. 6–43, Apr. 2013.

[61] D. K. Pin Tan *et al.*, "Integrated sensing and communication in 6G: Motivations, use cases, requirements, challenges and future directions," in *Proc. 1st IEEE Int. Online Symp. Joint Commun. Sens. (JC&S)*, Feb. 2021, pp. 1–6.

[62] Y. Zeng, Q. Wu, and R. Zhang, "Accessing from the sky: A tutorial on UAV communications for 5G and beyond," *Proc. IEEE*, vol. 107, no. 12, pp. 2327–2375, Dec. 2019.

[63] Q. Huang, H. Chen, and Q. Zhang, "Joint design of sensing and communication systems for smart Homes," *IEEE Netw.*, vol. 34, no. 6, pp. 191–197, Nov. 2020.

[64] Q. Huang, Z. Luo, J. Zhang, W. Wang, and Q. Zhang, "LoRadar: Enabling concurrent radar sensing and LoRa communication," *IEEE Trans. Mobile Comput.*, early access, Nov. 4, 2020, doi: 10.1109/TMC.2020.3035797.

[65] K. Niu, X. Wang, F. Zhang, R. Zheng, Z. Yao, and D. Zhang, "Rethinking Doppler effect for accurate velocity estimation with commodity WiFi devices," *IEEE J. Sel. Areas Commun.*, vol. 40, no. 8.

[66] K. Gao, H. Wang, and H. Lv, "Towards 5G NR high-precision indoor positioning via channel frequency response: A new paradigm and dataset generation method," *IEEE J. Sel. Areas Commun.*, to be published.

[67] W. Shoulberg, *Ces Comes Home: The Best Intros at the Show*. Mumbai, India: Forbes, Jan. 2021.

[68] Y. Ma, G. Zhou, and S. Wang, "WiFi sensing with channel state information: A survey," *ACM Comput. Surv.*, vol. 52, no. 3, pp. 1–36, May 2020, doi: 10.1145/3310194.

[69] *IMT Vision–Framework and Overall Objectives of the Future Development of IMT for 2020 and Beyond*, document Recommendation ITU, 2083, M. Series, 2015.

[70] IEEE 802.11bf Task Group. (2020). *WiFi Sensing Uses Cases*. [Online]. Available: https://mentor.ieee.org/802.11/dcn/20/11-20-1712-02-00bf-wifi-sensing-use-cases.xlsx

[71] J. Tregloan-Reed *et al.*, "First observations and magnitude measurement of Starlink's darksat," *Astron. Astrophys.*, vol. 637, p. L1, May 2020, doi: 10.1051/0004-6361/202037958.

[72] H. Messer, A. Zinevich, and A. Pinhas, "Environmental monitoring by wireless communication networks," *Science*, vol. 312, no. 5774, p. 713, 2006. [Online]. Available: https://science.sciencemag.org/content/312/5774/713

[73] J. Lien *et al.*, "Soli: Ubiquitous gesture sensing with millimeter wave radar," *ACM Trans. Graph.*, vol. 35, no. 4, pp. 1–19, 2016.

[74] S. Shekhar, S. K. Feiner, and W. G. Aref, "Spatial computing," *Commun. ACM*, vol. 59, no. 1, pp. 72–81, Dec. 2015, doi: 10.1145/2756547.

[75] Xiaomi. (2021). *XIAOMI Introduces Groundbreaking UWB Technology*. [Online]. Available: https://blog.mi.com/en/2020/10/13/xiaomi-introduces-groundbreaking-uwb-technology

[76] T. Luettel, M. Himmelsbach, and H.-J. Wuensche, "Autonomous ground vehicles-concepts and a path to the future," *Proc. IEEE*, vol. 100, pp. 1831–1839, May 2012, doi: 10.1109/JPROC.2012.2189803.

[77] O. Kaiwartya *et al.*, "Internet of vehicles: Motivation, layered architecture, network model, challenges, and future aspects," *IEEE Access*, vol. 4, pp. 5356–5373, 2016.

[78] M. Sybis *et al.*, "Communication aspects of a modified cooperative adaptive cruise control algorithm," *IEEE Trans. Intell. Transp. Syst.*, vol. 20, no. 12, pp. 4513–4523, Dec. 2019.

[79] T. Zeng, O. Semiari, W. Saad, and M. Bennis, "Joint communication and control for wireless autonomous vehicular platoon systems," *IEEE Trans. Commun.*, vol. 67, no. 11, pp. 7907–7922, Nov. 2019.

[80] L. Wang, Y. Duan, Y. Lai, S. Mu, and X. Li, "V2I-based platooning design with delay awareness," *IEEE Trans. Intell. Transp. Syst.*, to be published. [Online]. Available: https://arxiv.org/abs/2012.03243

[81] V. Milanes, J. Villagra, J. Godoy, J. Simo, J. Perez, and E. Onieva, "An intelligent V2I-based traffic management system," *IEEE Trans. Intell. Transp. Syst.*, vol. 13, no. 1, pp. 49–58, Mar. 2012.

[82] F. Liu, W. Yuan, C. Masouros, and J. Yuan, "Radar-assisted predictive beamforming for vehicular links: Communication served by sensing," *IEEE Trans. Wireless Commun.*, vol. 19, no. 11, pp. 7704–7719, Nov. 2020.

[83] W. Yuan, F. Liu, C. Masouros, J. Yuan, D. W. K. Ng, and N. Gonzalez-Prelcic, "Bayesian predictive beamforming for vehicular networks: A low-overhead joint radar-communication approach," *IEEE Trans. Wireless Commun.*, vol. 20, no. 3, pp. 1442–1456, Mar. 2021.

[84] C. B. Barneto *et al.*, "Millimeter-wave mobile sensing and environment mapping: Models, algorithms and validation," *IEEE Trans. Veh. Technol.*, early access, doi: 10.1109/TVT.2022.3146003.

[85] Y. Ge *et al.*, "A computationally efficient EK-PMBM filter for bistatic mmWave radio SLAM," *IEEE J. Sel. Areas Commun.*, vol. 40, no. 8.

[86] J. Yang, C.-K. Wen, and S. Jin, "Hybrid active and passive sensing for SLAM in wireless communication systems," *IEEE J. Sel. Areas Commun.*, vol. 40, no. 8.

[87] S. K. Rao and R. Prasad, "Impact of 5G technologies on industry 4.0," *Wireless Pers. Commun.*, vol. 100, no. 1, pp. 145–159, May 2018.

[88] P. Popovski *et al.*, "Wireless access in ultra-reliable low-latency communication (URLLC)," *IEEE Trans. Commun.*, vol. 67, no. 8, pp. 5783–5801, Aug. 2019.

[89] D. C. Schedl, I. Kurmi, and O. Bimber, "An autonomous drone for search and rescue in forests using airborne optical sectioning," *Sci. Robot.*, vol. 6, no. 55, Jun. 2021, Art. no. eabg1188. [Online]. Available: https://robotics.sciencemag.org/content/6/55/eabg1188

[90] "6G—Connecting a cyber-physical world," Ericsson, Stockholm, Sweden, White Paper GFTL-20:001402. [Online]. Available: https://www.ericsson.com/4927de/assets/local/reports-papers/white-papers/6g–connecting-a-cyber-physical-world.pdf

[91] "5G evolution and 6G," NTT DOCOMO, Tokyo, Japan, White Paper, 2020. [Online]. Available: https://www.nttdocomo.co.jp/english/binary/pdf/corporate/technology/whitepaper_6g/DOCOMO_6G_White_PaperEN_20200124.pdf

[92] J. Waring. (2020). *China Unicom, ZTE Explore 6G Options*. [Online]. Available: https://www.mobileworldlive.com/asia/asia-news/china-unicom-zte-explore-6g-options#:~:text=China%20Unicom%20and%20ZTE%20signed,exploring%20technical%20trends%20and%20standards

[93] C. Cordeiro. (Jul. 2020). *Next-Generation Wi-Fi: Wi-Fi 7 and beyond*. Intel Corporation. [Online]. Available: https://www.intel.com/content/dam/www/public/us/en/documents/pdf/wi-fi-7-and-beyond.pdf

[94] J. Waring. (2021). *Huawei Readies 5.5G as Bosses Push Evolution*. [Online]. Available: https://www.mobileworldlive.com/featured-content/home-banner/huawei-readies-5-5G-as-bosses-push-evolution

[95] M. Alloulah and H. Huang, "Future millimeter-wave indoor systems: A blueprint for joint communication and sensing," *Computer*, vol. 52, no. 7, pp. 16–24, Jul. 2019.

[96] F. Restuccia, "IEEE 802.11bf: Toward ubiquitous Wi-Fi sensing," 2021, *arXiv:2103.14918*.

[97] S. M. Kay, *Fundamentals of Statistical Signal Processing: Detection Theory*, vol. 2. Englewood Cliffs, NJ, USA: Prentice-Hall, 1998.

[98] S. M. Kay, *Fundamentals of Statistical Signal Processing: Estimation Theory*, vol. 2. Cliffs, NJ, USA: Prentice-Hall, 1998.

[99] P. Tait, *Introduction to Radar Target Recognition*, vol. 18. Edison, NJ, USA: IET, 2005.

[100] A. Goldsmith, *Wireless Communications*. Cambridge, U.K.: Cambridge Univ. Press, 2005.

[101] D. Tse and P. Viswanath, *Fundamentals of Wireless Communication*. Cambridge, U.K.: Cambridge Univ. Press, 2005.

[102] T. M. Cover, *Elements of Information Theory*. Hoboken, NJ, USA: Wiley, 1999.

[103] D. Guo, S. Shamai (Shitz), and S. Verdú, "Mutual information and minimum mean-square error in Gaussian channels," *IEEE Trans. Inf. Theory*, vol. 51, no. 4, pp. 1261–1282, Apr. 2005.

[104] A. Sutivong, T. M. Cover, and M. Chiang, "Tradeoff between message and state information rates," in *Proc. IEEE Int. Symp. Inf. Theory*, Jun. 2001, p. 303.

[105] A. Sutivong, T. M. Cover, M. Chiang, and Y.-H. Kim, "Rate vs. distortion trade-off for channels with state information," in *Proc. IEEE Int. Symp. Inf. Theory*, Jun. 2002, p. 226.

[106] A. Sutivong, M. Chiang, T. M. Cover, and Y.-H. Kim, "Channel capacity and state estimation for state-dependent Gaussian channels," *IEEE Trans. Inf. Theory*, vol. 51, no. 4, pp. 1486–1495, Apr. 2005.

[107] W. Zhang, S. Vedantam, and U. Mitra, "Joint transmission and state estimation: A constrained channel coding approach," *IEEE Trans. Inf. Theory*, vol. 57, no. 10, pp. 7084–7095, Oct. 2011.

[108] C. Choudhuri, Y.-H. Kim, and U. Mitra, "Causal state communication," *IEEE Trans. Inf. Theory*, vol. 59, no. 6, pp. 3709–3719, Jun. 2013.

[109] M. Kobayashi, G. Caire, and G. Kramer, "Joint state sensing and communication: Optimal tradeoff for a memoryless case," in *Proc. IEEE Int. Symp. Inf. Theory (ISIT)*, Jun. 2018, pp. 111–115.

[110] M. Kobayashi, H. Hamad, G. Kramer, and G. Caire, "Joint state sensing and communication over memoryless multiple access channels," in *Proc. IEEE Int. Symp. Inf. Theory (ISIT)*, Jul. 2019, pp. 270–274.

[111] M. Ahmadipour, M. Wigger, and M. Kobayashi, "Joint sensing and communication over memoryless broadcast channels," in *Proc. IEEE Inf. Theory Workshop (ITW)*, Apr. 2021, pp. 1–5.

[112] B. K. Chalise, M. G. Amin, and B. Himed, "Performance tradeoff in a unified passive radar and communications system," *IEEE Signal Process. Lett.*, vol. 24, no. 9, pp. 1275–1279, Sep. 2017.

[113] H. D. Griffiths and C. J. Baker, *An Introduction to Passive Radar*. Norwood, MA, USA: Artech House, 2017.

[114] B. K. Chalise and B. Himed, "Performance tradeoff in a unified multistatic passive radar and communication system," in *Proc. IEEE Radar Conf. (RadarConf)*, Apr. 2018, pp. 653–658.

[115] F. Liu, Y.-F. Liu, A. Li, C. Masouros, and Y. C. Eldar, "Cramér–Rao bound optimization for joint radar-communication beamforming," *IEEE Trans. Signal Process.*, vol. 70, pp. 240–253, 2022.

[116] Z. Ben-Haim and Y. C. Eldar, "On the constrained Cramér–Rao bound with a singular Fisher information matrix," *IEEE Signal Process. Lett.*, vol. 16, no. 6, pp. 453–456, Jun. 2009.

[117] X. Liu, T. Huang, N. Shlezinger, Y. Liu, J. Zhou, and Y. C. Eldar, "Joint transmit beamforming for multiuser MIMO communications and MIMO radar," *IEEE Trans. Signal Process.*, vol. 68, pp. 3929–3944, 2020.

[118] H. Hua, J. Xu, and T.-X. Han, "Optimal transmit beamforming for integrated sensing and communication," *IEEE Trans. Wireless Commun.*, to be published. [Online]. Available: https://arxiv.org/abs/2104.11871

[119] Z.-Q. Luo, W.-K. Ma, A. M.-C. So, Y. Ye, and S. Zhang, "Semidefinite relaxation of quadratic optimization problems," *IEEE Signal Process. Mag.*, vol. 27, no. 3, pp. 20–34, May 2010.

[120] F. Liu, C. Masouros, A. Li, H. Sun, and L. Hanzo, "MU-MIMO communications with MIMO radar: From co-existence to joint transmission," *IEEE Trans. Wireless Commun.*, vol. 17, no. 4, pp. 2755–2770, Apr. 2018.

[121] J. R. Guerci, R. M. Guerci, A. Lackpour, and D. Moskowitz, "Joint design and operation of shared spectrum access for radar and communications," in *Proc. IEEE Radar Conf. (RadarCon)*, May 2015, pp. 761–766.

[122] D. W. Bliss, "Cooperative radar and communications signaling: The estimation and information theory odd couple," in *Proc. IEEE Radar Conf.*, May 2014, pp. 50–55.

[123] A. R. Chiriyath, B. Paul, G. M. Jacyna, and D. W. Bliss, "Inner bounds on performance of radar and communications co-existence," *IEEE Trans. Signal Process.*, vol. 64, no. 2, pp. 464–474, Jan. 2016.

[124] G. Cui, H. Li, and M. Rangaswamy, "MIMO radar waveform design with constant modulus and similarity constraints," *IEEE Trans. Signal Process.*, vol. 62, no. 2, pp. 343–353, Jan. 2014.

[125] N. Mehrotra and A. Sabharwal, "On the degrees of freedom region for simultaneous imaging & uplink communication," *IEEE J. Sel. Areas Commun.*, to be published.

[126] G. Li *et al.*, "Rethinking the tradeoff in integrated sensing and communication: Recognition accuracy versus communication rate," *IEEE Trans. Mobile Comput.*, to be published. [Online]. Available: https://arxiv.org/abs/2107.09621

[127] J. B. Kenney, "Dedicated short-range communications (DSRC) standards in the United States," *Proc. IEEE*, vol. 99, no. 7, pp. 1162–1182, Jul. 2011.

[128] P. Kumari, J. Choi, N. Gonzalez-Prelcic, and R. W. Heath, Jr., "IEEE 802.11ad-based radar: An approach to joint vehicular communication-radar system," *IEEE Trans. Veh. Technol.*, vol. 67, no. 4, pp. 3012–3027, Apr. 2018.

[129] E. Grossi, M. Lops, L. Venturino, and A. Zappone, "Opportunistic radar in IEEE 802.11ad networks," *IEEE Trans. Signal Process.*, vol. 66, no. 9, pp. 2441–2454, Mar. 2018.

[130] H. Wymeersch, G. Seco-Granados, G. Destino, D. Dardari, and F. Tufvesson, "5G mmWave positioning for vehicular networks," *IEEE Wireless Commun.*, vol. 24, no. 6, pp. 80–86, Dec. 2017.

[131] Q. Zhang, H. Sun, X. Gao, X. Wang, and Z. Feng, "Time-division ISAC enabled connected automated vehicles cooperation algorithm design and performance evaluation," *IEEE J. Sel. Areas Commun.*, vol. 40, no. 8.

[132] M. Bica and V. Koivunen, "Radar waveform optimization for target parameter estimation in cooperative radar-communications systems," *IEEE Trans. Aerosp. Electron. Syst.*, vol. 55, no. 5, pp. 2314–2326, Oct. 2019.

[133] C. Shi, F. Wang, M. Sellathurai, J. Zhou, and S. Salous, "Power minimization-based robust OFDM radar waveform design for radar and communication systems in coexistence," *IEEE Trans. Signal Process.*, vol. 66, no. 5, pp. 1316–1330, Mar. 2018.

[134] R. Fu, S. Mulleti, T. Huang, Y. Liu, and Y. C. Eldar, "Hardware prototype demonstration of a cognitive radar with sparse array antennas," *Electron. Lett.*, vol. 56, pp. 1210–1212, Oct. 2020.

[135] S. Sodagari, A. Khawar, T. C. Clancy, and R. McGwier, "A projection based approach for radar and telecommunication systems coexistence," in *Proc. IEEE Global Commun. Conf. (GLOBECOM)*, Dec. 2012, pp. 5010–5014.

[136] M. Jamil, H.-J. Zepernick, and M. I. Pettersson, "On integrated radar and communication systems using oppermann sequences," in *Proc. MILCOM IEEE Mil. Commun. Conf.*, Nov. 2008, pp. 1–6.

[137] Z. Ye, Z. Zhou, P. Fan, Z. Liu, X. Lei, and X. Tang, "Low ambiguity zone: Theoretical bounds and Doppler-resilient sequence design in integrated sensing and communication systems," *IEEE J. Sel. Areas Commun.*, vol. 40, no. 6.

[138] X. Chen, Z. Feng, Z. Wei, P. Zhang, and X. Yuan, "Code-division OFDM joint communication and sensing system for 6G machine-type communication," *IEEE Internet Things J.*, vol. 8, no. 15, pp. 12093–12105, Aug. 2021.

[139] F. Liu and C. Masouros, "A tutorial on joint radar and communication transmission for vehicular networks—Part I: Background and fundamentals," *IEEE Commun. Lett.*, vol. 25, no. 2, pp. 322–326, Feb. 2021.

[140] A. Hassanien, M. G. Amin, Y. D. Zhang, and F. Ahmad, "Dual-function radar-communications: Information embedding using sidelobe control and waveform diversity," *IEEE Trans. Signal Process.*, vol. 64, no. 8, pp. 2168–2181, Apr. 2016.

[141] T. Huang, N. Shlezinger, X. Xu, Y. Liu, and Y. C. Eldar, "MAJoRCom: A dual-function radar communication system using index modulation," *IEEE Trans. Signal Process.*, vol. 68, pp. 3423–3438, 2020.

[142] D. Ma *et al.*, "Spatial modulation for joint radar-communications systems: Design, analysis, and hardware prototype," *IEEE Trans. Veh. Technol.*, vol. 70, no. 3, pp. 2283–2298, Mar. 2021.

[143] D. Ma, N. Shlezinger, T. Huang, Y. Liu, and Y. Eldar, "FRaC: FMCW-based joint radar-communications system via index modulation," *IEEE J. Sel. Topics Signal Process.*, vol. 15, no. 6, pp. 1348–1364, Nov. 2021.

[144] L. Chen, F. Liu, W. Wang, and C. Masouros, "Joint radar-communication transmission: A generalized Pareto optimization framework," *IEEE Trans. Signal Process.*, vol. 69, pp. 2752–2765, 2021.

[145] A. Hassanien, M. G. Amin, Y. D. Zhang, F. Ahmad, and B. Himed, "Non-coherent PSK-based dual-function radar-communication systems," in *Proc. IEEE Radar Conf. (RadarConf)*, May 2016, pp. 1–6.

[146] E. BouDaher, A. Hassanien, E. Aboutanios, and M. G. Amin, "Towards a dual-function MIMO radar-communication system," in *Proc. IEEE Radar Conf. (RadarConf)*, May 2016, pp. 1–6.

[147] T. Huang, N. Shlezinger, X. Xu, D. Ma, Y. Liu, and Y. C. Eldar, "Multi-carrier agile phased array radar," *IEEE Trans. Signal Process.*, vol. 68, pp. 5706–5721, 2020.

[148] J. Johnston, L. Venturino, E. Grossi, M. Lops, and X. Wang, "MIMO-OFDM dual-function radar-communication under error rate and beampattern constraints," *IEEE J. Sel. Areas Commun.*, vol. 40, no. 6.

[149] M. F. Keskin, H. Wymeersch, and V. Koivunen, "MIMO-OFDM joint radar-communications: Is ICI friend or foe?" *IEEE J. Sel. Topics Signal Process.*, vol. 15, no. 6, pp. 1393–1408, Nov. 2021.

[150] L. Chen, Z. Wang, Y. Du, Y. Chen, and F. R. Yu, "Generalized transceiver beamforming for DFRC with MIMO radar and MU-MIMO communication," *IEEE J. Sel. Areas Commun.*, vol. 40, no. 6.

[151] X. Liu, T. Huang, and Y. Liu, "Transmit design for joint MIMO radar and multiuser communications with transmit covariance constraint," *IEEE J. Sel. Areas Commun.*, vol. 40, no. 6.

[152] S. K. Mohammed and E. G. Larsson, "Per-antenna constant envelope precoding for large multi-user MIMO systems," *IEEE Trans. Commun.*, vol. 61, no. 3, pp. 1059–1071, Mar. 2013.

[153] N. Nartasilpa, A. Salim, D. Tuninetti, and N. Devroye, "Communications system performance and design in the presence of radar interference," *IEEE Trans. Commun.*, vol. 66, no. 9, pp. 4170–4185, Sep. 2018.

[154] S. Shahi, D. Tuninetti, and N. Devroye, "On the capacity of the AWGN channel with additive radar interference," *IEEE Trans. Commun.*, vol. 66, no. 2, pp. 629–643, Feb. 2018.

[155] L. Zheng, M. Lops, and X. Wang, "Adaptive interference removal for uncoordinated radar/communication coexistence," *IEEE J. Sel. Topics Signal Process.*, vol. 12, no. 1, pp. 45–60, Feb. 2018.

[156] M. L. Rahman, J. A. Zhang, X. Huang, Y. J. Guo, and R. W. Heath, "Framework for a perceptive mobile network using joint communication and radar sensing," *IEEE Trans. Aerosp. Electron. Syst.*, vol. 56, no. 3, pp. 1926–1941, Jun. 2020.

[157] Z. Ni, J. A. Zhang, X. Huang, K. Yang, and J. Yuan, "Uplink sensing in perceptive mobile networks with asynchronous transceivers," *IEEE Trans. Signal Process.*, vol. 69, pp. 1287–1300, 2021.

[158] X. Lin *et al.*, "5G new radio: Unveiling the essentials of the next generation wireless access technology," *IEEE Commun. Standards Mag.*, vol. 3, no. 3, pp. 30–37, Sep. 2019.

[159] A. Sabharwal, P. Schniter, D. Guo, D. W. Bliss, S. Rangarajan, and R. Wichman, "In-band full-duplex wireless: Challenges and opportunities," *IEEE J. Sel. Areas Commun.*, vol. 32, no. 9, pp. 1637–1652, Sep. 2014.

[160] Z. Xiao and Y. Zeng, "Waveform design and performance analysis for full-duplex integrated sensing and communication," *IEEE J. Sel. Areas Commun.*, vol. 40, no. 6.

[161] C. Baquero Barneto *et al.*, "Full-duplex OFDM radar with LTE and 5G NR waveforms: Challenges, solutions, and measurements," *IEEE Trans. Microw. Theory Techn.*, vol. 67, no. 10, pp. 4042–4054, Oct. 2019.

[162] L. Pucci, E. Paolini, and A. Giorgetti, "System-level analysis of joint sensing and communication based on 5G new radio," *IEEE J. Sel. Areas Commun.*, vol. 40, no. 8.

[163] Q. Zhang, Z. Li, X. Gao, and Z. Feng, "Performance evaluation of radar and communication integrated system for autonomous driving vehicles," in *Proc. IEEE INFOCOM Conf. Comput. Commun. Workshops (INFOCOM WKSHPS)*, May 2021, pp. 1–2.

[164] Q. Zhang, X. Wang, Z. Li, and Z. Wei, "Design and performance evaluation of joint sensing and communication integrated system for 5G mmWave enabled CAVs," *IEEE J. Sel. Topics Signal Process.*, vol. 15, no. 6, pp. 1500–1514, Nov. 2021.

[165] Y. Shen, H. Wymeersch, and M. Z. Win, "Fundamental limits of wideband localization— Part II: Cooperative networks," *IEEE Trans. Inf. Theory*, vol. 56, no. 10, pp. 4981–5000, Oct. 2010.

[166] M. Z. Win *et al.*, "Network localization and navigation via cooperation," *IEEE Commun. Mag.*, vol. 49, no. 5, pp. 56–62, May 2011.

[167] N. Patwari, J. N. Ash, S. Kyperountas, A. O. Hero, R. L. Moses, and N. S. Correal, "Locating the nodes: Cooperative localization in wireless sensor networks," *IEEE Signal Process. Mag.*, vol. 22, no. 4, pp. 54–69, Jul. 2005.

[168] I. Guvenc and C.-C. Chong, "A survey on TOA based wireless localization and NLOS mitigation techniques," *IEEE Commun. Surveys Tuts.*, vol. 11, no. 3, pp. 107–124, 3rd Quart., 2009.

[169] H. Godrich, A. M. Haimovich, and R. S. Blum, "Target localization accuracy gain in MIMO radar-based systems," *IEEE Trans. Inf. Theory*, vol. 56, no. 6, pp. 2783–2803, Jun. 2010.

[170] M. Peng, C. Wang, V. Lau, and H. V. Poor, "Fronthaul-constrained cloud radio access networks: Insights and challenges," *IEEE Wireless Commun.*, vol. 22, no. 2, pp. 152–160, Apr. 2015.

[171] M. Peng, Y. Sun, X. Li, Z. Mao, and C. Wang, "Recent advances in cloud radio access networks: System architectures, key techniques, and open issues," *IEEE Commun. Surveys Tuts.*, vol. 18, no. 3, pp. 2282–2308, 3rd Quart., 2016.

[172] J. Wu, Z. Zhang, Y. Hong, and Y. Wen, "Cloud radio access network (C-RAN): A primer," *IEEE Netw.*, vol. 29, no. 1, pp. 35–41, Jan. 2015.

[173] L. Wang, K.-K. Wong, M. Elkashlan, A. Nallanathan, and S. Lambotharan, "Secrecy and energy efficiency in massive MIMO aided heterogeneous C-RAN: A new look at interference," *IEEE J. Sel. Topics Signal Process.*, vol. 10, no. 8, pp. 1375–1389, Dec. 2016.

[174] X. Li *et al.*, "Indotrack: Device-free indoor human tracking with commodity Wi-Fi," *Proc. ACM Interact. Mob. Wearable Ubiquitous Technol.*, vol. 1, no. 3, pp. 1–22, Sep. 2017, doi: 10.1145/3130940.

[175] D. Cohen, S. Tsiper, and Y. C. Eldar, "Analog-to-digital cognitive radio: Sampling, detection, and hardware," *IEEE Signal Process. Mag.*, vol. 35, no. 1, pp. 137–166, Jan. 2018.

[176] T. Yucek and H. Arslan, "A survey of spectrum sensing algorithms for cognitive radio applications," *IEEE Commun. Surveys Tuts.*, vol. 11, no. 1, pp. 116–130, 1st Quart., 2009.

[177] Y.-C. Liang, Y. Zeng, E. C. Y. Peh, and A. T. Hoang, "Sensing-throughput tradeoff for cognitive radio networks," *IEEE Trans. Wireless Commun.*, vol. 7, no. 4, pp. 1326–1337, Apr. 2008.

[178] J. Wang *et al.*, "Beam codebook based beamforming protocol for multi-Gbps millimeter-wave WPAN systems," *IEEE J. Sel. Areas Commun.*, vol. 27, no. 8, pp. 1390–1399, Oct. 2009.

[179] A. Alkhateeb, O. El Ayach, G. Leus, and R. W. Heath, Jr., "Channel estimation and hybrid precoding for millimeter wave cellular systems," *IEEE J. Sel. Topics Signal Process.*, vol. 8, no. 5, pp. 831–846, Oct. 2014.

[180] C. Aydogdu, F. Liu, C. Masouros, H. Wymeersch, and M. Rydstrom, "Distributed radar-aided vehicle-to-vehicle communication," in *Proc. IEEE Radar Conf. (RadarConf20)*, Sep. 2020, pp. 1–6.

[181] N. Gonzalez-Prelcic, R. Mendez-Rial, and R. W. Heath, "Radar aided beam alignment in mmWave V2I communications supporting antenna diversity," in *Proc. Inf. Theory Appl. Workshop (ITA)*, Jan. 2016, pp. 1–7.

[182] A. Ali, N. Gonzalez-Prelcic, R. W. Heath, and A. Ghosh, "Leveraging sensing at the infrastructure for mmWave communication," *IEEE Commun. Mag.*, vol. 58, no. 7, pp. 84–89, Jul. 2020.

[183] J. Zhang, Y. Huang, J. Wang, X. You, and C. Masouros, "Intelligent interactive beam training for millimeter wave communications," *IEEE Trans. Wireless Commun.*, vol. 20, no. 3, pp. 2034–2048, Mar. 2021.

[184] D. Zhu, J. Choi, and R. W. Heath, Jr., "Auxiliary beam pair enabled AoD and AoA estimation in closed-loop large-scale millimeter-wave MIMO systems," *IEEE Trans. Wireless Commun.*, vol. 16, no. 7, pp. 4770–4785, Jul. 2017.

[185] F. Liu and C. Masouros, "A tutorial on joint radar and communication transmission for vehicular networks—Part II: State of the art and challenges ahead," *IEEE Commun. Lett.*, vol. 25, no. 2, pp. 327–331, Feb. 2021.

[186] Q. Zhang, H. Sun, Z. Wei, and Z. Feng, "Sensing and communication integrated system for autonomous driving vehicles," in *Proc. IEEE INFOCOM Conf. Comput. Commun. Workshops (INFOCOM WKSHPS)*, Jul. 2020, pp. 1278–1279.

[187] S. Kang, S. Choi, G. Lee, and S. Bahk, "A dual-connection based handover scheme for ultra-dense millimeter-wave cellular networks," in *Proc. IEEE Global Commun. Conf. (GLOBECOM)*, Dec. 2019, pp. 1–6.

[188] J. Huang *et al.*, "V2X-communication assisted interference minimization for automotive radars," *China Commun.*, vol. 16, no. 10, pp. 100–111, Oct. 2019.

[189] C. Aydogdu, M. F. Keskin, N. Garcia, H. Wymeersch, and D. W. Bliss, "RadChat: Spectrum sharing for automotive radar interference mitigation," *IEEE Trans. Intell. Transp. Syst.*, vol. 22, no. 1, pp. 416–429, Jan. 2021.

[190] H. Yang *et al.*, "Queue-aware dynamic resource allocation for the joint communication-radar system," *IEEE Trans. Veh. Technol.*, vol. 70, no. 1, pp. 754–767, Jan. 2021.

[191] J. Zhang and C. Masouros, "Beam drift in millimeter wave links: Beamwidth tradeoffs and learning based optimization," *IEEE Trans. Commun.*, vol. 69, no. 10, pp. 6661–6674, Oct. 2021.

[192] G. R. Muns, K. V. Mishra, C. B. Guerra, Y. C. Eldar, and K. R. Chowdhury, "Beam alignment and tracking for autonomous vehicular communication using IEEE 802.11ad-based radar," in *Proc. IEEE INFOCOM Conf. Comput. Commun. Workshops (INFOCOM WKSHPS)*, Apr. 2019, pp. 535–540.

[193] F. Liu and C. Masouros, "Joint localization and predictive beamforming in vehicular networks: Power allocation beyond water-filling," in *Proc. IEEE Int. Conf. Acoust., Speech Signal Process. (ICASSP)*, Jun. 2021, pp. 8393–8397.

[194] L. Wu, K. V. Mishra, B. Shankar, and B. Ottersten, "Resource allocation in heterogeneously-distributed joint radar-communications under asynchronous Bayesian tracking framework," *IEEE J. Sel. Areas Commun.*, vol. 40, no. 8.

[195] J. L. Massey, "An introduction to contemporary cryptology," *Proc. IEEE*, vol. 76, no. 5, pp. 533–549, May 1988.

[196] N. Su, F. Liu, and C. Masouros, "Secure radar-communication systems with malicious targets: Integrating radar, communications and jamming functionalities," *IEEE Trans. Wireless Commun.*, vol. 20, no. 1, pp. 83–95, Jan. 2021.

[197] A. Dimas, M. A. Clark, B. Li, K. Psounis, and A. P. Petropulu, "On radar privacy in shared spectrum scenarios," in *Proc. IEEE Int. Conf. Acoust., Speech Signal Process. (ICASSP)*, May 2019, pp. 7790–7794.

[198] A. Dimas, B. Li, M. Clark, K. Psounis, and A. Petropulu, "Spectrum sharing between radar and communication systems: Can the privacy of the radar be preserved?" in *Proc. 51st Asilomar Conf. Signals, Syst., Comput.*, Oct. 2017, pp. 1285–1289.

[199] A. A. Hilli, A. Petropulu, and K. Psounis, "MIMO radar privacy protection through gradient enforcement in shared spectrum scenarios," in *Proc. IEEE Int. Symp. Dyn. Spectr. Access Netw. (DySPAN)*, Nov. 2019, pp. 1–5.

[200] Y. Liang, H. V. Poor, and S. Shamai (Shitz), "Secure communication over fading channels," *IEEE Trans. Inf. Theory*, vol. 54, no. 6, pp. 2470–2492, Jun. 2008.

[201] N. Su, F. Liu, Z. Wei, Y. Liu, and C. Masouros, "Secure dual-functional radar-communication transmission: Exploiting interference for resilience against target eavesdropping," *IEEE Trans. Wireless Commun.*, early access.

[202] Z. Wei, F. Liu, N. Su, and P. Athina, "Towards multi-functional 6G wireless networks: Integrating sensing, communication and security," *IEEE Wireless Commun. Mag.*, early access. [Online]. Available: https://arxiv.org/pdf/2107.07735.pdf

[203] K. B. Letaief, W. Chen, Y. Shi, J. Zhang, and Y. A. Zhang, "The roadmap to 6G: AI empowered wireless networks," *IEEE Commun. Mag.*, vol. 57, no. 8, pp. 84–90, Aug. 2019.

[204] Y. Mao, C. You, J. Zhang, K. Huang, and K. B. Letaief, "A survey on mobile edge computing: The communication perspective," *IEEE Commun. Surveys Tuts.*, vol. 19, no. 4, pp. 2322–2358, 4th Quart., 2017.

[205] F. Wang, J. Xu, and S. Cui, "Optimal energy allocation and task offloading policy for wireless powered mobile edge computing systems," *IEEE Trans. Wireless Commun.*, vol. 19, no. 4, pp. 2443–2459, Apr. 2020.

[206] C. Ding, J.-B. Wang, H. Zhang, M. Lin, and G. Y. Li, "Joint MIMO precoding and computation resource allocation for integrated communication and radar systems with mobile edge computing," *IEEE J. Sel. Areas Commun.*, vol. 40, no. 8.

[207] F. Sohrabi, T. Jiang, W. Cui, and W. Yu, "Active sensing for communications via learning," *IEEE J. Sel. Areas Commun.*, vol. 40, no. 6.

[208] G. Zhu, D. Liu, Y. Du, C. You, J. Zhang, and K. Huang, "Toward an intelligent edge: Wireless communication meets machine learning," *IEEE Commun. Mag.*, vol. 58, no. 1, pp. 19–25, Jan. 2020.

[209] T. Gafni, N. Shlezinger, K. Cohen, Y. C. Eldar, and H. V. Poor, "Federated learning: A signal processing perspective," *IEEE Signal Process. Mag.*, to be published. [Online]. Available: https://arxiv.org/abs/2103.17150

[210] T. Zhang, S. Wang, G. Li, F. Liu, G. Zhu, and R. Wang, "Accelerating edge intelligence via integrated sensing and communication," in *Proc. IEEE Int. Conf. Commun. (ICC)*, Seoul, South Korea, 2022.

[211] G. Zhu, J. Xu, K. Huang, and S. Cui, "Over-the-air computing for wireless data aggregation in massive IoT," 2020, *arXiv:2009.02181*.

[212] X. Cao, G. Zhu, J. Xu, Z. Wang, and S. Cui, "Optimized power control design for over-the-air federated edge learning," 2021, *arXiv:2106.09316*.

[213] X. Cao, G. Zhu, J. Xu, and K. Huang, "Optimized power control for over-the-air computation in fading channels," *IEEE Trans. Wireless Commun.*, vol. 19, no. 11, pp. 7498–7513, Nov. 2020.

[214] X. Cao, G. Zhu, J. Xu, and K. Huang, "Cooperative interference management for over-the-air computation networks," *IEEE Trans. Wireless Commun.*, vol. 20, no. 4, pp. 2634–2651, Apr. 2021.

[215] T. Sery, N. Shlezinger, K. Cohen, and Y. Eldar, "Over-the-air federated learning from heterogeneous data," *IEEE Trans. Signal Process.*, vol. 69, pp. 3796–3811, 2021.

[216] Q. Wu, S. Zhang, B. Zheng, C. You, and R. Zhang, "Intelligent reflecting surface-aided wireless communications: A tutorial," *IEEE Trans. Commun.*, vol. 69, no. 5, pp. 3313–3351, May 2021.

[217] M. Di Renzo *et al.*, "Smart radio environments empowered by reconfigurable intelligent surfaces: How it works, state of research, and the road ahead," *IEEE J. Sel. Areas Commun.*, vol. 38, no. 11, pp. 2450–2525, Nov. 2020.

[218] Z. Wang, Z. Liu, Y. Shen, A. Conti, and M. Z. Win, "Location awareness in beyond 5G networks via reconfigurable intelligent surfaces," *IEEE J. Sel. Areas Commun.*, vol. 40, no. 8.

[219] X. Shao, C. You, W. Ma, X. Chen, and R. Zhang, "Target sensing with intelligent reflecting surface: Architecture and performance," *IEEE J. Sel. Areas Commun.*, vol. 40, no. 8.

[220] Q. Wu *et al.*, "A comprehensive overview on 5G-and-Beyond networks with UAVs: From communications to sensing and intelligence," *IEEE J. Sel. Areas Commun.*, vol. 39, no. 10, pp. 2912–2945, Oct. 2021.

[221] B. Chang, W. Tang, X. Yan, X. Tong, and Z. Chen, "Integrated scheduling of sensing, communication, and control for mmWave/THz communications in cellular connected UAV networks," *IEEE J. Sel. Areas Commun.*, vol. 40, no. 8.

[222] X. Chen, Z. Feng, Z. Wei, F. Gao, and X. Yuan, "Performance of joint sensing-communication cooperative sensing UAV network," *IEEE Trans. Veh. Technol.*, vol. 69, no. 12, pp. 15545–15556, Dec. 2020.

[223] M. Giordani and M. Zorzi, "Non-terrestrial networks in the 6G era: Challenges and opportunities," *IEEE Netw.*, vol. 35, no. 2, pp. 244–251, Mar./Apr. 2021.

[224] O. Kodheli, "Satellite communications in the new space era: A survey and future challenges," *IEEE Commun. Surveys Tuts.*, vol. 23, no. 1, pp. 70–109, 4th Quart., 2021.

[225] T. S. Rappaport *et al.*, "Wireless communications and applications above 100 GHz: Opportunities and challenges for 6G and beyond," *IEEE Access*, vol. 7, pp. 78729–78757, 2019.

[226] I. F. Akyildiz, J. M. Jornet, and C. Han, "TeraNets: Ultra-broadband communication networks in the terahertz band," *IEEE Wireless Commun.*, vol. 21, no. 4, pp. 130–135, Aug. 2014.

[227] Y. Lu, X. Huang, K. Zhang, S. Maharjan, and Y. Zhang, "Low-latency federated learning and blockchain for edge association in digital twin empowered 6G networks," *IEEE Trans. Ind. Informat.*, vol. 17, no. 7, pp. 5098–5107, Jul. 2021.
[228] H. X. Nguyen, R. Trestian, D. To, and M. Tatipamula, "Digital twin for 5G and beyond," *IEEE Commun. Mag.*, vol. 59, no. 2, pp. 10–15, Feb. 2021.
[229] R. Hadani *et al.*, "Orthogonal time frequency space modulation," in *Proc. IEEE Wireless Commun. Netw. Conf. (WCNC)*, Mar. 2017, pp. 1–6.
[230] L. Gaudio, M. Kobayashi, G. Caire, and G. Colavolpe, "On the effectiveness of OTFS for joint radar parameter estimation and communication," *IEEE Trans. Wireless Commun.*, vol. 19, no. 9, pp. 5951–5965, Sep. 2020.
[231] S. Li *et al.*, "A novel ISAC transmission framework based on spatially-spread orthogonal time frequency space modulation," *IEEE J. Sel. Areas Commun.*, vol. 40, no. 6.

Fan Liu (Member, IEEE) received the B.Eng. and Ph.D. degrees from the Beijing Institute of Technology (BIT), Beijing, China, in 2013 and 2018, respectively.

He has previously held academic positions at University College London (UCL), first as a Visiting Researcher from 2016 to 2018 and then as a Marie Curie Research Fellow from 2018 to 2020. He is currently an Assistant Professor with the Department of Electronic and Electrical Engineering, Southern University of Science and Technology (SUSTech). His research interests include the general area of signal processing and wireless communications, and in particular in the area of integrated sensing and communications (ISAC). He is a member of the IMT-2030 (6G) ISAC Task Group. He was listed in the World's Top 2% Scientists by Stanford University for citation impact in 2021. He has ten publications selected as IEEE ComSoc Besting Readings in ISAC. He was the recipient of the IEEE Signal Processing Society Young Author Best Paper Award of 2021, the Best Ph.D. Thesis Award of the Chinese Institute of Electronics of 2019, and the EU Marie Curie Individual Fellowship in 2018, and has been named as an Exemplary Reviewer for IEEE TRANSACTIONS ON WIRELESS COMMUNICATIONS, IEEE TRANSACTIONS ON COMMUNICATIONS, and IEEE COMMUNICATIONS LETTERS for five times. He was an Organizer and the Co-Chair for numerous workshops, special sessions, and tutorials in flagship IEEE conferences, including ICC, GLOBECOM, ICASSP, and SPAWC. He is the TPC Co-Chair of the 2nd IEEE Joint Communication and Sensing Symposium (JC&S) and will serve as the Track Co-Chair for the IEEE WCNC 2024. He is the Founding Academic Chair of the IEEE ComSoc ISAC Emerging Technology Initiative (ISAC-ETI), an Associate Editor of the IEEE COMMUNICATIONS LETTERS, the Lead Guest Editor for the Special Issue on Integrated Sensing and Communication of the IEEE JOURNAL ON SELECTED AREAS IN COMMUNICATIONS, and a Guest Editor for the Special Issue on Integrated Sensing and Communications for 6G of the IEEE WIRELESS COMMUNICATIONS.

Yuanhao Cui (Member, IEEE) received the B.Eng. degree (Hons.) from Henan University and the Ph.D. degree from the Beijing University of Posts and Telecommunications (BUPT). He has been the CTO and the Co-Founder of two startup companies, where he has invested more than $3 million dollars. He holds more than 20 granted patents. His research interests include precoding and protocol designs for ISAC. He is a member of the IMT-2030 (6G) ISAC Task Group. He received the Best Paper Award from IWCMC 2021. He is the Founding Secretary of the IEEE ComSoc ISAC Emerging Technology Initiative (ISAC-ETI) and the CCF Science Communication Working Committee. He was the Organizer and the Co-Chair for a number of workshops and special sessions in flagship IEEE conferences, including ICC, ICASSP, WCNC, and VTC. He is the Lead Guest Editor for the Special Issue on Integrated Sensing and Communication for 6G of the IEEE OPEN JOURNAL OF THE COMMUNICATIONS SOCIETY and the Guest Editor for the Special Issue on Integrated Sensing and Communications for Future Green Networks of the IEEE TRANSACTIONS ON GREEN COMMUNICATIONS AND NETWORKING.

Christos Masouros (Senior Member, IEEE) received the Diploma degree in electrical and computer engineering from the University of Patras, Greece, in 2004, and the M.Sc. by research and Ph.D. degrees in electrical and electronic engineering from The University of Manchester, U.K., in 2006 and 2009, respectively.

In 2008, he was a Research Intern at Philips Research Labs, U.K. Between 2009 and 2010, he was a Research Associate with The University of Manchester and a Research Fellow at Queen's University Belfast between 2010 and 2012. In 2012, he joined University College London as a Lecturer. He has held a Royal Academy of Engineering Research Fellowship between 2011 and 2016. Since 2019, he has been a Full Professor of signal processing and wireless communications with the Information and Communication Engineering Research Group, Department of Electrical and Electronic Engineering, and affiliated with the Institute for Communications and Connected Systems, University College London. His research interests lie in the field of wireless communications and signal processing with particular focus on green communications, large scale antenna systems, integrated sensing and communications, interference mitigation techniques for MIMO, and multicarrier communications. He was the co-recipient of the 2021 IEEE SPS Young Author Best Paper Award. He was the recipient of the Best Paper Awards in the IEEE GlobeCom 2015 and IEEE WCNC 2019 conferences, and has been recognized as an Exemplary Editor for the IEEE COMMUNICATIONS LETTERS and as an Exemplary Reviewer for the IEEE TRANSACTIONS ON COMMUNICATIONS. He is a founding member and the Vice-Chair of the IEEE Emerging Technology Initiative on Integrated Sensing and Communications, the Vice Chair of the IEEE Special Interest Group on Integrated Sensing and Communications (ISAC), and the Chair of the IEEE Special Interest Group on Energy Harvesting Communication Networks. He is an Editor of IEEE TRANSACTIONS ON COMMUNICATIONS, IEEE TRANSACTIONS ON WIRELESS COMMUNICATIONS, the IEEE OPEN JOURNAL OF SIGNAL PROCESSING; and the Editor-at-Large of IEEE OPEN JOURNAL OF THE COMMUNICATIONS SOCIETY. He has been an Associate Editor of IEEE COMMUNICATIONS LETTERS and a Guest Editor for a number of IEEE JOURNAL OF SELECTED TOPICS IN SIGNAL PROCESSING and IEEE JOURNAL ON SELECTED AREAS IN COMMUNICATIONS issues.

Jie Xu (Member, IEEE) received the B.E. and Ph.D. degrees from the University of Science and Technology of China in 2007 and 2012, respectively. From 2012 to 2014, he was a Research Fellow with the Department of Electrical and Computer Engineering, National University of Singapore. From 2015 to 2016, he was a Post-Doctoral Research Fellow with the Engineering Systems and Design Pillar, Singapore University of Technology and Design. From 2016 to 2019, he was a Professor with the School of Information Engineering, Guangdong University of Technology, China. He is currently an Associate Professor with the School of Science and Engineering, The Chinese University of Hong Kong, Shenzhen, China. His research interests include wireless communications, wireless information and power transfer, UAV communications, edge computing and intelligence, and integrated sensing and communication (ISAC). He was a recipient of the 2017 IEEE Signal Processing Society Young Author Best Paper Award, the IEEE/CIC ICCC 2019 Best Paper Award, the 2019 IEEE Communications Society Asia–Pacific Outstanding Young Researcher Award, and the 2019 Wireless Communications Technical Committee Outstanding Young Researcher Award. He is the Symposium Co-Chair of the IEEE GLOBECOM 2019 Wireless Communications Symposium, the workshop co-chair of several IEEE ICC and GLOBECOM workshops, the Tutorial Co-Chair of the IEEE/CIC ICCC 2019, and the Vice Co-Chair of the IEEE Emerging Technology Initiative (ETI) on ISAC. He served or is serving as an Editor for the IEEE TRANSACTIONS ON WIRELESS COMMUNICATIONS, IEEE TRANSACTIONS ON COMMUNICATIONS, IEEE WIRELESS COMMUNICATIONS LETTERS, and *Journal of Communications and Information Networks*; an Associate Editor for IEEE ACCESS; and a Guest Editor for the IEEE WIRELESS COMMUNICATIONS, IEEE JOURNAL ON SELECTED AREAS IN COMMUNICATIONS, and *Science China Information Sciences*.

Tony Xiao Han (Senior Member, IEEE) received the B.E. degree in electrical engineering from Sichuan University and the Ph.D. degree in communication engineering from Zhejiang University, Hangzhou, China.

He was a Post-Doctoral Research Fellow with the National University of Singapore. He is currently a Principal Engineer with Huawei Technologies Company Ltd. His research interests include wireless communication, signal processing, integrated sensing and communication (ISAC), and standardization of wireless communication. He was the Chair of the IEEE 802.11 WLAN Sensing Topic Interest Group (TIG) and the 802.11 WLAN Sensing Study Group (SG), and he is currently serving as the Chair for the IEEE 802.11bf WLAN Sensing Task Group (TG). He has served as the ISAC Workshop Co-Chair for the IEEE GLOBECOM 2020. He is the Industry Chair of IEEE ComSoc Integrated Sensing and Communication Emerging Technology Initiative (ISAC-ETI), the Vice Chair of the IEEE WTC Special Interest Group (SIG) on ISAC, and a Guest Editor for the Special Issue on Integrated Sensing and Communications of the IEEE JOURNAL ON SELECTED AREAS IN COMMUNICATIONS (JSAC).

Yonina C. Eldar (Fellow, IEEE) received the B.Sc. degree in physics and the B.Sc. degree in electrical engineering from Tel Aviv University (TAU), Tel Aviv-Yafo, Israel, in 1995 and 1996, respectively, and the Ph.D. degree in electrical engineering and computer science from the Massachusetts Institute of Technology (MIT), Cambridge, in 2002.

She is currently a Professor with the Department of Mathematics and Computer Science, Weizmann Institute of Science, Rehovot, Israel. She was previously a Professor with the Department of Electrical Engineering, Technion. She is also a Visiting Professor at MIT, a Visiting Scientist at the Broad Institute, and an Adjunct Professor at Duke University, and was a Visiting Professor at Stanford. She is an author of the book *Sampling Theory: Beyond Bandlimited Systems* and a coauthor of five other books published by Cambridge University Press. Her research interests are in the broad areas of statistical signal processing, sampling theory and compressed sensing, learning and optimization methods, and their applications to biology, medical imaging, and optics.

Dr. Eldar was a member of the Young Israel Academy of Science and Humanities, the Israel Committee for Higher Education, and the IEEE Signal Processing Theory and Methods and Bio Imaging Signal Processing Technical Committees. She is a member of the Israel Academy of Sciences and Humanities (elected 2017) and the IEEE Sensor Array and Multichannel Technical Committee, and serves on several other IEEE committees. She is a fellow of EURASIP, a Horev Fellow of the Leaders in Science and Technology Program at the Technion, and a fellow of Alon. She has received many awards for excellence in research and teaching, including the IEEE Signal Processing Society Technical Achievement Award in 2013, the IEEE/AESS Fred Nathanson Memorial Radar Award in 2014, and the IEEE Kiyo Tomiyasu Award in 2016. She received the Michael Bruno Memorial Award from the Rothschild Foundation, the Weizmann Prize for Exact Sciences, the Wolf Foundation Krill Prize for Excellence in Scientific Research, the Henry Taub Prize for Excellence in Research (twice), the Hershel Rich Innovation Award (three times), the Award for Women with Distinguished Contributions, the Andre and Bella Meyer Lectureship, the Career Development Chair at the Technion, the Muriel and David Jacknow Award for Excellence in Teaching, and the Technion's Award for Excellence in Teaching (two times). She also received several best paper awards and best demo awards together with her research students and colleagues including the SIAM Outstanding Paper Prize, the UFFC Outstanding Paper Award, the Signal Processing Society Best Paper Award, and the *IET Circuits, Devices and Systems* Premium Award. She was selected as one of the 50 most influential women in Israel and Asia, and is a Highly Cited Researcher. She was the co-chair and the technical co-chair of several international conferences and workshops. She was a Signal Processing Society Distinguished Lecturer and served as an Associate Editor for the IEEE TRANSACTIONS ON SIGNAL PROCESSING, the *EURASIP Journal on Advances in Signal Processing*, the *SIAM Journal on Matrix Analysis and Applications*, and the *SIAM Journal on Imaging Sciences*. She is the Editor-in-Chief of *Foundations and Trends in Signal Processing*.

Stefano Buzzi (Senior Member, IEEE) received the M.Sc. degree *(summa cum laude)* in electronic engineering and the Ph.D. degree in electrical and computer engineering from the University of Naples Federico II in 1994 and 1999, respectively. He has had short-term research appointments at Princeton University, Princeton, NJ, USA, from 1999 to 2001 and in 2006. He is a Full Professor with the University of Cassino and Southern Lazio, Italy. He is currently the Principal Investigator of the EU-funded Innovative Training Network Project METAWIRELESS, on the application of metasurfaces to wireless communications. He has coauthored about 170 technical peer-reviewed journals and conference papers. His research interests are in the broad field of communications and signal processing, with emphasis on wireless communications and beyond-5G systems. His research interests also lie in the field of statistical signal processing and wireless communications, with emphasis on beyond-5G and 6G wireless systems. He also serves regularly as a TPC Member for several international conferences. He is a former Associate Editor of the IEEE SIGNAL PROCESSING LETTERS and IEEE COMMUNICATIONS LETTERS. He has been the Guest Editor for four IEEE JOURNAL ON SELECTED AREAS IN COMMUNICATIONS special issues, and he was an Editor of the IEEE TRANSACTIONS ON WIRELESS COMMUNICATIONS from 2014 to 2020.